Electronic Supplementary Material (ESI) for Organic Chemistry Frontiers.

Electronic Supplementary Materials for

Chemical transformation of Doubly N-Confused Porphodimethene to variants of (anti)Aromatic Doubly N-Confused Porphyrinoids and σ aromatic Doubly N-Confused Isophlorinoid

Nyancy Halder,[a] Raja Narayanasamy,[b] Dandamudi Usharani * [b,c] and Harapriya Rath*[a]

[a] *School of Chemical Sciences, Indian Association for The Cultivation of Science, 2A/2B Raja S. C. Mullick Road, Jadavpur, Kolkata 700 032, India, E-mail: ichr@iacs.res.in*
[b] *Department of Food Safety and Analytical Quality Control Laboratory, CSIR-Central Food Technological Research Institute, Mysuru 570020 Karnataka, India, E-mail: ushad@cftri.res.in*
[c] *Academy of Scientific and Innovative Research (AcSIR), CSIR-HRDC, Ghaziabad, Uttar Pradesh, India*

Table of Contents

Materials and Methods:

1.1 Electronic absorption spectra were measured with a Perkin Elmer Lambda 950 UV-visible-NIR spectrophotometer. ^{1}H NMR spectra were recorded on a Bruker AVIII 500 MHz spectrometer, Bruker AVIII 400 MHz, Bruker DPX-300 MHz spectrometer and chemical shifts were reported as the delta scale in ppm relative to $CHCl_3$ (δ = 7.26 ppm) and CH_2Cl_2 (δ = 5.32 ppm) as internal reference for ^{1}H and ^{13}C NMR $CHCl_3$ (δ = 77.00 ppm) and CH_2Cl_2 (δ = 55.00 ppm). MALDI-TOF MS data were recorded using Bruker Daltonics flex Analyser and ESI HR-MS data were recorded using Waters QTOF Micro YA263 spectrometer. Cyclic voltammograms were recorded using a platinum working electrode, a platinum wire counter electrode and a Ag/AgCl reference electrode in Bioanalytical Systems EC epsilon. The measurements were carried out in CH_2Cl_2 solution using 0.1 M Bu_4NPF_6 as the supporting electrolyte at a scan rate of 0.1 V/s. Peak potentials were determined from differential pulse voltammetry experiments. The Fc/Fc^{+} redox couple was used as an internal standard. All solvents and chemicals were of reagent grade quality, obtained commercially and used without further purification except as noted. For spectral measurements, anhydrous dichloromethane was obtained by refluxing and distillation over CaH_2. Dry THF was obtained by refluxing and distillation over pressed Sodium metal. Thin layer chromatography (TLC) was carried out on alumina sheets coated with silica gel 60 F_{254} (Merck 5554) and gravity column chromatography were performed using Merck Silica Gel 230-400 mesh. Aluminum Oxide (Basic) grade II was purchased from Sigma Aldrich.

1.2 X-Ray structure determination.

A specimen of $C_{57}H_{35}F_{10}N_5$, approximate dimensions 0.150 mm x 0.200 mm x 0.300 mm, was used for the X-ray crystallographic analysis of **7**. The X-ray intensity data were measured on a Bruker APEX-II CCD system (Mo, λ = 0.71073 Å). The total exposure time was 4.14 hours. The frames were integrated with the Bruker SAINT software package using a narrow-frame algorithm. The integration of the data using a triclinic unit cell yielded a total of 25138 reflections to a maximum θ angle of 25.50° (0.83 Å resolution), of which 10089 were independent (average redundancy 2.492, completeness = 99.1%, R_{int} = 6.97%, R_{sig} = 8.69%) and 7315 (72.50%) were greater than $2\sigma(F^2)$. The final cell constants of a = 11.498(3) Å, b = 12.936(2) Å, c = 20.787(4) Å, α = 76.103(6)°, β = 77.831(7)°, γ = 66.872(6)°, volume = 2736.5(9) $Å^3$, are based upon the refinement of the XYZ-centroids of 9228 reflections above 20 σ(I) with 4.870° < 2θ < 56.62°. The ratio of minimum to maximum apparent transmission was 0.753. The calculated minimum and maximum transmission coefficients (based on crystal size) are 0.8910 and 0.9430. The structure was solved and refined using the Bruker SHELXTL Software Package, using the space group P -1, with Z = 2 for the formula unit, $C_{57}H_{35}F_{10}N_5$. The final anisotropic full-matrix least-squares refinement on F^2 with 733 variables converged at R1 = 9.72%, for the observed data and wR2 = 30.67% for all data. The goodness-of-fit was 1.050. The largest peak in the final difference electron density synthesis was 1.432 e-/$Å^3$ and the largest hole was -1.225 e-/$Å^3$ with an RMS deviation of 0.131 e-/$Å^3$. On the basis of the final model, the calculated density was 1.498 g/cm^3 and F(000), 1256 e^-. The Alert B due to the Cl atom is part of solvent (prone to disorder) and is not ideally shaped due to low quality of data, however, this does not indicate an incorrect atom-type assignment.

A suitable shinning green crystal of size 0.1 x 0.1 x 0.09mm^3 of free base **8** was mounted on a Bruker APEX-III CCD diffractometer with a fine- focus sealed tube Mo-Kα radiation (λ = 0.71073Å) X-ray source. Total 1800 frames were collected at 100 K for free base form of **8** with the exposure time of 20s per frame. Unit cell determination using both high angle and low angle diffraction reveal that compound crystallizes in monoclinic P 2yb space group for **8**. The structures were solved by SHELX-2018/3 using SHELXTL suite of programme. The final refinement of the structure was carried out using least-squares method on F^2 using SHELXL-2018/3. The final refinement of the solved structure converged at the R value of 0.0777 for free base form of **8**. All non-hydrogen atoms were refined anisotropically. All the hydrogen atoms were located from difference Fourier maps. But the data is not sufficient to define the structure and the bond precision is poor, which raises an Alert A and Alert B.

A specimen of $C_{46}H_{24}F_8N_4O_4$, approximate dimensions 0.050 mm x 0.100 mm x 0.200 mm, was used for the X-ray crystallographic analysis of **10**. The X-ray intensity data were measured (λ = 0.71073 Å). The total exposure time was 1.63 hours. The frames were integrated with the Bruker SAINT software package using a narrow-frame algorithm. The integration of the data using a triclinic unit cell yielded a total of 10661 reflections to a maximum θ angle of 28.36° (0.75 Å resolution), of which 4525 were independent (average redundancy 2.356, completeness = 98.1%, R_{int} = 5.55%, R_{sig} = 8.26%) and 3006 (66.43%) were greater than 2σ(F^2). The final cell constants of a = 7.0383(11) Å, b = 10.8268(16) Å, c = 12.680(2) Å, α = 96.192(6)°, β = 98.435(6)°, γ = 103.370(5)°, volume = 919.7(3) Å^3, are based upon the refinement of the XYZ-centroids of 2882 reflections above 20 σ(I) with 4.720° < 2θ < 56.54°. Data were corrected for absorption effects using the Multi-Scan method (SADABS). The ratio of minimum to maximum apparent transmission was 0.773. The calculated minimum and maximum transmission coefficients (based on crystal size) are 0.9750 and 0.9940. The structure was solved and refined using the Bruker SHELXTL Software Package, using the space group P -1, with Z = 1 for the formula unit, $C_{46}H_{24}F_8N_4O_4$. The final anisotropic full-matrix least-squares refinement on F^2 with 281 variables converged at R1 = 6.36%, for the observed data and wR2 = 18.00% for all data. The goodness-of-fit was 1.042. The largest peak in the final difference electron density synthesis was 0.423 e^-/Å^3 and the largest hole was -0.382 e^-/Å^3 with an RMS deviation of 0.088 e^-/Å^3. On the basis of the final model, the calculated density was 1.532 g/cm^3 and F(000), 432 e^-.

1.3 Theoretical Calculation

Theoretical calculations were performed using Gaussian 16 (rev A 03) program suite.[1] The geometric structures of doubly N-confused porphodimethene (**6**, **11**) were modeled based on observed ^{1}H NMR data. Starting from X-ray crystal structures of **7** and oxidized congeners of **6** such as N-confused monooxoporphyrinoid (**8**), N-confused dioxoporphyrinoid (**9**) and N-confused isophlorinoid (**10**), unsubstituted N-methyl and *meso* aryl structures **8a**, **9a** and **10a** are modeled. Geometry optimizations for all these structures were carried out employing hybrid density functional B3LYP [2a-c] and 6-31G(d,p) basis set. [2d-e] Harmonic vibrational frequency analysis at the same level of theory has ascertain optimized geometry structures as local minima. Enol forms of 1**0**‘ are converged to tetraoxo isophlorinoid (**10**). Further simulated absorption spectrum in presence of dichloromethane solvent

using polarizable continuum model[3] and time dependent density functional formulism,[4] natural population analysis,[5] Anisotropy induced current density plots (AICD) [6a] based on continuous set of gauge transformations (CSGT) [6b,c] methods and Nuclear Independent Chemical Shifts (NICS) values[7a] with gauge independent atomic orbital (GIAO) method[7b,c] were obtained at the same level of theory. To understand the extent of π delocalization Nuclear Independent Chemical Shifts (NICS) has been calculated at 1 - 5Å above the molecular plane (NICS(1), isotropic chemical shift) and the ZZ component of the chemical shift tensor represent NICSzz values) Further based on Stranger method,[8] NICS values are scanned along the trajectory orthogonal to the plane of macrocycle where the ghost atoms above the geometric center are separated at an interval of 0.2 Å. To probe the aromatic nature, the decomposition of NBO-Wiberg bond Index[9] as σ and π contribution of bonds and π reconstruction pathways using localized orbital locator (LOL) topology analysis based on natural bonding orbital theory was obtained using multifunctional wave functional analyzer Multiwfn software. [10]

References:

1. M. J. Frisch, G. W. Trucks, H. B. Schlegel, G. E. Scuseria, M. A. Robb, J. R. Cheeseman, G. Scalmani, V. Barone, G. A. Petersson, H. Nakatsuji, X. Li, M. Caricato, A. V. Marenich, J. Bloino, B. G. Janesko, R. Gomperts, B. Mennucci, H. P. Hratchian, J. V. Ortiz, A. F. Izmaylov, J. L. Sonnenberg, F. Ding, F. Lipparini, F. Egidi, J. Goings, B. Peng, A. Petrone, T. Henderson, D. Ranasinghe, V. G. Zakrzewski, J. Gao, N. Rega, G. Zheng, W. Liang, M. Hada, M. Ehara, K. Toyota, R. Fukuda, J. Hasegawa, M. Ishida, T. Nakajima, Y. Honda, O. Kitao, H. Nakai, T. Vreven, K. Throssell, Jr. J. A. Montgomery, J. E. Peralta, F. Ogliaro, M. J. Bearpark, J. J. Heyd, E. N. Brothers, K. N. Kudin, V. N. Staroverov, T. A. Keith, R. Kobayashi, J. Normand, K. Raghavachari, A. P. Rendell, J. C. Burant, S. S. Iyengar, J. Tomasi, M. Cossi, J. M. Millam, M. Klene, C. Adamo, R. Cammi, J. W. Ochterski, R. L. Martin, K. Morokuma, O. Farkas, J. B. Foresman, D. J. Fox, *Gaussian 16 Rev. C.01*: Wallingford, CT, **2016**.
2. (a) A. D. Becke, A new mixing of Hartree–Fock and local density-functional theories, *J. Chem. Phys.,* 1993**, 98**, 1372-1377; (b) A. D. Becke, Density-functional thermochemistry. I. The effect of the exchange-only gradient correction, *J. Chem. Phys.,* 1992, **96**, 2155-2160; (c) C. Lee, W. Yang and R. G. Parr, Development of the Colle-Salvetti correlation-energy formula into a functional of the electron density, *Phys. Rev. B* 1988, **37**, 785-789; (d) P. J. Hay and W. R. Wadt, *Ab initio* effective core potentials for molecular calculations. Potentials for the transition metal atoms Sc to Hg, *J. Chem. Phys.,* 1985, **82**, 270-283; (e) W. R. Wadt and P. J. Hay, *J. Chem. Phys.,* 1985, **82**, 284-298. (f) T. H. Dunning and P. J. Hay, Gaussian basis sets for molecular calculations. In *Methods of electronic structure theory*, Springer1977; pp 1-27.
3. (a) S. Miertus and J. Tomasi, Approximate evaluations of the electrostatic free energy and internal energy changes in solution processes, *Chem. Phys.,* 1982, **65**, 239-245; (b) M. Cossi and V. Barone, *J.* Solvent effect on vertical electronic transitions by the polarizable continuum model, *J. Chem. Phys.,* 2000, **112**, 2427-2435.
4. (a) C. Adamo and D. Jacquemin, The calculations of excited-state properties with Time-Dependent Density Functional Theory, *Chem. Soc. Rev.,* 2013, **42**, 845-856; (b) G. Scalmani, M. J. Frisch, B. Mennucci, J. Tomasi, R. Cammi and V. Barone, Geometries and properties of excited states in the gas phase and in solution: Theory and application of a time-dependent density functional theory polarizable continuum model, *J. Chem. Phys.,* 2006, **124**, 094107.
5. (a) F. *J.* Weinhold, Natural bond orbital analysis: a critical overview of relationships to alternative bonding perspectives, *J. Comput. Chem.,* 2012, **33**, 2363-2379; (b) E. D.

Glendening, C. R. Landis and F. Weinhold, NBO 6.0: Natural bond orbital analysis program, *J. Comput. Chem.,* 2013, **34**, 1429-1437.

6. (a) D. Geuenich, K. Hess, F. Köhler and R. Herges, Anisotropy of the induced current density (ACID), a general method to quantify and visualize electronic delocalization, *Chem. Rev.,* 2005, **105**, 3758-3772; (b) J. R. Cheeseman, G. W. Trucks, T. A. Keith and M. J. Frisch, A comparison of models for calculating nuclear magnetic resonance shielding tensors, *J. Chem. Phys.,* 1996, **104**, 5497-5509; (c) T. A. Keith and R. F. W. Bader, Calculation of magnetic response properties using a continuous set of gauge transformations, *Chem. Phys. Lett.,* 1993, **210**, 223-231.
7. (a) P. v. R. Schleyer, C. Maerker, A. Dransfeld, H. Jiao and N. J. R. van Eikema Hommes, Nucleus-independent chemical shifts: a simple and efficient aromaticity probe, *J. Am. Chem. Soc.,* 1996**, 118**, 6317-6318; (b) K. Wolinski, J. F. Hinton and P. Pulay, Efficient implementation of the gauge-independent atomic orbital method for NMR chemical shift calculations, *J. Am. Chem. Soc.,* 1990**, 112**, 8251-8260; (c) F. London, Théorie quantique des courants interatomiques dans les combinaisons aromatiques, *J. phys. Radium,* 1937**, 8**, 397-409.
8. A. Stanger, Nucleus-independent chemical shifts (NICS): distance dependence and revised criteria for aromaticity and antiaromaticity, *J. Org. Chem.,* 2006**, 71**, 883-893.
9. K. B. Wiberg, The concept of strain in organic chemistry, *Angew. Chem. Int. Ed.,* 1986**, 25**, 312-322.
10. (a) T. Lu and F. Chen, Multiwfn: a multifunctional wavefunction analyzer, *J. Comput. Chem.,* 2012**, 33**, 580-592; (b) T. Lu and Q. Chen, mwfn: A strict, concise and extensible format for electronic wavefunction storage and exchange. **2021**.

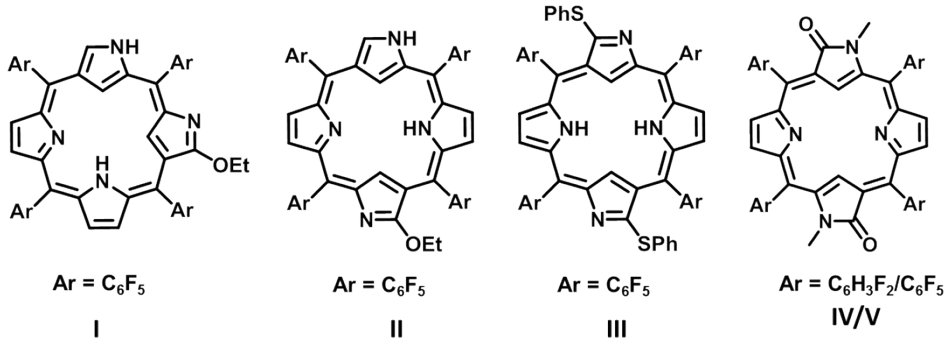

Chart S1. Representative examples of doubly N-confused Porphyrinoids

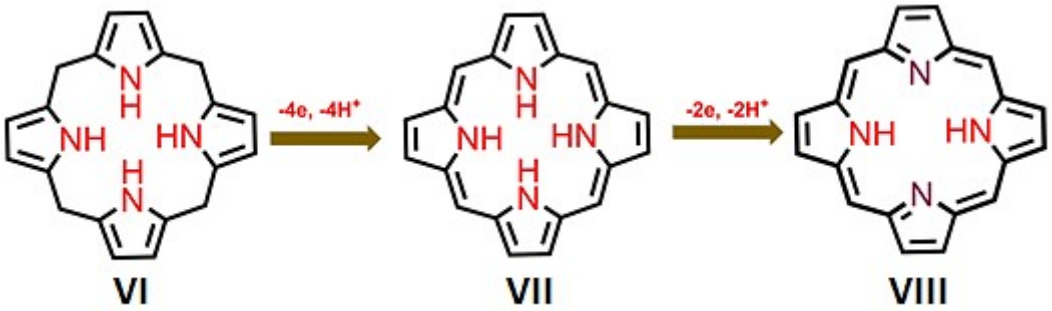

Chart S2 Proton Coupled Electron Transfer Induced Oxidation of Porphyrinogen (VI) into a Porphyrin (VIII) through Isophlorin (VII).

1.4 Synthesis:

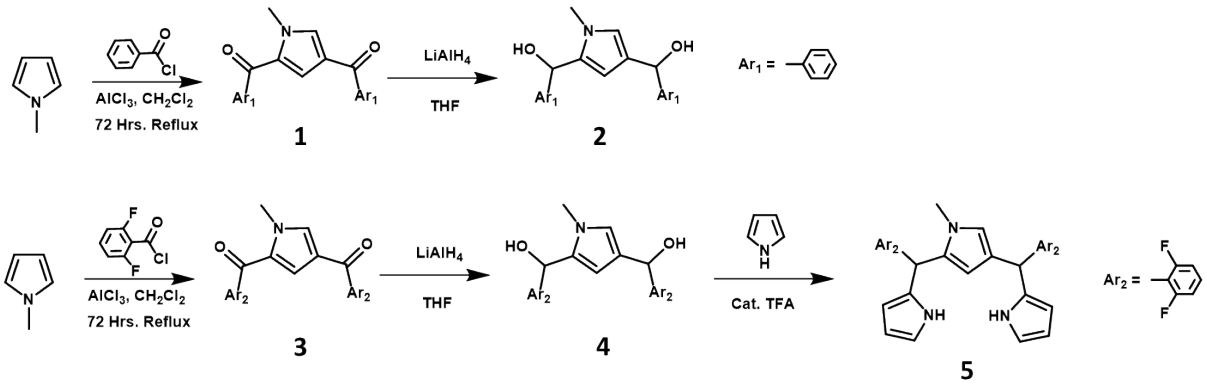

Scheme S1. Synthesis of all precursors used for the macrocycles reported in the manuscript

Synthesis of **6** and **7**: Tripyrrane **5** (0.463 g, 1 mmol) and diol **4** (0.365 g, 1 mmol) were taken in a round bottom flask, to it 740 mL of dry CH_2Cl_2 was added and stirred for 15 minutes under nitrogen atmosphere to get a clear solution. *p*-Toluenesulfonic acid (0.035 g, 0.185 mmol) was added to the reaction mixture and stirred for 90 minutes under dark condition. After that, *p*-chloranil (0.367 g, 1.5 mmol) was added and the resulting mixture was refluxed for 90 minutes in open air. After complete removal of solvent from reaction mixture by rotary evaporator, the compound was filtered through a short pad of basic alumina column. The crude mixture was purified by silica gel (200-400 mesh) column chromatography using dichloromethane/hexane as eluent. The red colored **6** and brown colored **7** collected from column were evaporated and recrystallized from CH_2Cl_2/Hexane yielding **6** as green crystalline solid and **7** as brown crystalline solid.

[**6**]: Yield. ~321 mg (~40%). R_f = 0.2 (CH_2Cl_2/ Hexane = 6:4). Mp > 350°C.

HR-ESI-TOF MS (*m/z*): 805.2208 $[M+H]^+$ (804.2145 calc. for $[C_{46}H_{28}F_8N_4O]^+$). Elemental analysis Calc. for $C_{46}H_{28}F_8N_4O$: C, 68.57; H, 3.63; N, 6.95. Found: C, 68.61; H, 3.67; N, 6.94. UV-vis (CH_2Cl_2, λ [nm], (ϵ [M^{-1} $cm^{-1}x10^3$]), 298K): 316 (15.43), 493 (14.25), 603 (1.45). ^{1}H NMR (500 MHz, $CDCl_3$, δ [ppm], 298 K): 9.04 (br, 1H, Pyrrole- NH), 8.94 (s, 1H, βH-N-Me-pyrrole), 7.47 (s, 1H, N-Me-Pyrrole-βH), 6.86-7.42 (m, 12H, Phenyl-H), 6.61 (d, 1H, J = 5.5 Hz, Pyrrole-βH), 6.45 (s, 1H, N-Me Pyrrole- αH), 6.05 (d, 1H, J = 5.5 Hz, Pyrrole-βH), 5.83 (m, 2H, Pyrrole-βH), 5.73 (s, 1H, *meso*-H), 5.71 (s, 1H, *meso*-H), 3.30 (s, 3H, N-methyl CH), 2.63 (s, 3H, N-methyl CH).^{13}C NMR (125 MHz, $CDCl_3$, δ[ppm]): 171.18, 168.24, 162.49, 160.57, 153.55, 144.21, 137.25, 136.01, 134.75, 134.38, 129.49, 129.07, 128.98, 127.30, 122.59, 114.57, 112.37, 112.18, 112.0, 111.80, 111.52, 111.42, 108.01, 107.85, 34.37, 32.68, 31.92, 29.85.

[**7**]: Yield. ~39mg (~4%). R_f = 0.3 (CH_2Cl_2/Hexane = 9:1). Mp > 350°C.

HR-ESI-TOF MS (*m/z*): 980.2806 $[M+H]^+$ (979.2733 calc. for $[C_{57}H_{35}F_{10}N_5]^+$). Elemental analysis Calc. for $C_{57}H_{35}F_{10}N_5$: C, 69.87; H, 3.60; N, 7.15. Found: C, 69.90; H, 3.65; N, 7.14. UV-vis (CH_2Cl_2, λ [nm], (ϵ [M^{-1} $cm^{-1}x10^3$]), 298K): 406 (49.43), 642 (24.05). ^{1}H NMR (500 MHz, CD_2Cl_2, δ [ppm], 298 K): 7.60 (br, 1H, Pyrrole- NH), 7.38 (br, 1H, Pyrrole- NH), 7.15-7.35 (m, 5H, Phenyl-H), 6.83-7.02 (m, 10H, Phenyl-H), 6.79 (br, 1H, N-Me Pyrrole- αH), 6.69 (s, 1H, N-Me Pyrrole- αH), 6.51 (d, 1H, J = 5 Hz,

Pyrrole-βH), 6.46 (d, 1H, J = 4.5 Hz, Pyrrole-βH), 6.32 (d, 1H, J = 5 Hz, Pyrrole-βH), 6.20 (d, 1H, J = 4.5 Hz, Pyrrole-βH), 6.19 (s, 1H, N-Me-Pyrrole-βH), 5.87 (s, 1H, N-Me-Pyrrole-βH), 5.77 (m, 1H, Pyrrole-βH), 5.72 (s, 1H, *meso*-H), 5.62 (s, 1H, *meso*-H), 5.58 (d, 1H, J = 5.5 Hz, Pyrrole-βH), 3.57 (s, 3H, N-methyl CH), 3.28 (s, 3H, N-methyl CH). ^{13}C NMR (125 MHz, CD_2Cl_2, δ[ppm]): 171.18, 168.09, 163.16, 163.09,162.49, 160.88, 156.64, 153.55, 150.26, 147.39, 144.21, 137.25, 136.01, 134.75, 134.38, 133.89, 133.35,131.62,131.61, 129.49, 129.07, 128.98, 128.61, 127.82, 127.30, 127.04, 124.83, 122.59, 121.61, 119.39, 117.94, 117.89, 114.57, 112.37, 112.18, 111.80, 111.52, 111.42, 108.35, 107.85, 105.99, 105.04, 104.38, 36.18, 34.55, 32.23, 31.97.

Synthesis of **8**: **6** (0.8 g, 1 mmol) was taken in a round bottom flask, to it 10 mL of dry CH_2Cl_2 and excess of basic alumina (~3 g) was added. The reaction mixture was stirred for 1 hour under air. The reaction mixture was filtered, the filtrate was evaporated in a rotary evaporator and was recrystalized from CH_2Cl_2/Hexane to obtain compounds **8** as air stable green solid. Yield. ~762 mg (~95%). R_f = 0.2 (CH_2Cl_2/ Hexane = 8:2). Mp > 350°C.

HR-ESI-TOF MS (*m/z*): 803.2052 $[M+H]^+$ (802.1979 calc. for $[C_{46}H_{26}F_8N_4O]^+$. Elemental analysis Calc. for $C_{46}H_{26}F_8N_4O$: C, 68.83; H, 3.26; N, 6.98. Found: C, 68.88; H, 3.28; N 6.95. UV-vis (CH_2Cl_2, λ [nm], (ϵ [$M^{-1}cm^{-1}x10^4$]), 298K): 438 (21.02), 660 (3.78), 717 (3.98).^{1}H NMR (500 MHz, CD_2Cl_2, δ [ppm], 298 K): 7.56-7.59 (m, 4H, Phenyl-CH), 7.45 (d, 1H, Pyrrole-β-CH, J = 5 Hz), 7.37 (d, 1H, Pyrrole-β-CH, J = 4.5 Hz), 7.28 (d, 1H, Pyrrole-β-CH, J = 4.5 Hz), 7.08-7.21 (m, 8H, Phenyl-CH), 7.05 (s, 1H, N-Me Pyrrole-α-CH), 6.95 (d, 1H, Pyrrole-β-CH, J = 5 Hz), 3.70 (s, 1H, N-Me-Pyrrole-β-CH), 3.45 (s, 3H, Methyl CH), 2.91 (s, 3H, Methyl CH), 2.36 (s, 1H, N-Me-Pyrrole-β-CH). ^{13}C NMR (125 MHz, CD_2Cl_2, δ[ppm]): 170.97, 166.09, 163.48, 163.25, 162.96, 162.66, 161.49, 161.33, 160.73, 160.62, 155.18, 153.84, 147.05, 145.47, 141.31, 134.23, 131.40, 131.28, 129.51, 123.22, 128.54, 128.36, 119.59, 111.85, 111.69, 111.50, 100,14, 37.40, 28.77.

Synthesis of **9**: **6** (0.8 g, 1 mmol) was taken in a round bottom flask, to it 10 mL of dry CH_2Cl_2 and *p*-chloranil (0.490 g, 2 mmol) was added and stirred under reflux for 30 minutes in air. The reaction mixture was evaporated in a rotary evaporator and was purified by silica gel column chromatography to obtain compound **9**. Yield. ~736 mg (~90%).

Synthesis of **10**: **6** (0.8 g, 1 mmol) was taken in a round bottom flask, to it 10 mL of dry CH_2Cl_2 and DDQ (0.454 g, 2 mmol) was added and stirred at room temperature for 30 minutes in air. After complete removal of solvent from crude mixture by rotary evaporator, the compound was purified by silica gel column chromatography using 10% EtOAc/CH_2Cl_2 as eluent. The desired macrocycle **10** was isolated as extra pure deep green crystalline solid upon further recrystallization from CH_2Cl_2/Hexane.
Yield. ~780 mg (~92%). R_f = 0.1 (EtOAc/CH_2Cl_2 = 1:9). Mp > 350°C.

HR-ESI-TOF MS (*m/z*): 849.1748 $[M+H]^+$ (848.1670 calc. for $[C_{46}H_{24}F_8N_4O_4]^+$). Elemental analysis Calc. for $C_{46}H_{24}F_8N_4O_4$: C, 65.10; H, 2.85; N, 6.60. Found: C, 65.18; H, 2.87; N, 6.59. UV-vis (CH_2Cl_2, λ [nm], (ϵ [M^{-1} $cm^{-1}x10^3$]), 298K): 329 (9.02), 455 (7.78), 586 (2.98).^{1}H NMR (500 MHz, $CDCl_3$, δ [ppm], 298 K): 13.77 (br, 2H, Py-NH), 7.01-7.71 (m, 12H, Phenyl-CH), 6.58 (br, 2H, Pyrrole-β-CH), 6.09 (br, 2H, Pyrrole-β-CH), 2.78 (s, 6H, Methyl CH).

Synthesis of Compound **11**: Tripyrrane **5** (0.571 g, 1 mmol) and diol **2** (0.365 g, 1 mmol) were taken in a round bottom flask, to it 740 mL of dry CH_2Cl_2 was added and stirred for 15 minutes under nitrogen atmosphere to get a clear solution. *p*-Toluenesulfonic acid (0.035 g, 0.185 mmol) was added to the reaction mixture and stirred for 90 minutes under dark condition. After that, *p*-chloranil (0.367 g, 1.5 mmol) was added and the resulting mixture was refluxed for 90 minutes in open air. After complete removal of solvent from crude mixture by rotary evaporator, the compound was purified using basic alumina followed by repeated silica gel (200-400 mesh) column chromatography to obtain compound **11** as red solid. Yield. ~440 mg (~60%). R_f = 0.4 (CH_2Cl_2/ Hexane = 8:2). Mp > 350°C.

HR-ESI-TOF MS (*m/z*): 733.2585 $[M+H]^+$ (732.2512 calc. for $[C_{46}H_{32}F_4N_4O]^+$). Elemental analysis Calc. for $C_{46}H_{32}F_4N_4O$: C, 75.40; H, 4.40; N, 7.65. Found: C, 75.48; H, 4.47; N, 7.64. UV-vis (CH_2Cl_2, λ [nm], (ϵ [M^{-1} $cm^{-1}x10^3$]), 298K): 317 (22.23), 497 (22.25). ^{1}H NMR (500 MHz, $CDCl_3$, δ [ppm], 298 K): 8.71 (s, 1H, βH-N-Me-pyrrole), 8.66 (br, 1H, Pyrrole- NH), 7.23-7.50 (m, 12H, Phenyl-H), 7.07 (s, 1H, N-Me-Pyrrole-βH), 6.85-6.99 (m, 4H, Phenyl-H), 6.73 (d, 1H, J = 4 Hz, Pyrrole-βH), 6.52 (s, 1H, N-Me Pyrrole- αH), 6.11 (d, 1H, J = 4.5 Hz, Pyrrole-βH), 5.90 (m, 1H, Pyrrole-βH), 5.62 (s, 1H, *meso*-H), 5.52 (m, 1H, Pyrrole-βH), 5.35 (s, 1H, *meso*-H), 3.26 (s, 3H, N-methyl CH), 2.62 (s, 3H, N-methyl CH).^{13}C NMR (125 MHz, $CDCl_3$, δ[ppm]): 170.97, 166.47, 162.3, 160.3, 152.4, 152.30, 148.9, 142.80, 140.4, 140.2, 139.91,137.41, 137.36, 137.00, 135.69, 134.16, 133.86, 132.69, 132.56, 131.7, 131.51, 129.4, 128.9, 128.73, 127.5, 127.3, 126.1, 125.99, 123.52, 115.59, 111.7, 107.89, 107.42, 43.26, 40.95, 34.53, 31.92.

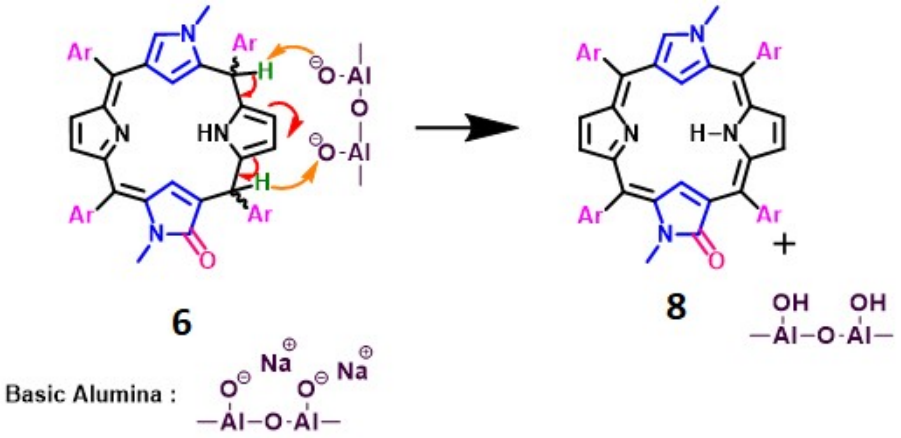

Scheme S2:Proposed mechanism for the formation of **8** from **6** [11-12]

References:

11. G. H. Posner, Organic Reactions at Alumina Surfaces, *Angew. Chem. Int. Ed. Engl.,* 1978, **17**, 487-496.

12. D.H. Burns, Y. H. Li, D. C. Shi and M. O. Delaney, C–H Bond activation by alumina: facile hydroxylation of chlorins at their saturated b-carbon by molecular oxygen and alumina, *Chem. Commun*, 1998, 1677.and references therein,

2. Supplementary Data:

2.1 Mass Spectra

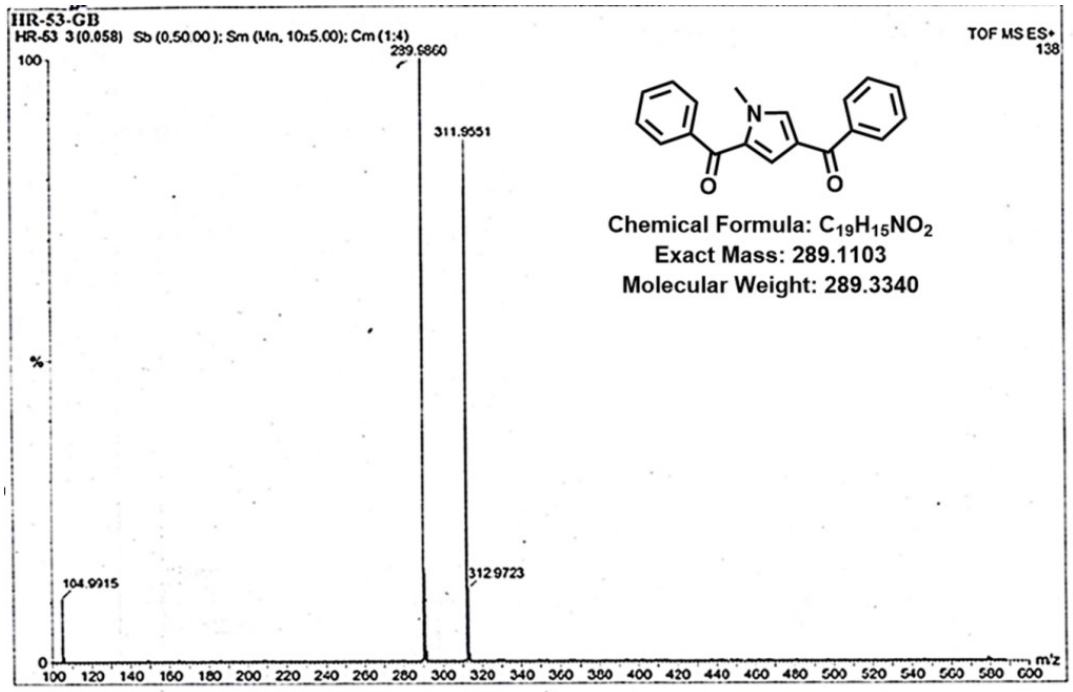

Fig. S1 HRMS Spectra of **1**

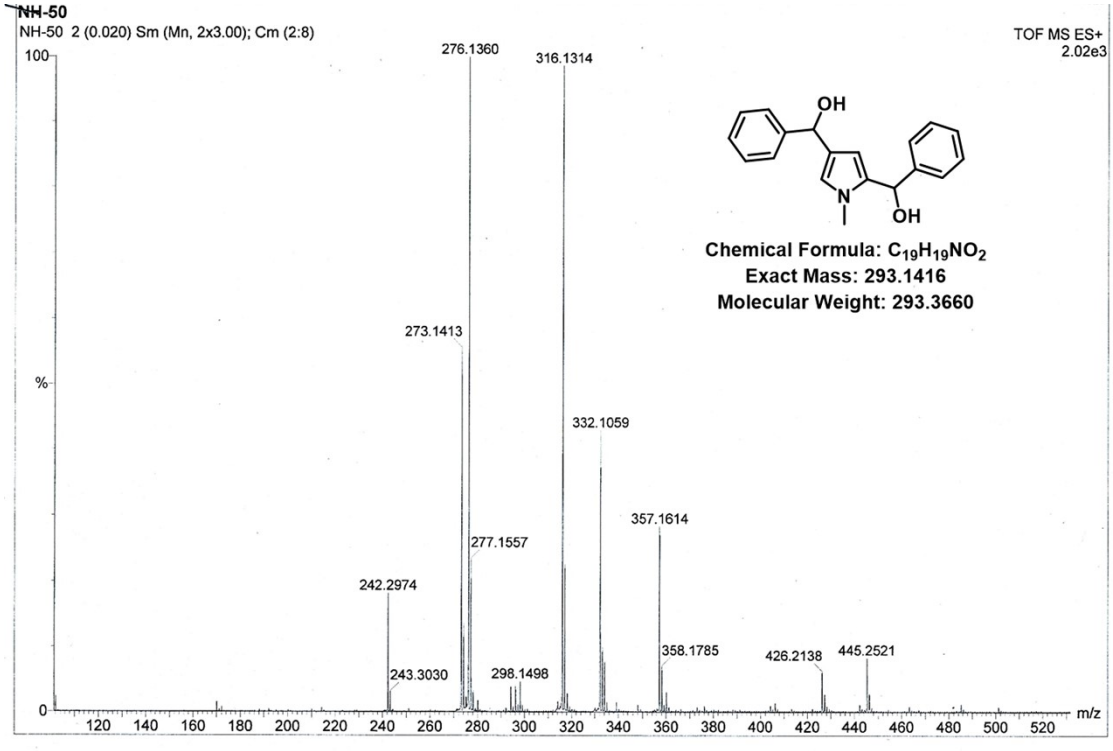

Fig. S2 HRMS Spectra of **2**

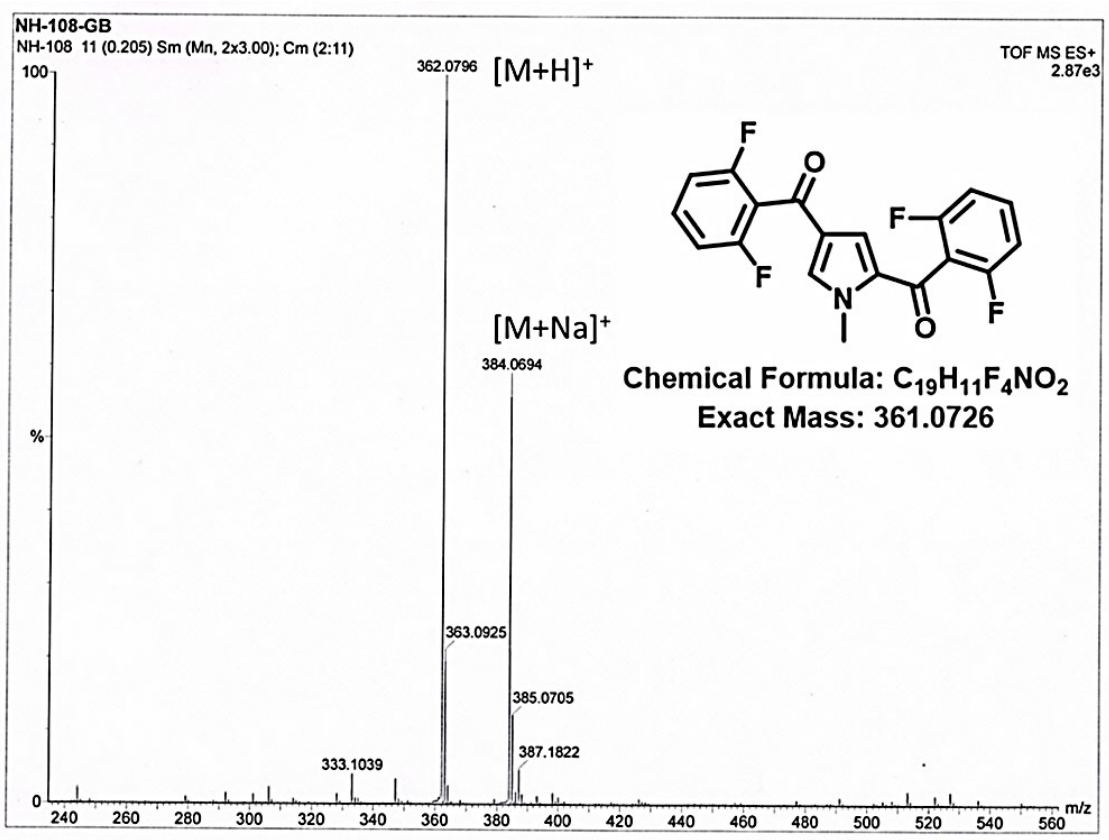

Fig. S3 HRMS Spectra of **3**

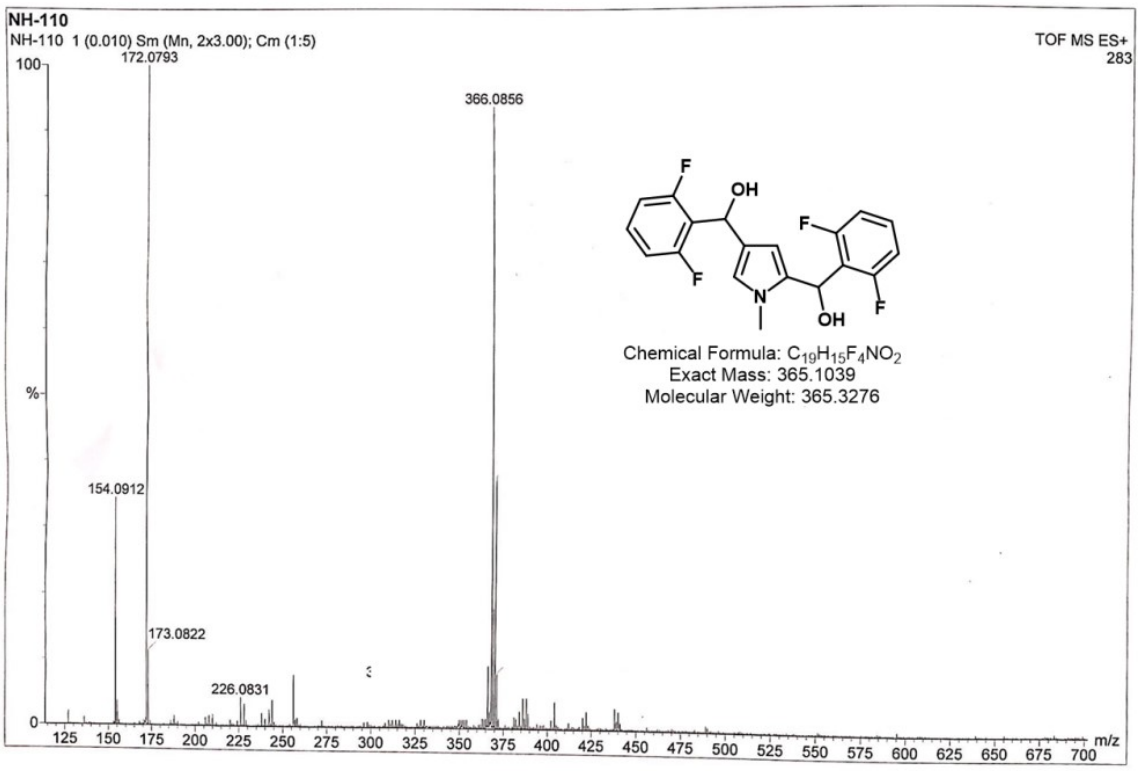

Fig. S4 HRMS Spectra of **4**

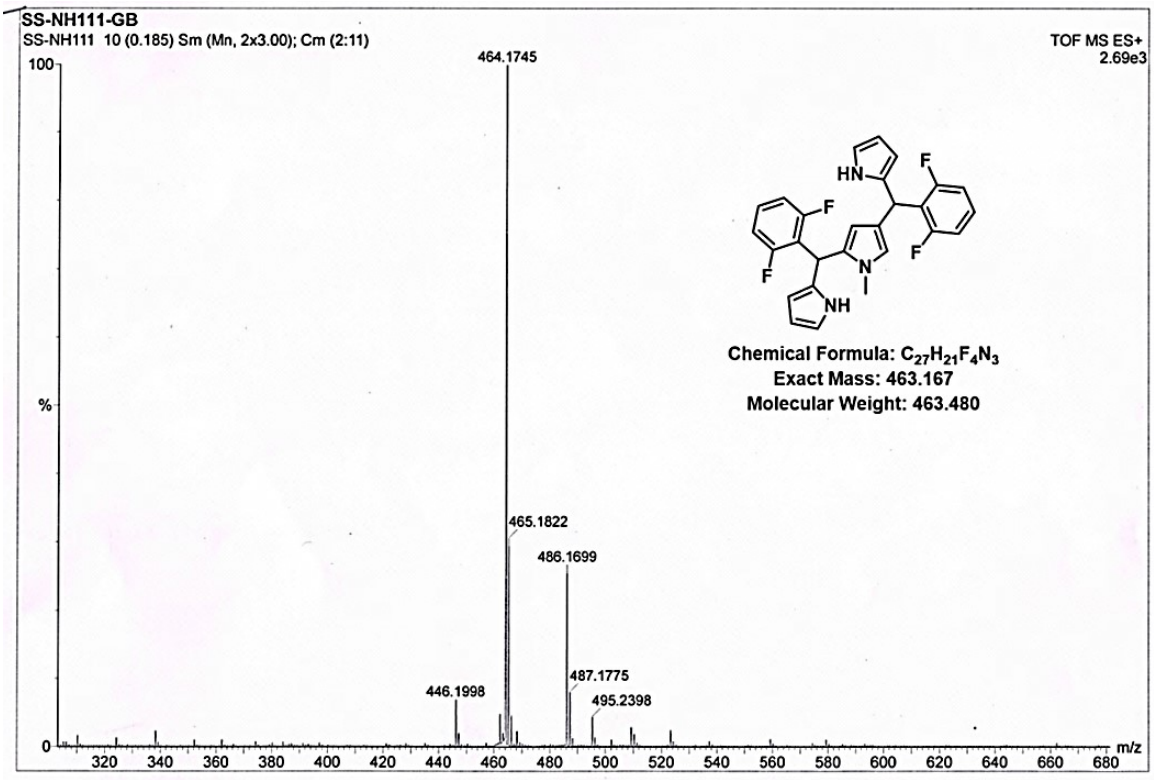

Fig. S5 HRMS Spectra of **5**

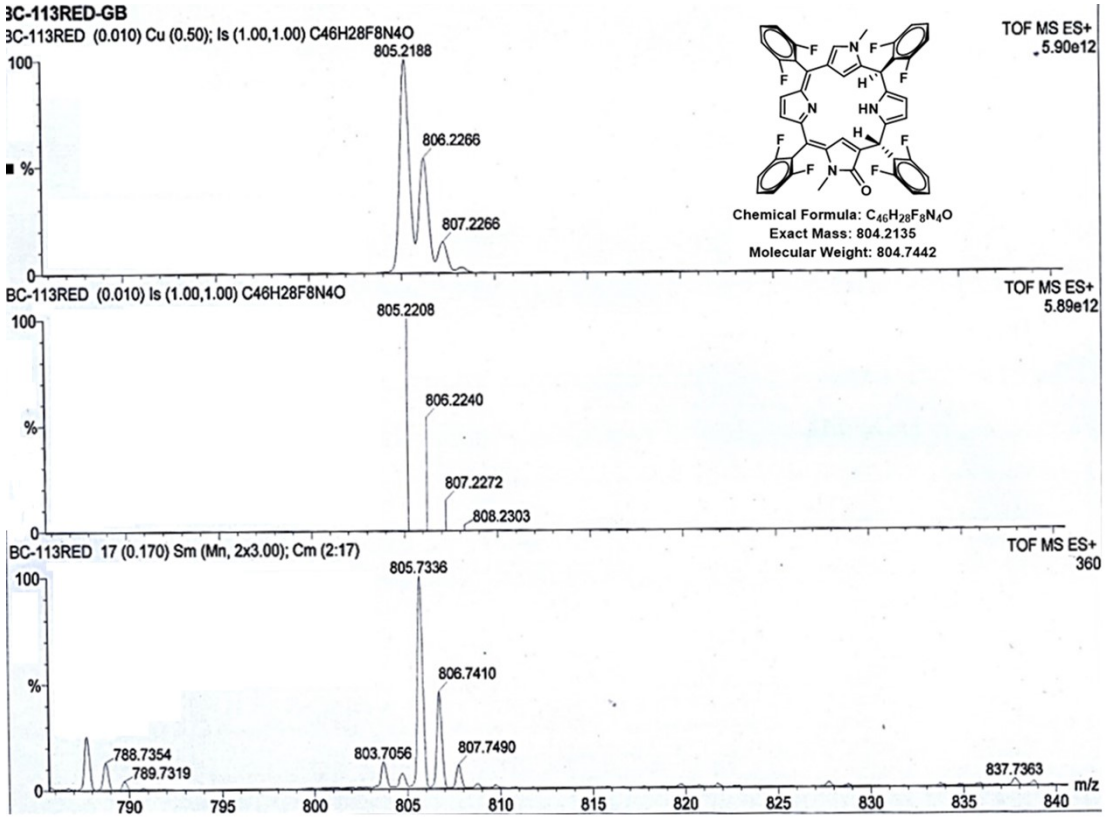

Fig. S6 HRMS Spectra of **6**

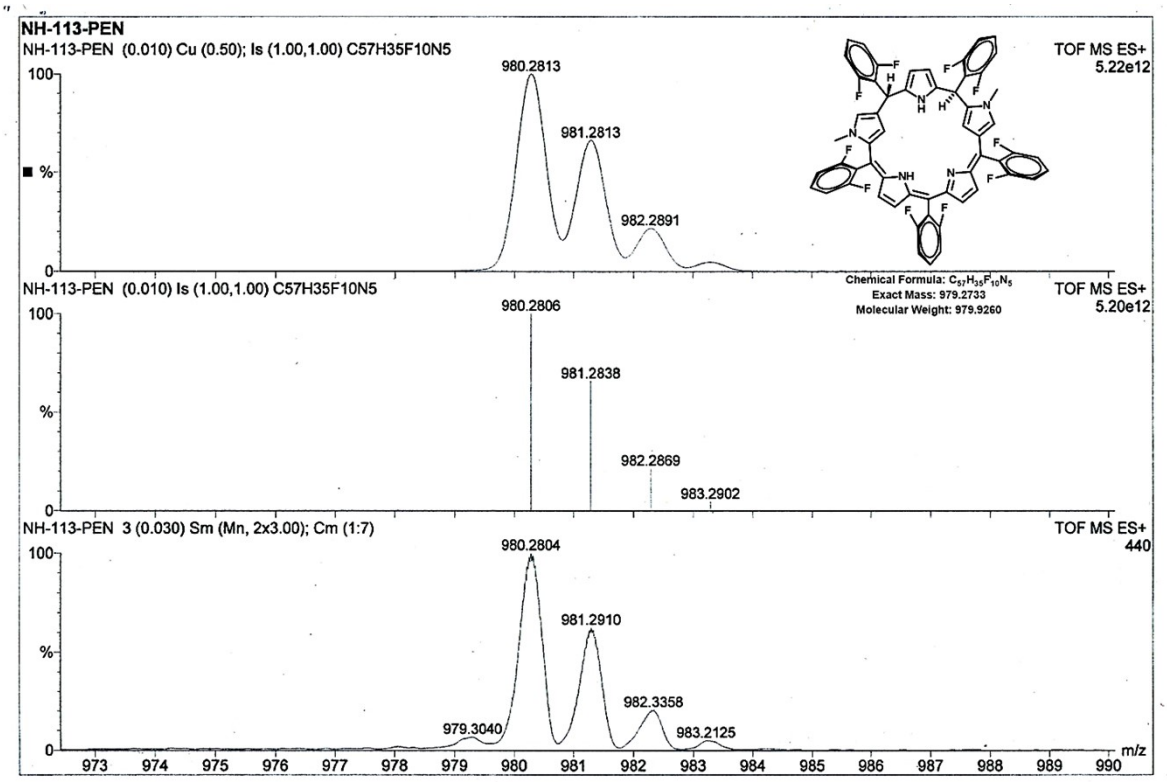

Fig. S7 HRMS Spectra of **7**

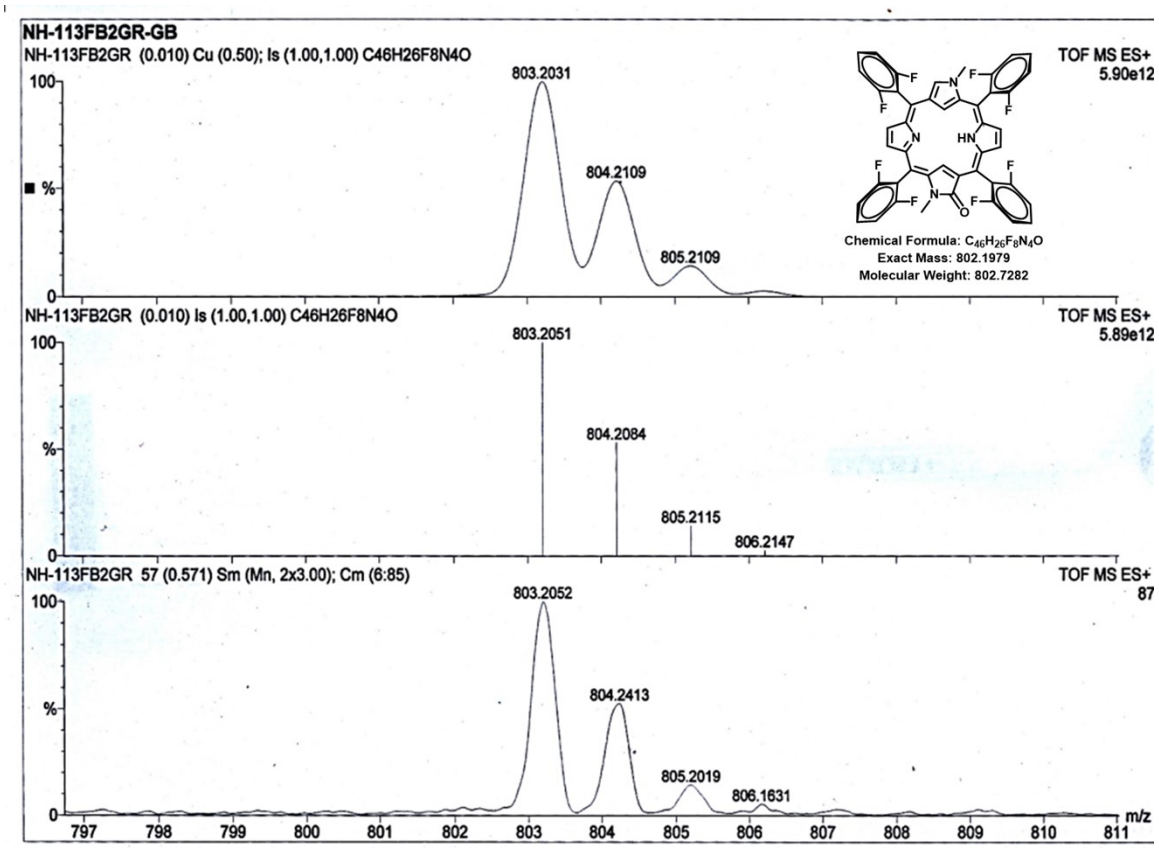

Fig. S8 HRMS Spectra of **8**

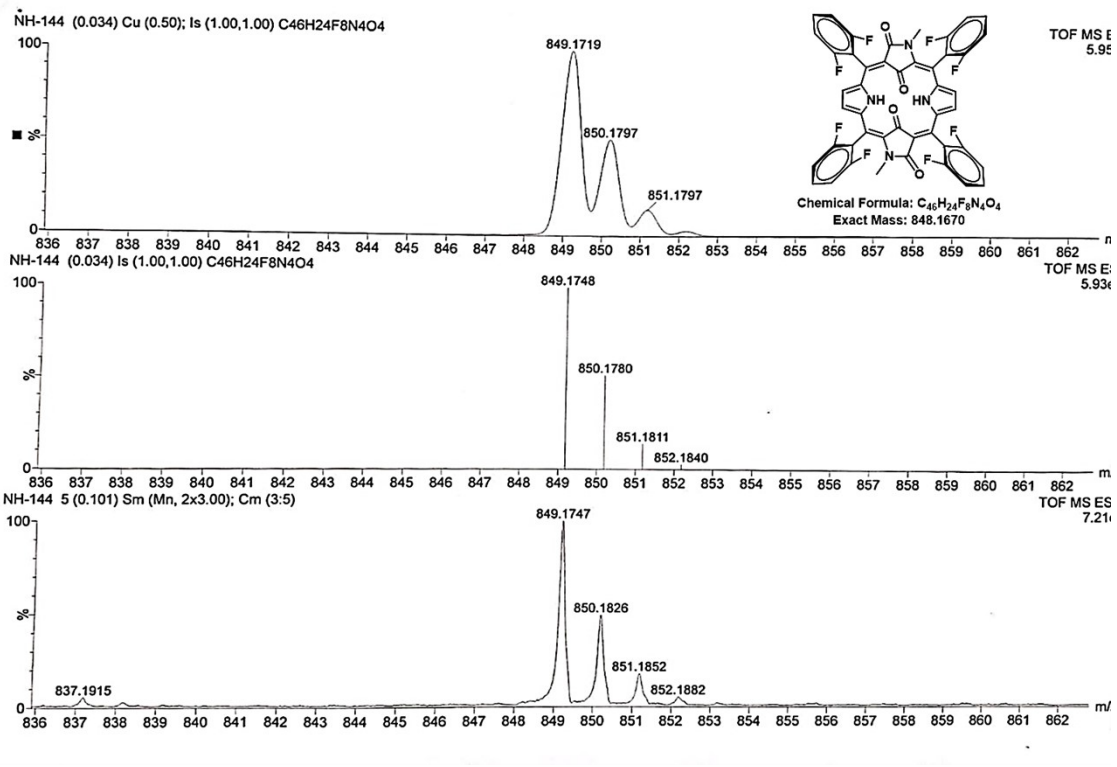

Fig. S9 HRMS Spectra of **10**

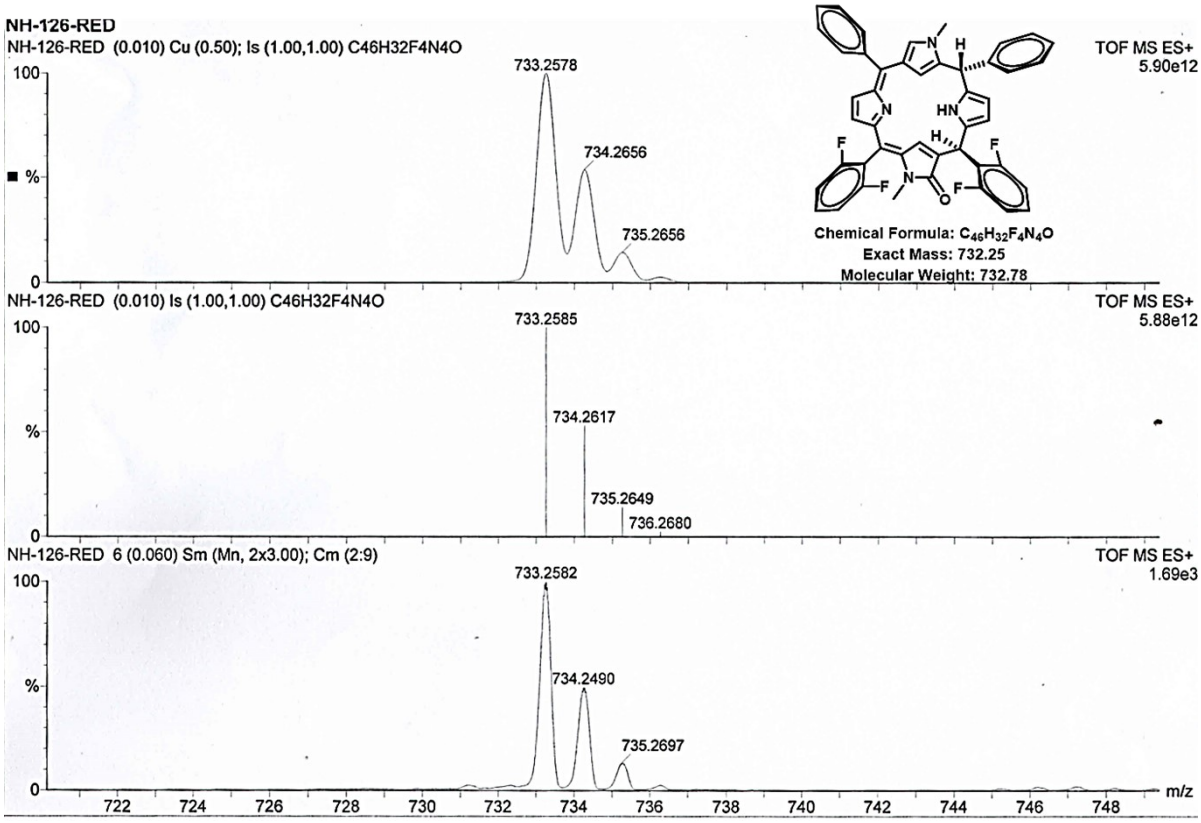

Fig. S10 HRMS Spectra of **11**

2.2 UV-vis spectra:

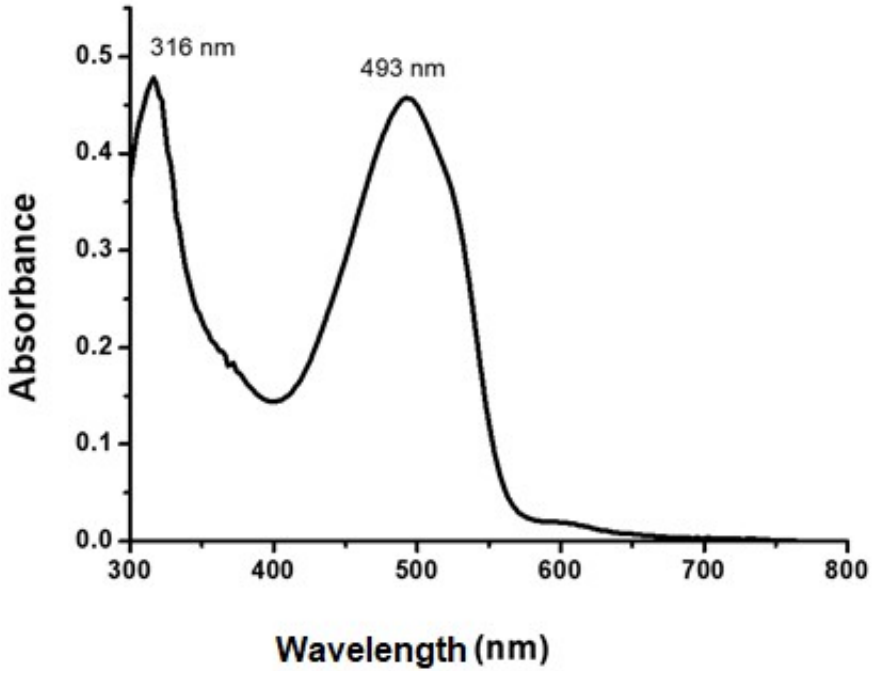

Fig. S11 UV-vis Spectrum of **6**

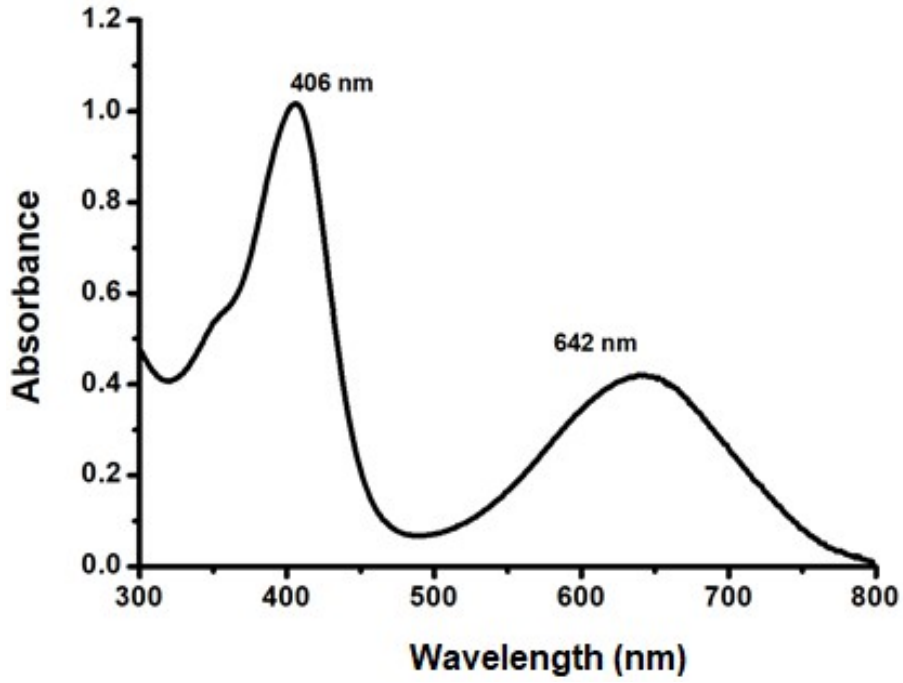

Fig. S12 UV-vis Spectrum of **7**

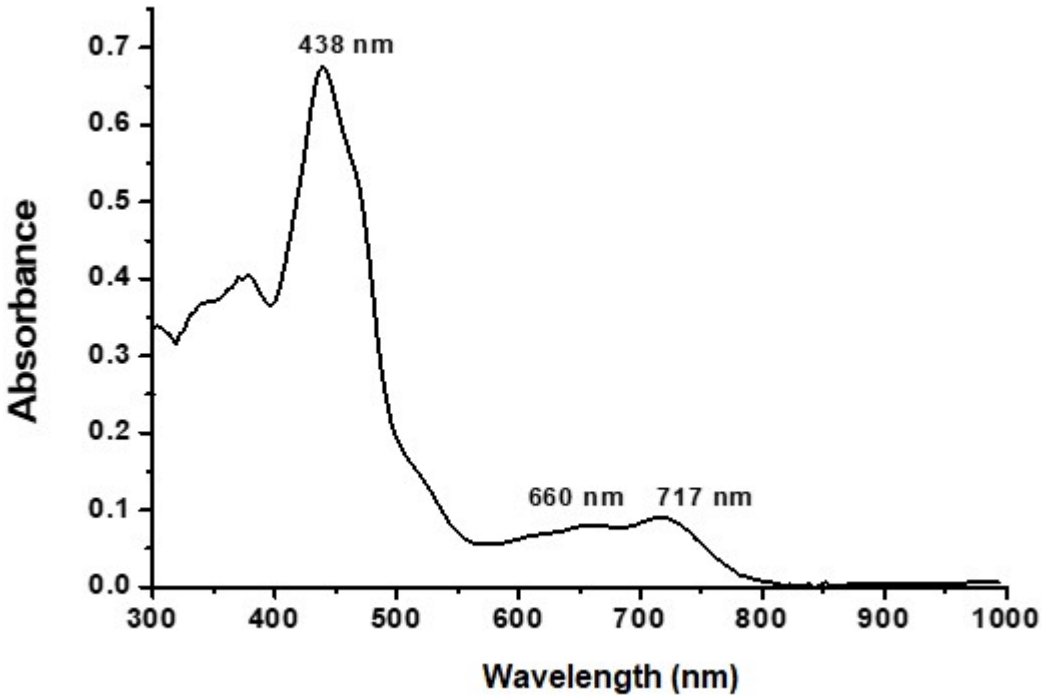

Fig. S13 UV-vis Spectrum of **8**

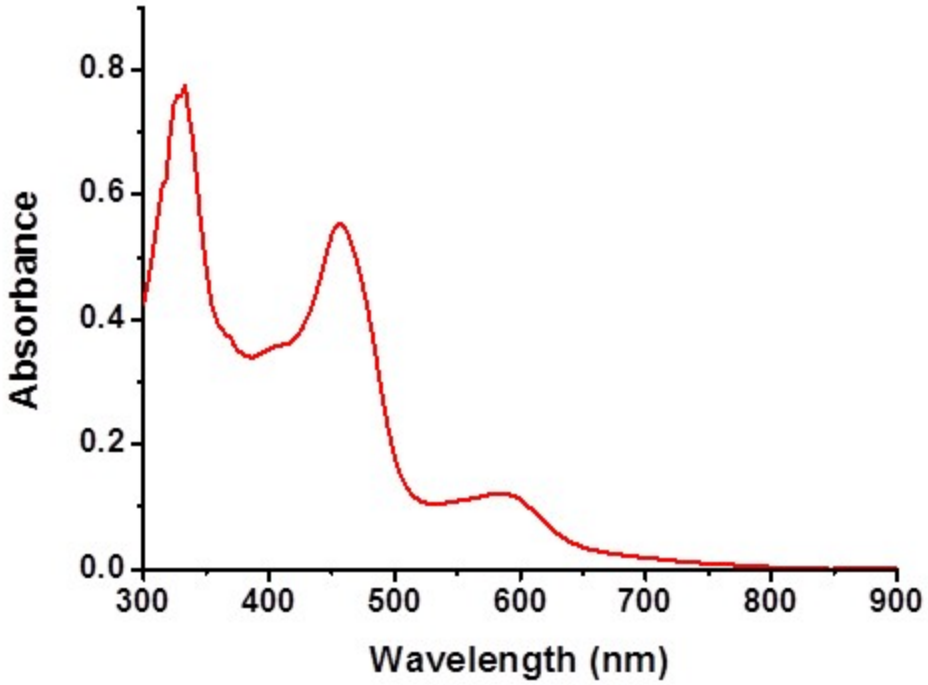

Fig. S14 UV-vis Spectrum of **10**

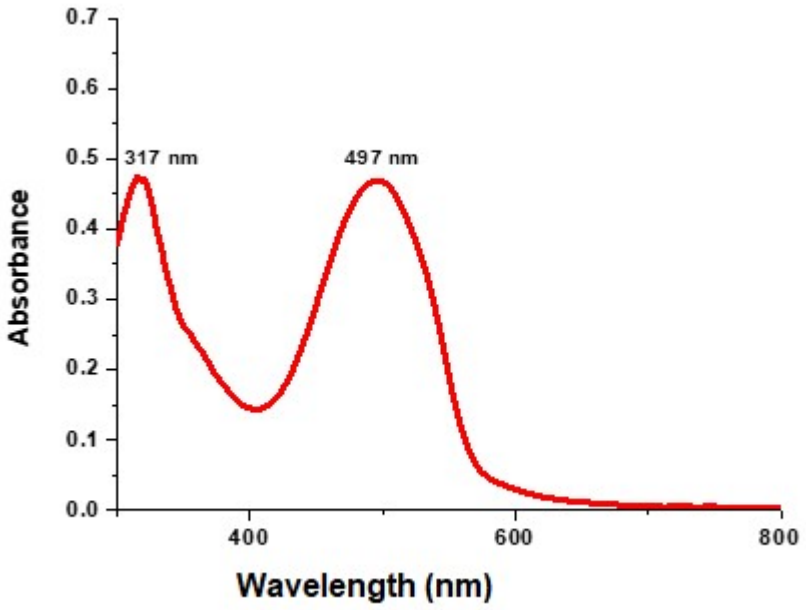

Fig. S15 UV-vis Spectrum of **11**

2.3 IR spectra:

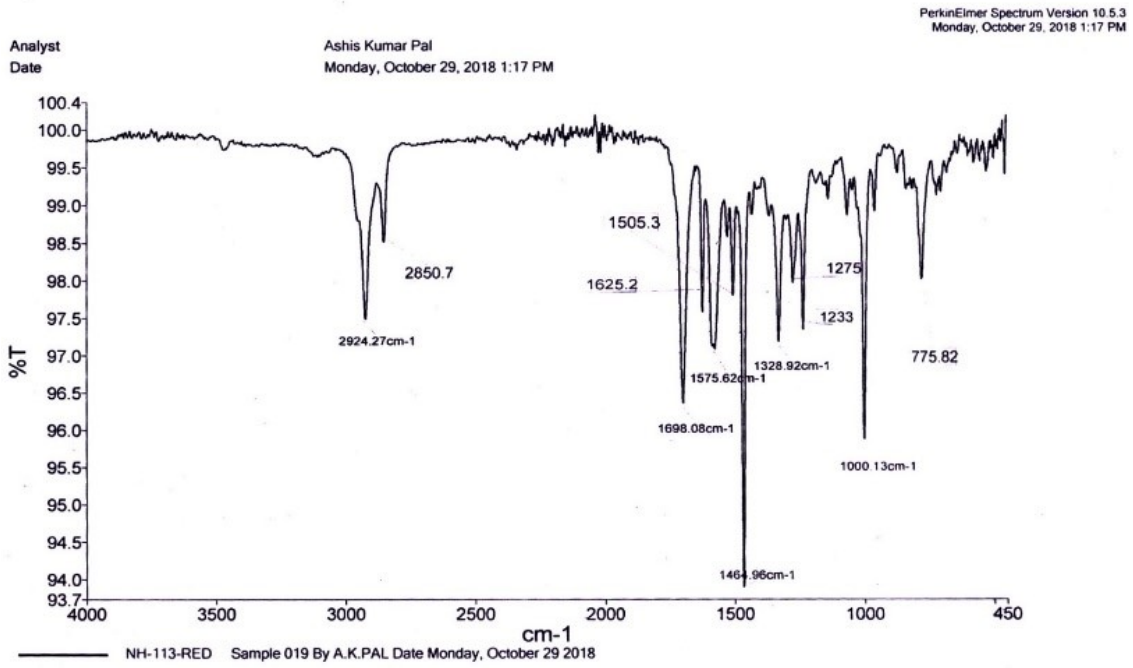

Fig. S16 IR Spectrum of **6**

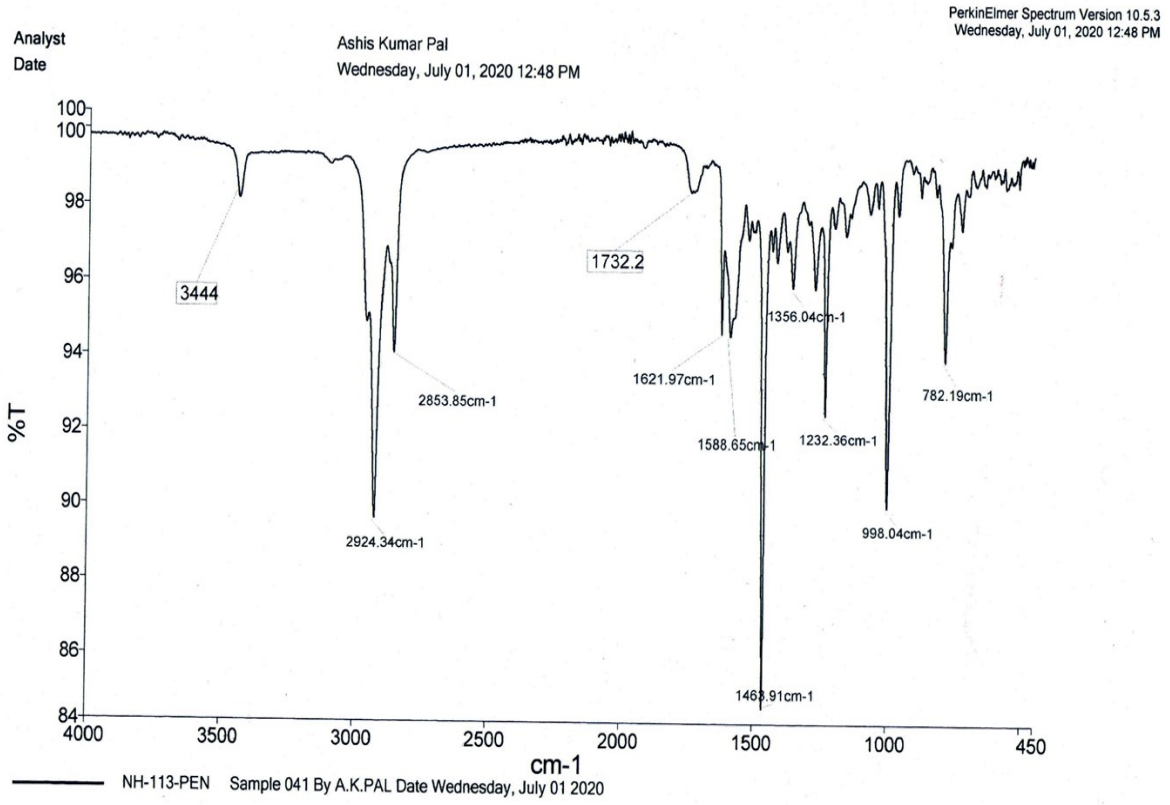

Fig. S17 IR Spectrum of **7**

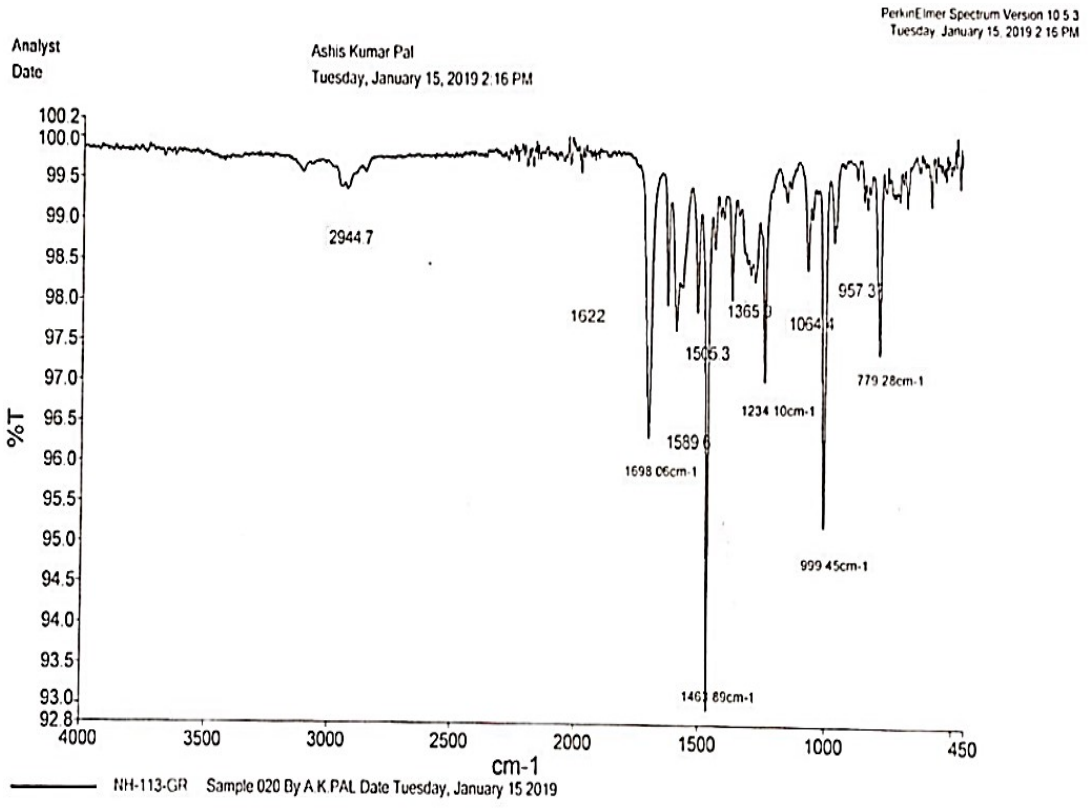

Fig. S18 IR Spectrum of **8**

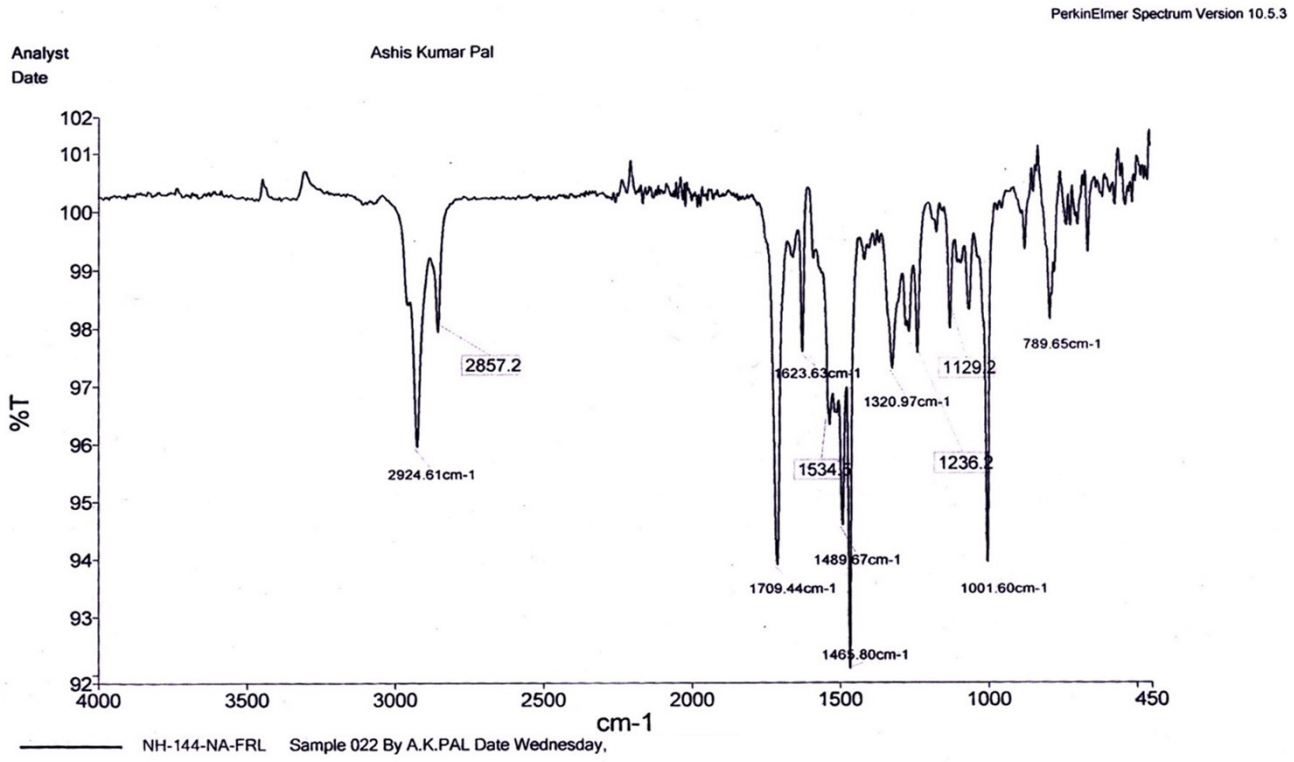

Fig. S19 IR Spectrum of **10**

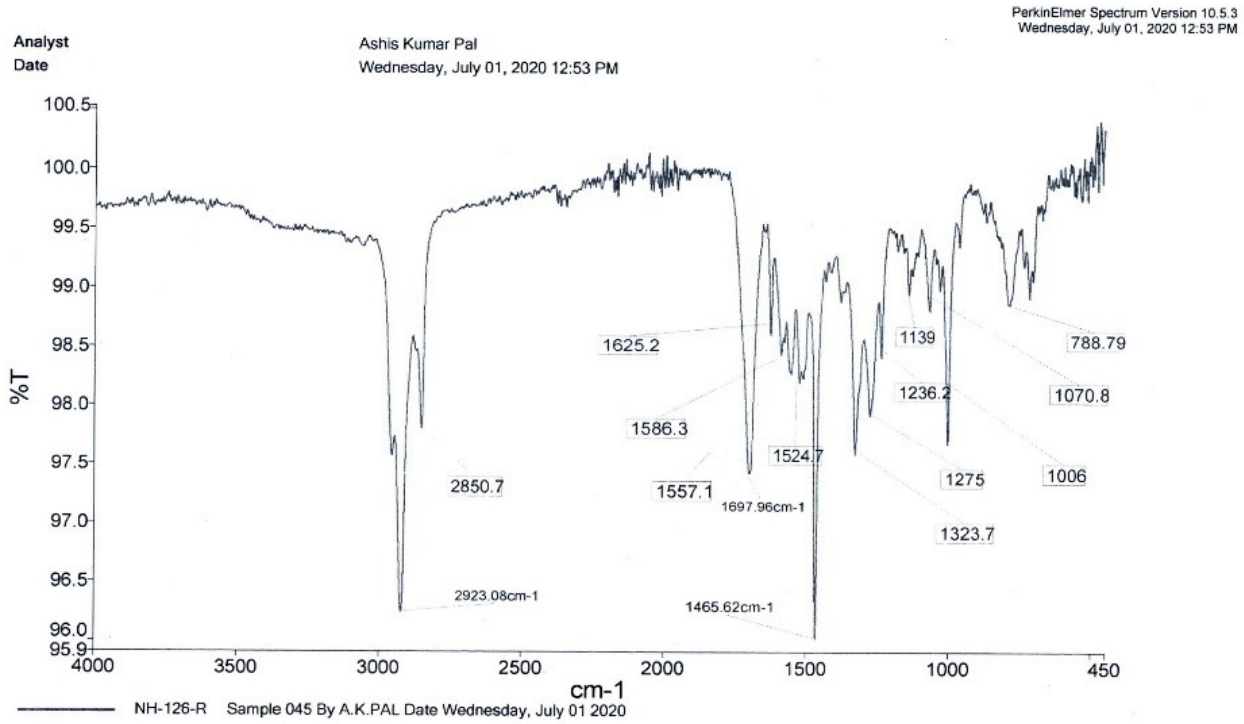

Fig. S20 IR Spectrum of **11**

2.4 NMR spectra:

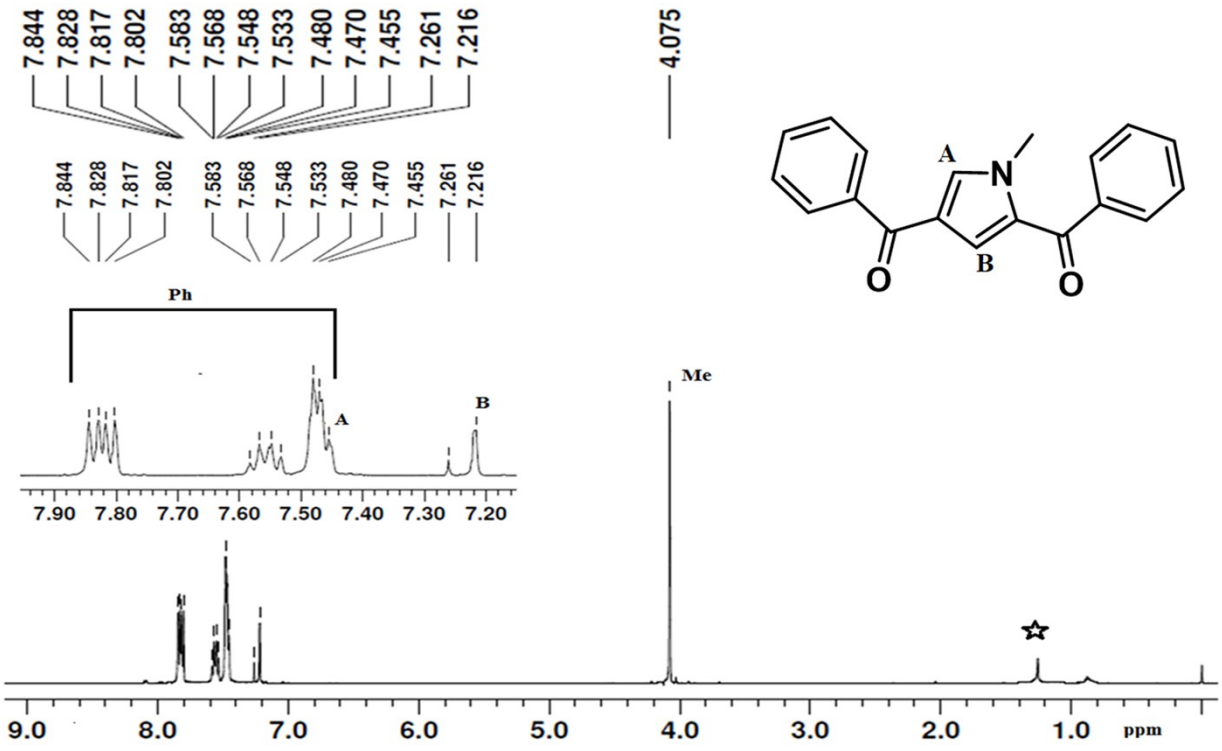

Fig. S21 ^{1}H NMR spectra of **1** in $CDCl_3$ at 298 K

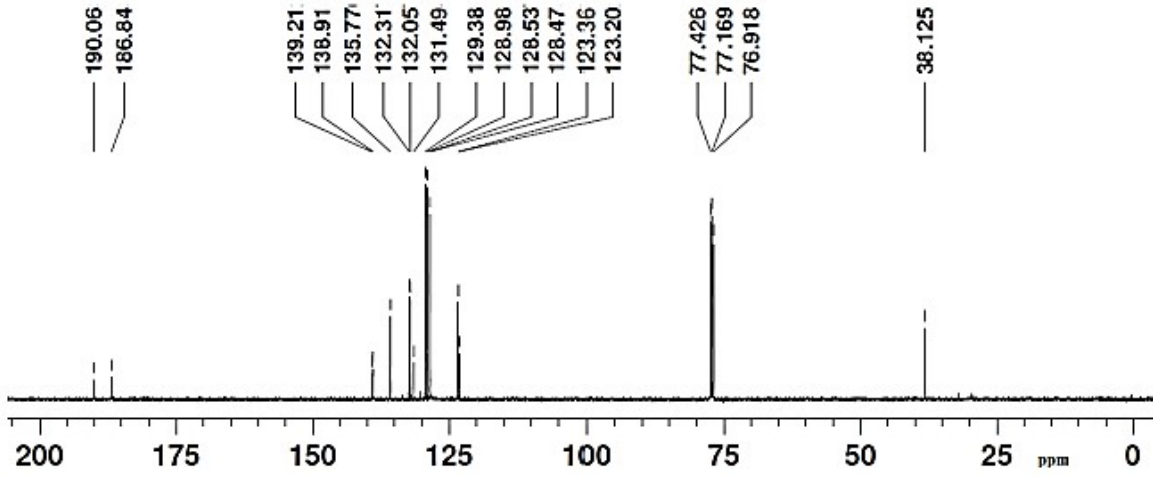

Fig. S22 ^{13}C NMR spectra of **1** in $CDCl_3$ at 298 K

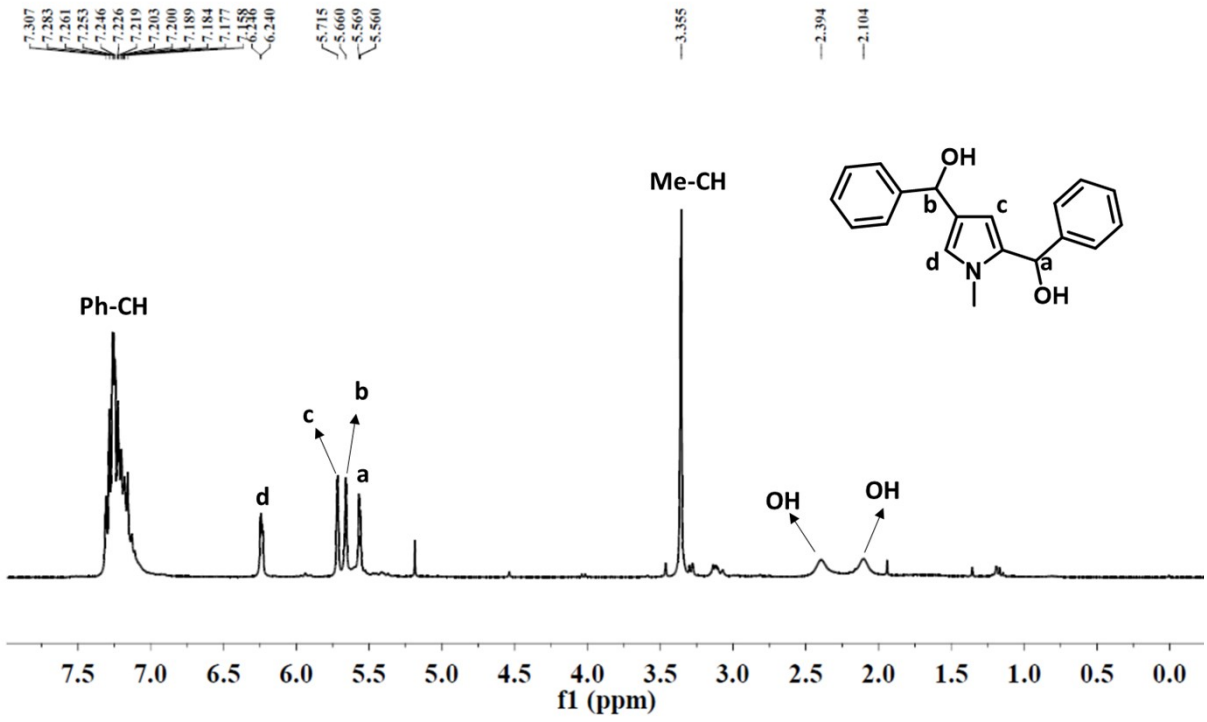

Fig. S23 ^{1}H NMR spectra of **2** in $CDCl_3$ at 298 K

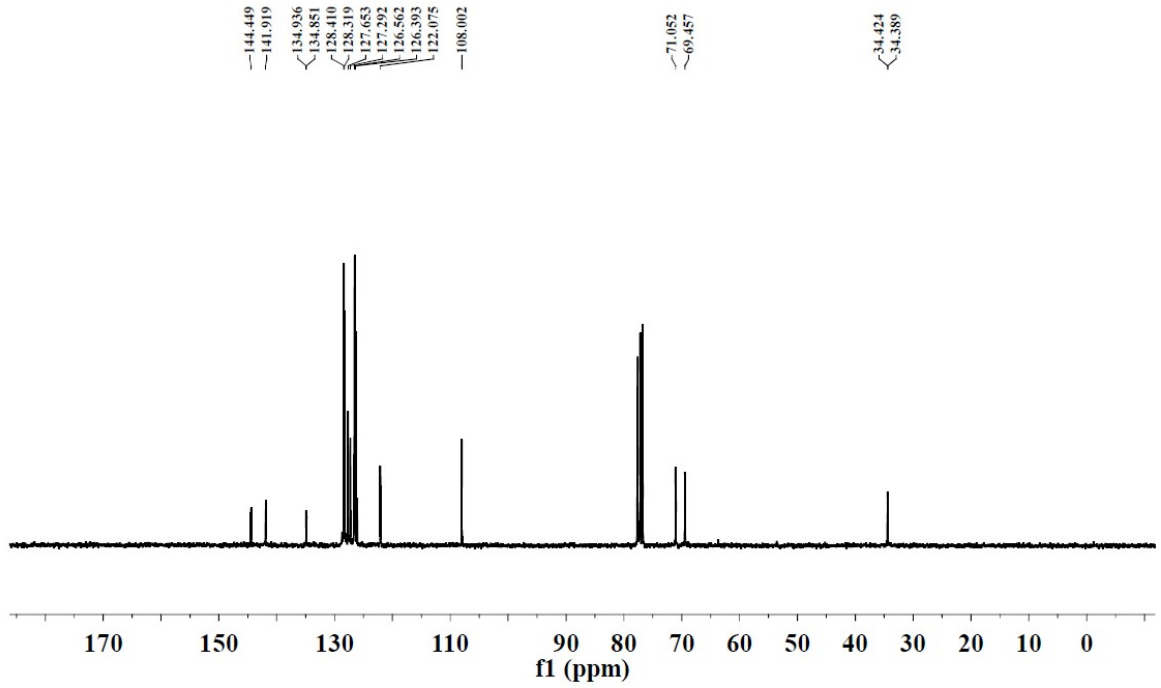

Fig. S24 ^{13}C NMR spectra of **2** in $CDCl_3$ at 298 K

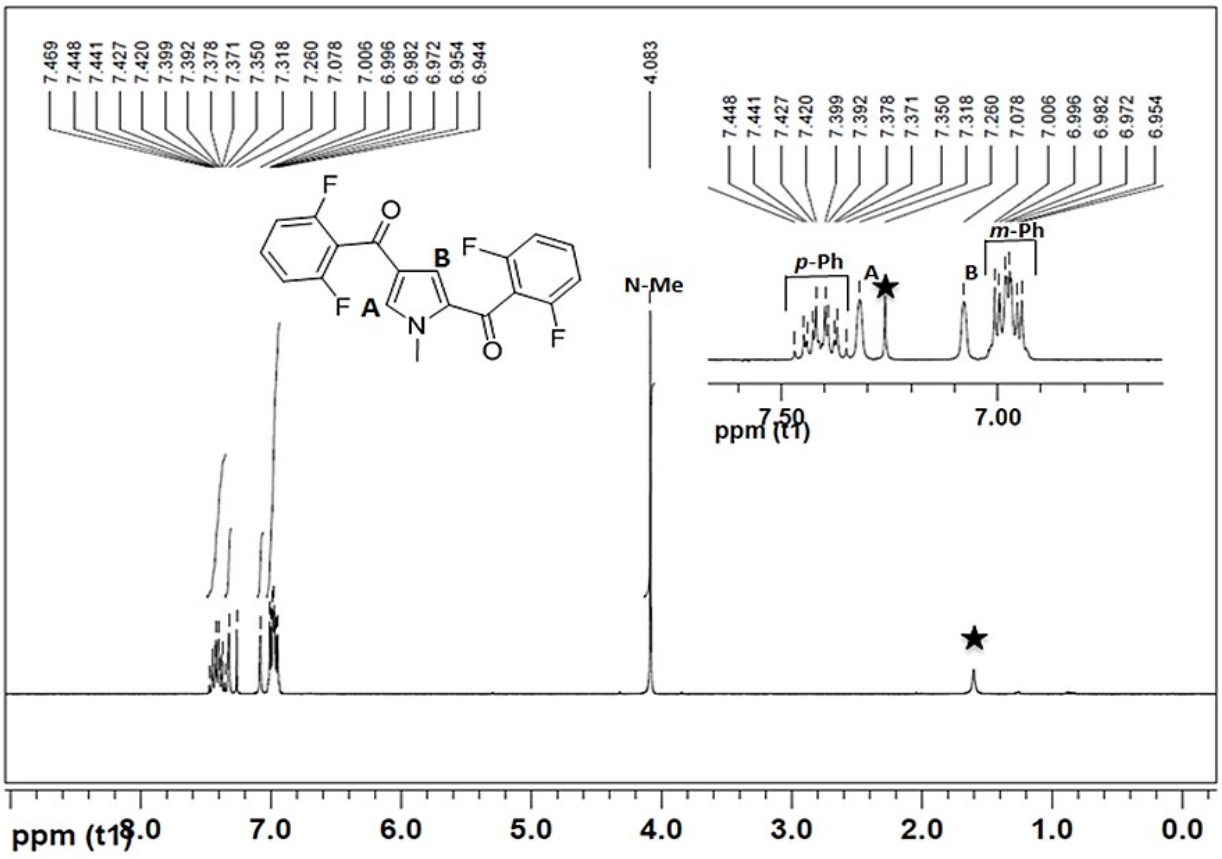

Fig. S25 ^{1}H NMR spectra of **3** in $CDCl_3$ at 298 K

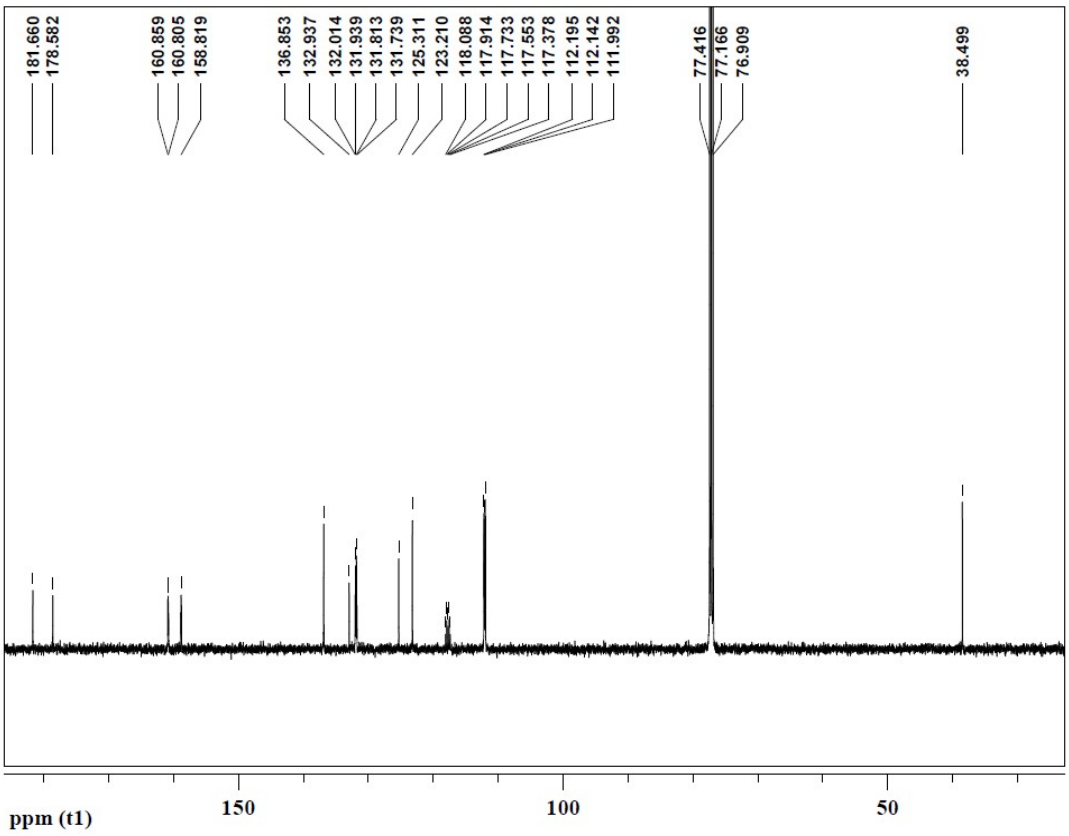

Fig. S26 ^{13}C NMR spectra of **3** in $CDCl_3$ at 298 K

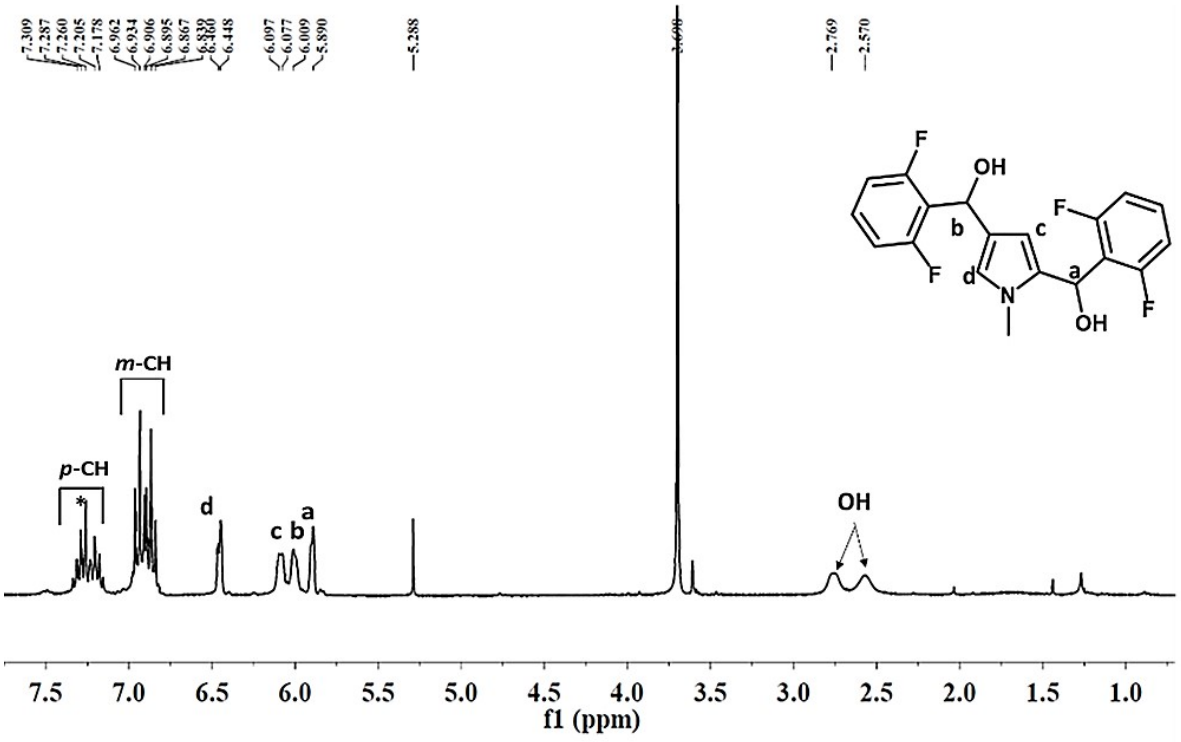

Fig. S27 ^{1}H NMR spectra of **4** in $CDCl_3$ at 298 K

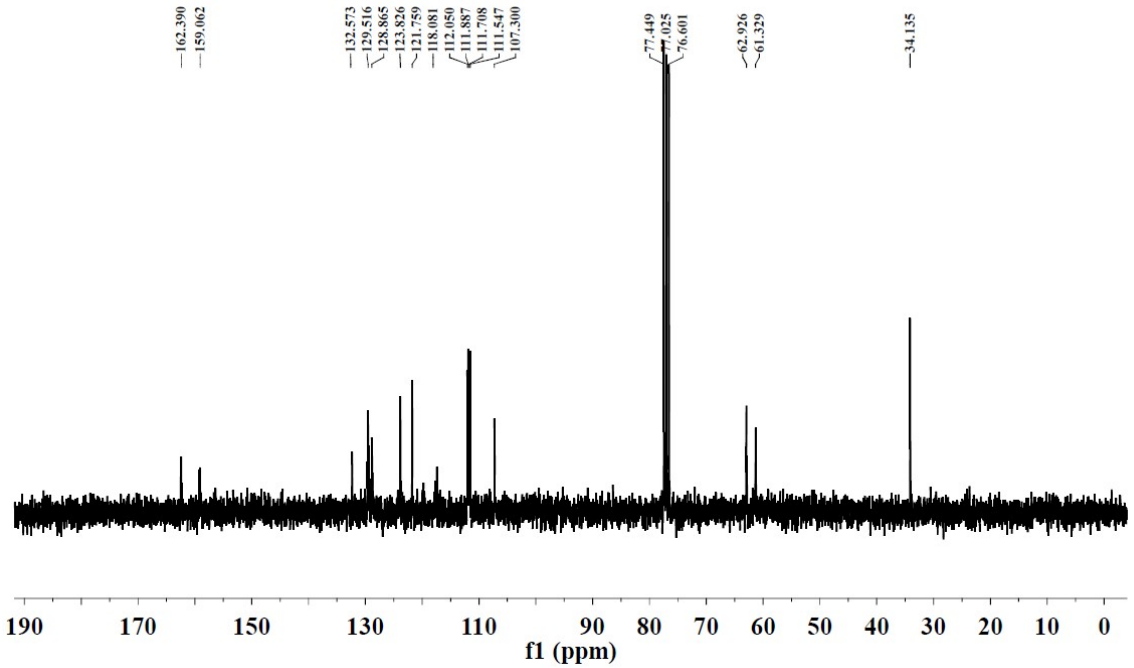

Fig. S28 ^{13}C NMR spectra of **4** in $CDCl_3$ at 298 K

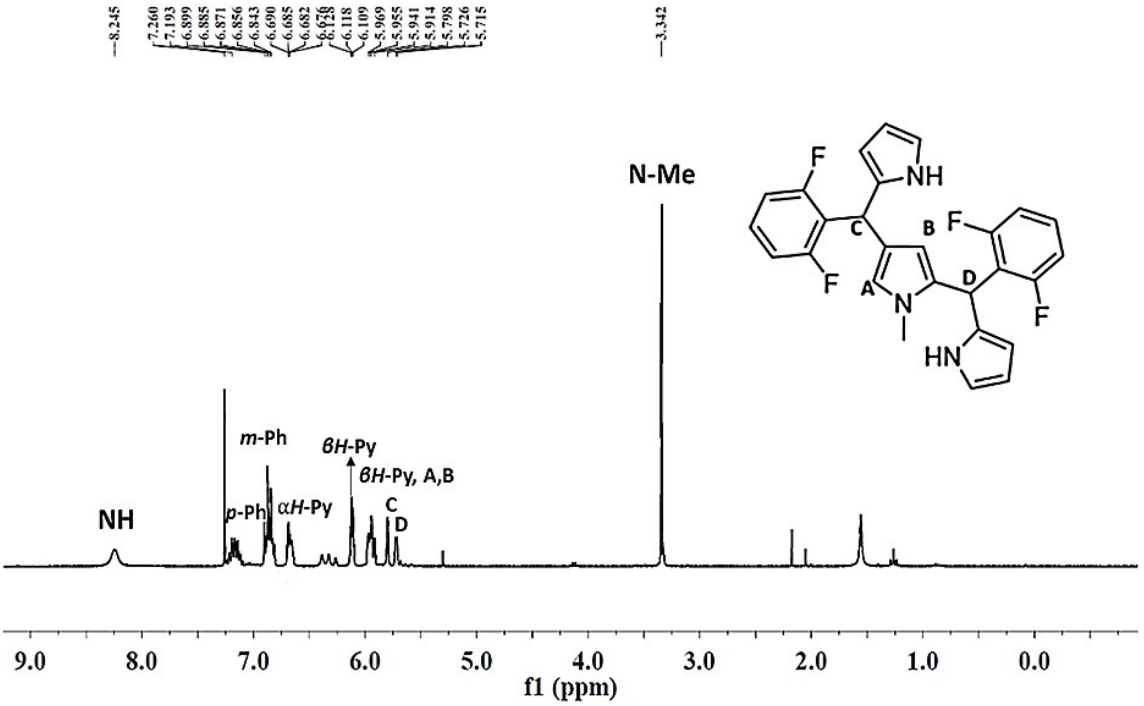

Fig. S29 ^{1}H NMR spectra of **5** in $CDCl_3$ at 298 K

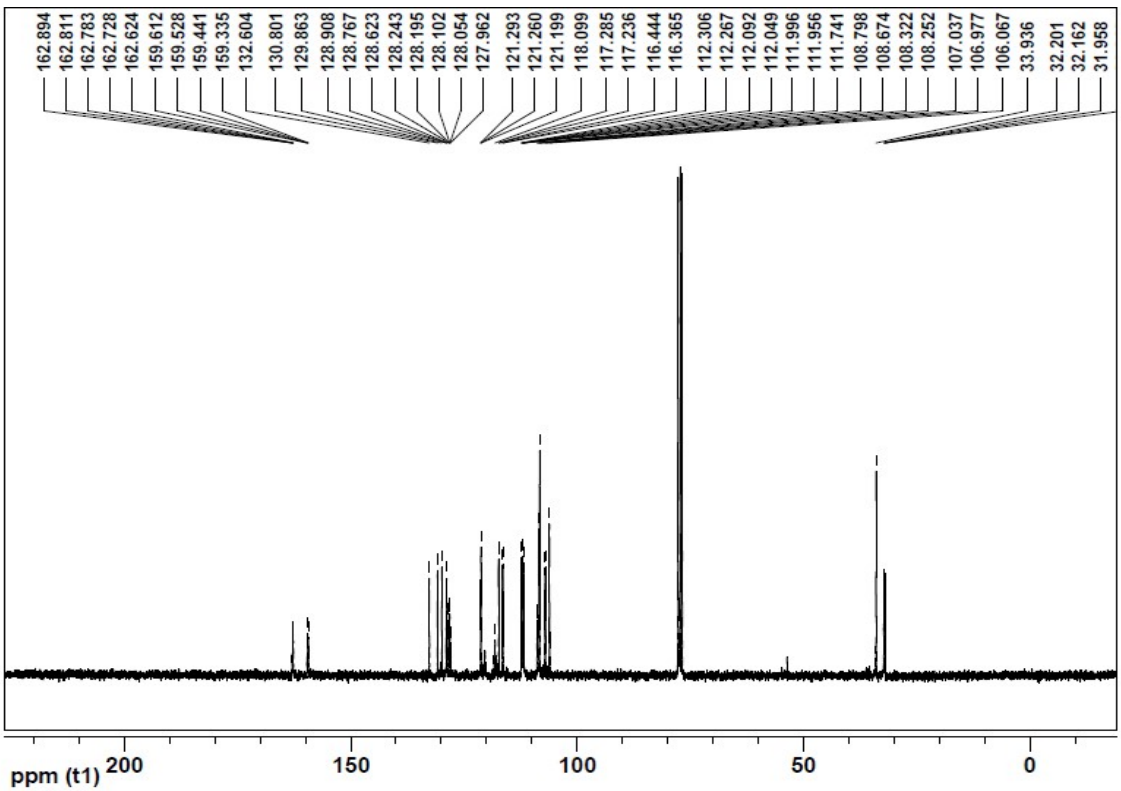

Fig.S30 ^{13}C NMR spectra of **5** in $CDCl_3$ at 298 K

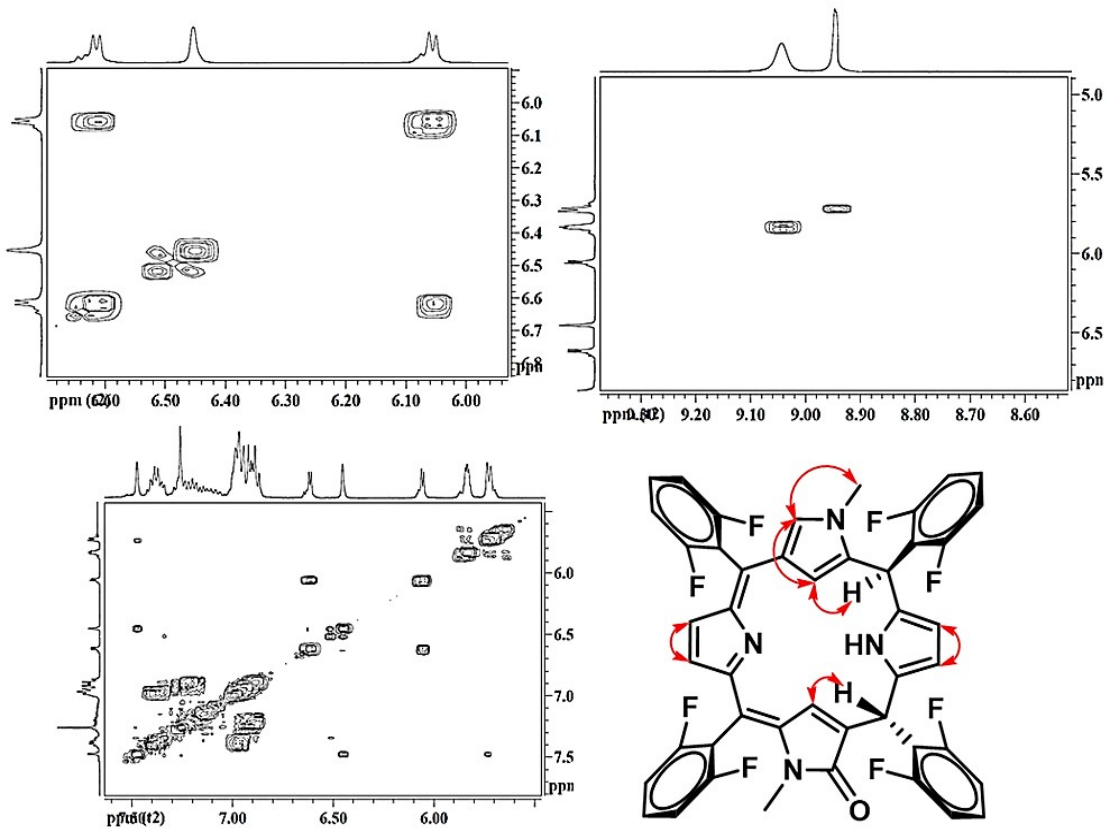

Fig. S31 ^{1}H- ^{1}H 2D COSY NMR spectra of **6** in $CDCl_3$ at 298 K

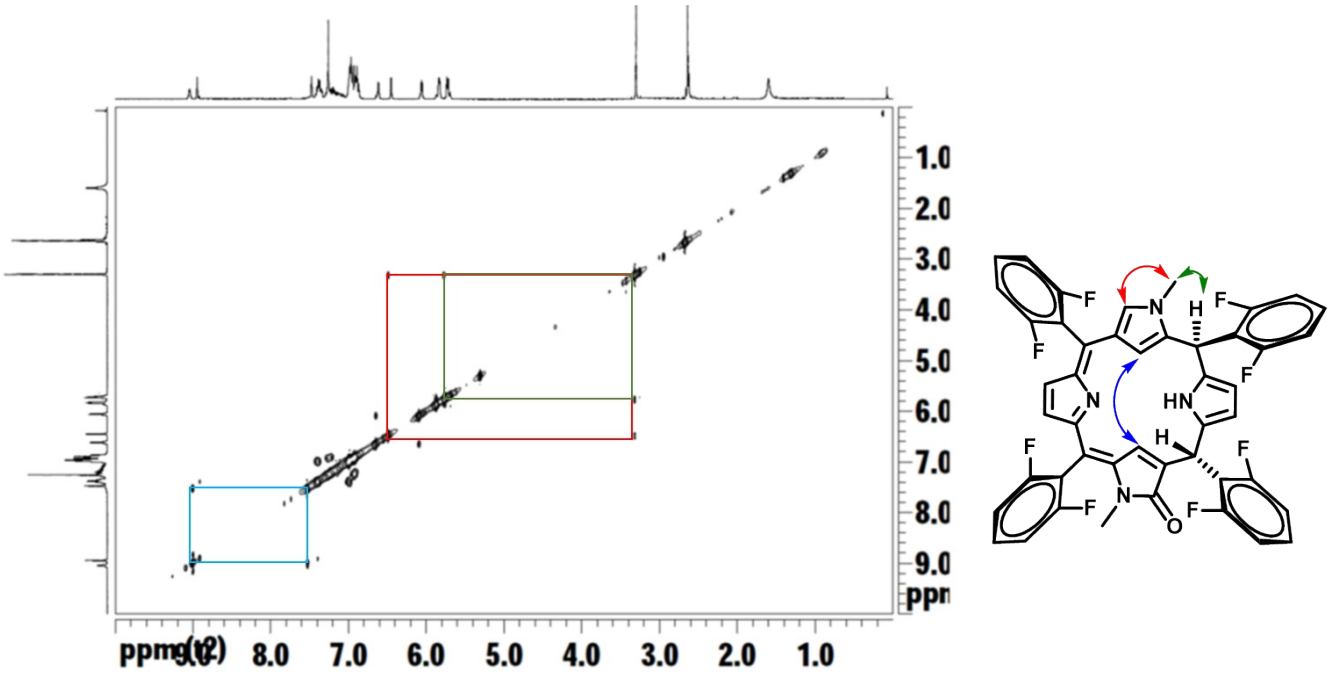

Fig. S32 ^{1}H- ^{1}H 2D ROESY NMR spectrum of **6** in $CDCl_3$ at 298 K

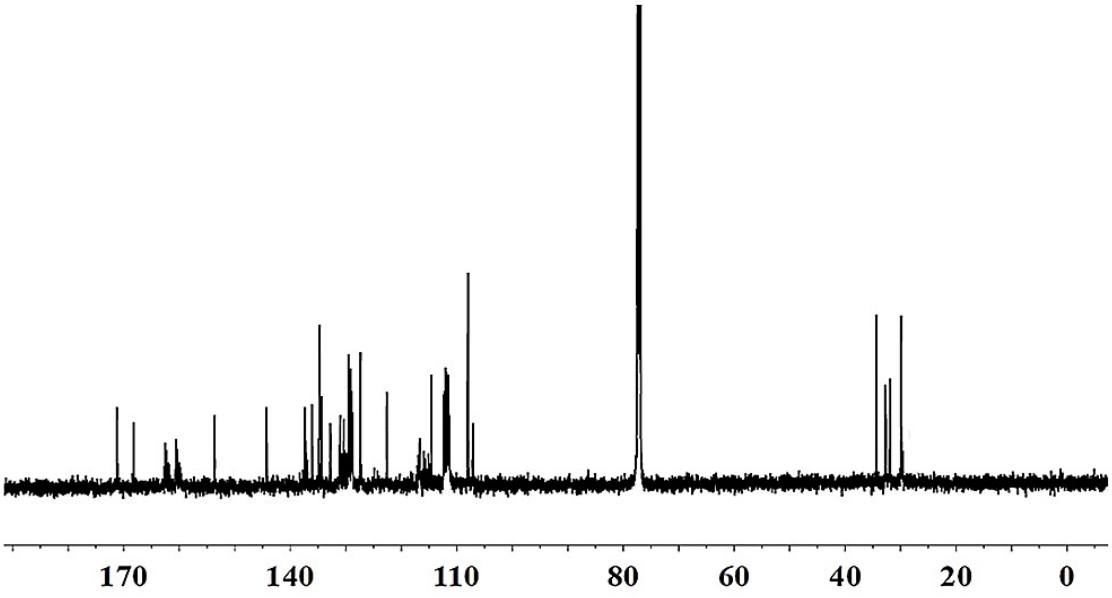

Fig. S33 ^{13}C NMR spectra of **6** in $CDCl_3$ at 298 K

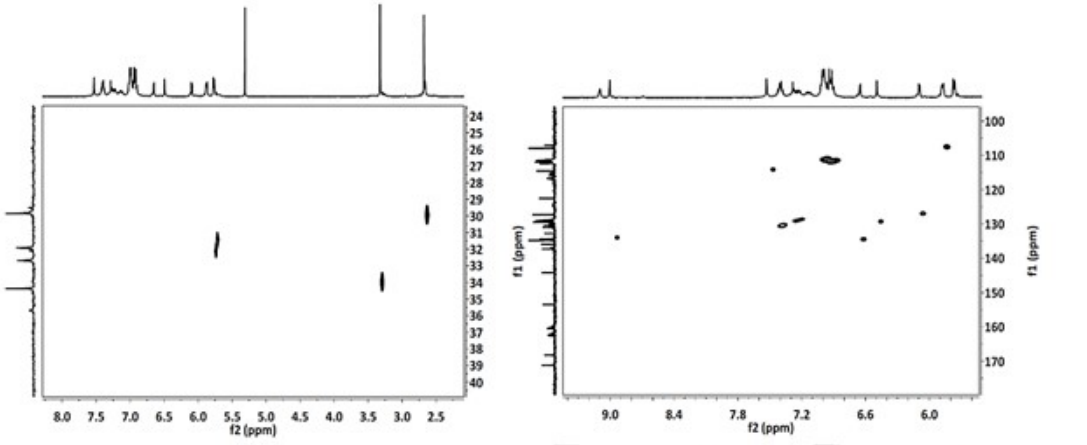

^{1}H	ppm	^{13}C	ppm	^{1}H	ppm	^{13}C	ppm
a	6.45	1	129.07	g	6.05	18	127.30
b	7.47	3	114.57	h	5.71	5	31.92
c,d	5.83	7,8	107.85	i	5.73	10	32.68
e	8.94	13	134.38	j	3.30	22	34.37
f	6.61	17	134.75	k	2.63	21	29.85
NH	9.04						

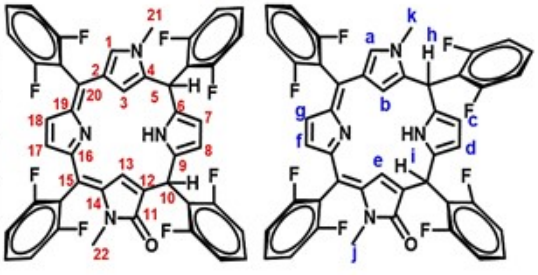

Fig. S34 HSQC NMR spectra of **6** in $CDCl_3$ at 298 K

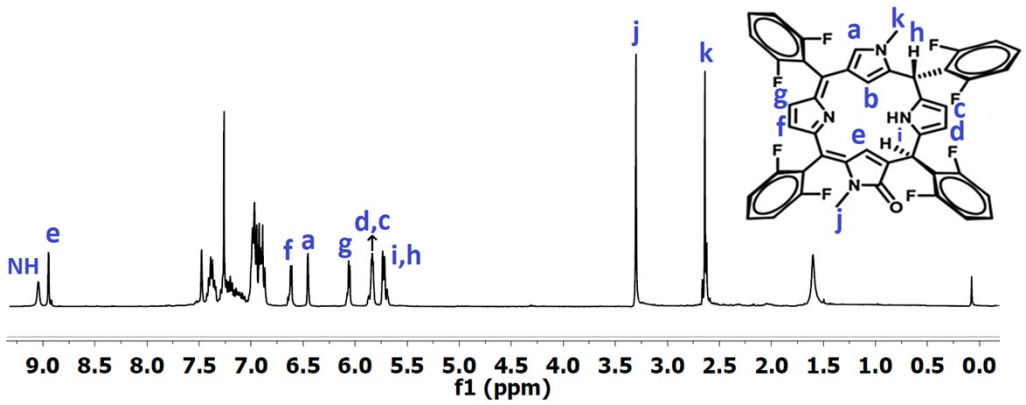

Fig. S35 Completely assigned ^{1}H NMR spectrum of **6** in $CDCl_3$ at 298 K

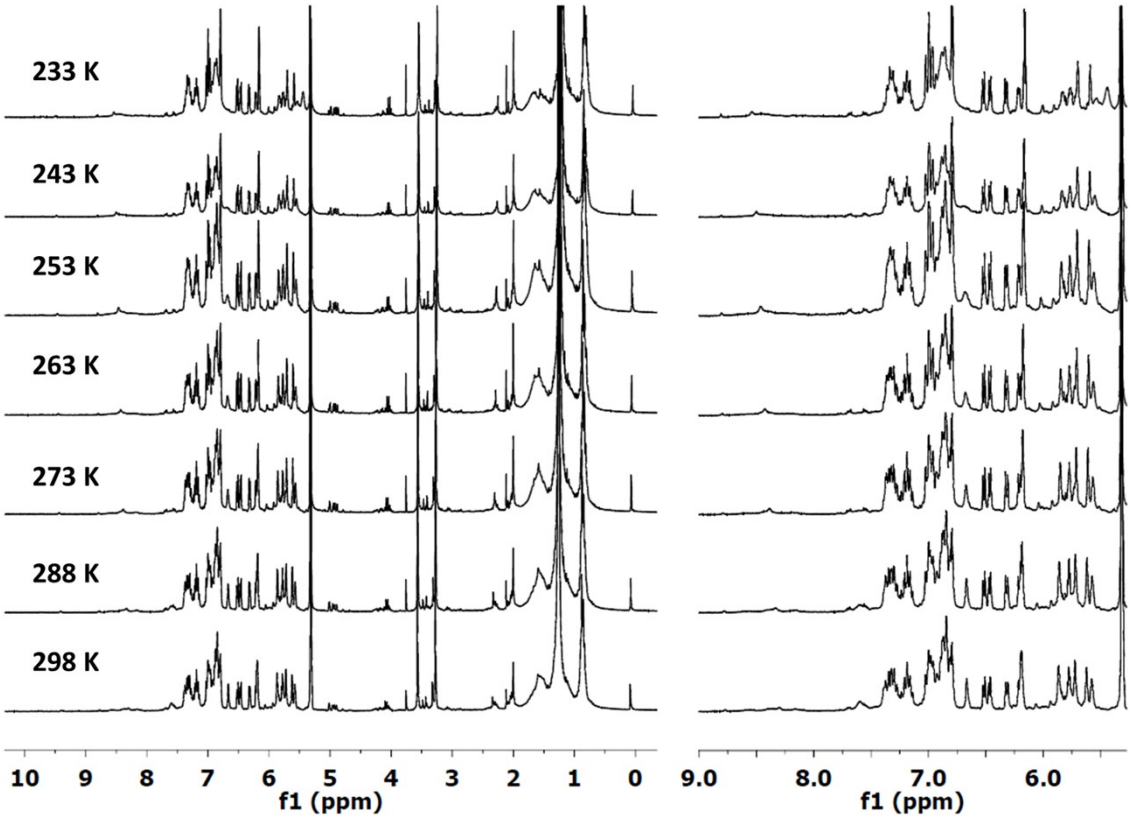

Fig. S36 Low VT ^{1}H NMR spectra of **7** in CD_2Cl_2

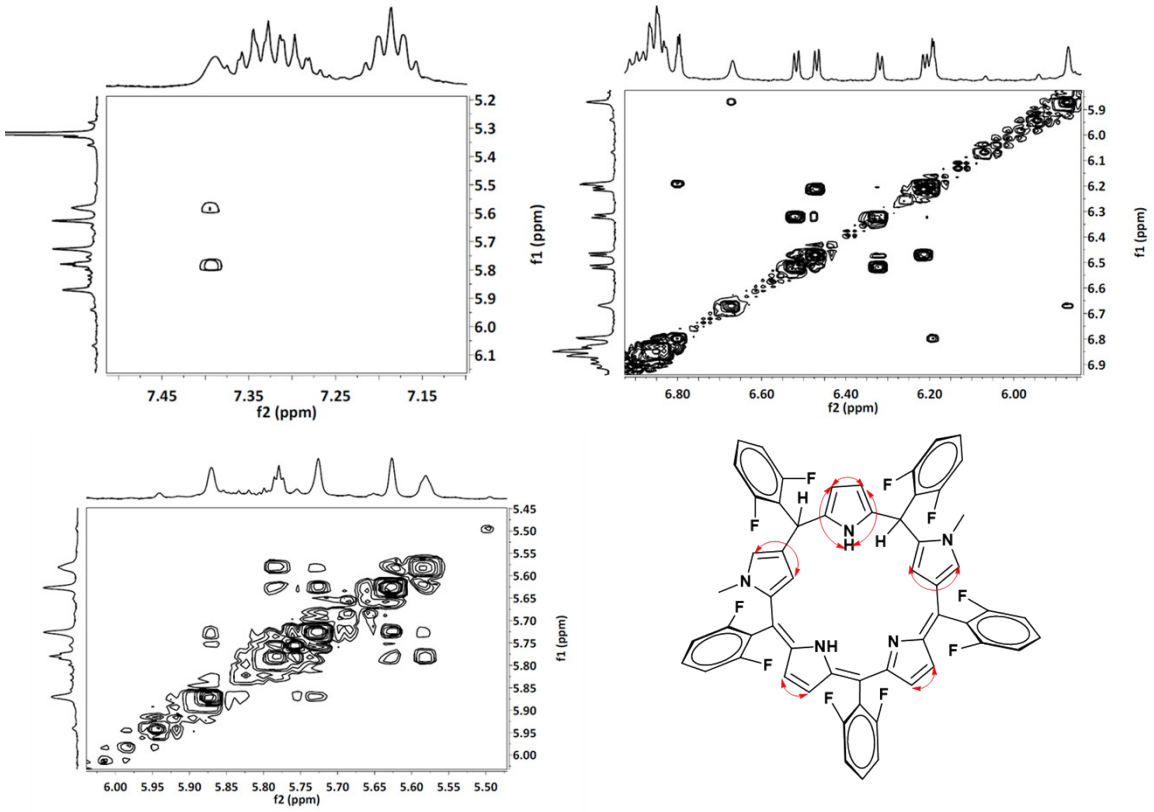

Fig. S37 ^{1}H -^{1}H 2D COSY NMR spectra of **7** in CD_2Cl_2 at 298 K

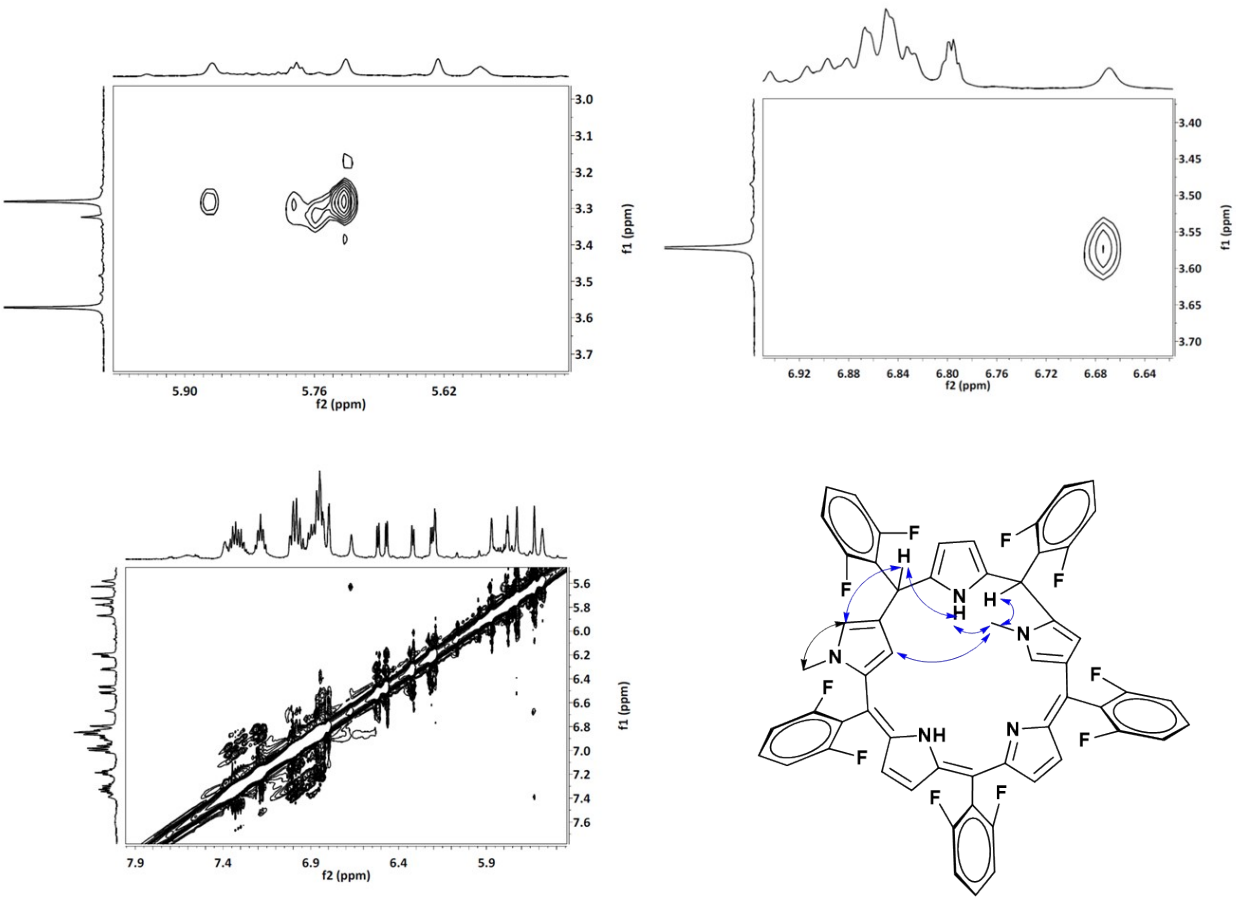

Fig. S38 ^{1}H -^{1}H 2D ROESY NMR spectra of **7** in CD_2Cl_2 at 298 K

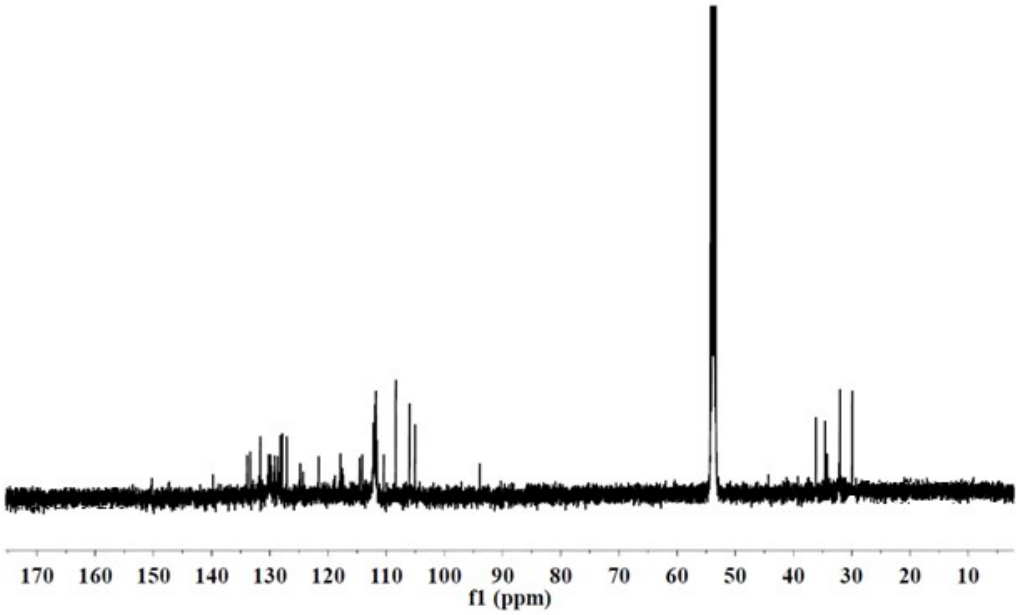

Fig. S39 ^{13}C NMR spectra of **7** in CD_2Cl_2 at 298 K

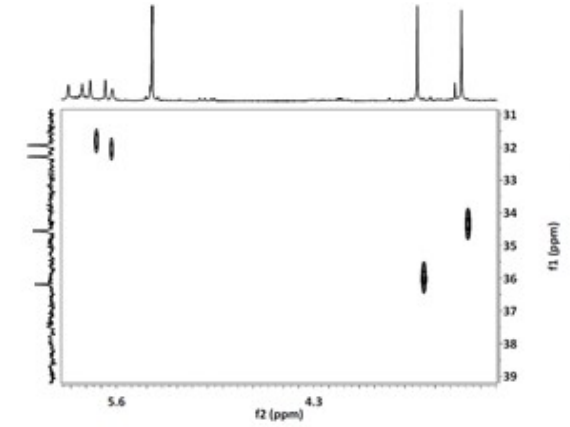

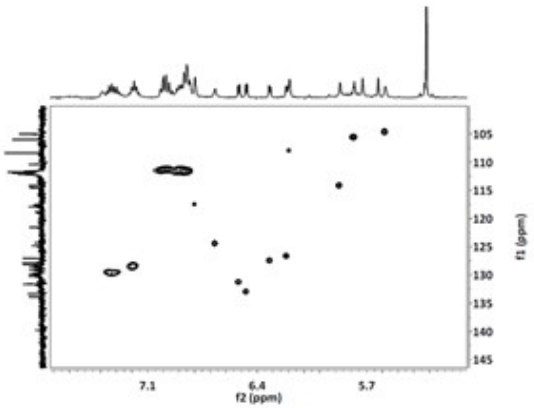

^1H	ppm	^{13}C	ppm	^1H	ppm	^{13}C	ppm
a	6.69	1	124.83	h	6.19	18	108.35
b	5.87	3	114.57	i	5.77	22	105.99
c	6.20	7	127.04	j	5.58	23	105.04
d	6.46	8	133.35	k	3.57	26	36.18
e	6.32	12	127.82	l	3.28	27	34.55
f	6.51	13	131.61	m	7.38		
g	6.79	16	117.89	n	7.60		
o	5.72	20	31.97	p	5.62	25	32.23

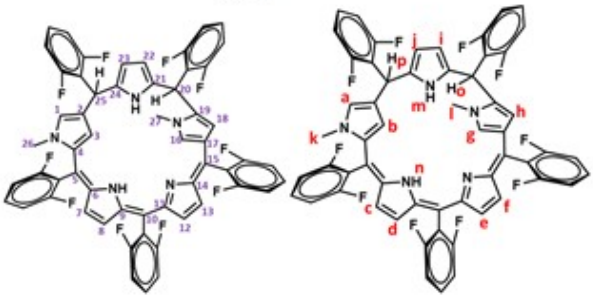

Fig. S40 HSQC NMR spectra of **7** in CD_2Cl_2 at 298 K

^{1}H	ppm	^{13}C	ppm	^{1}H	ppm	^{13}C	ppm
a	6.69	3 4 2	114.57 104.38 133.89	h	6.19	16 20	117.89 31.97
b	5.87	25 1 4 2	32.23 124.83 104.38 133.89	i	5.77	20 23 21 24	31.97 105.04 131.61 128.61
c	6.20	8 6 5	133.35 150.26 163.16	j	5.58	25 22 21 24	31.97 105.99 131.61 128.61
d	6.46	7 9	127.041 150.26	k	3.57	1 4	124.83 133.89
e	6.32	13 11	131.61 147.39	l	3.28	16 19	117.89 131.62
f	6.51	12 15 14	127.82 156.64 147.39	m	7.38	22 23 21 24	105.99 105.04 131.61 128.61
g	6.79	18 27	108.35 34.55	n	7.60	6 7 8	150.26 127.04 133.35
o	5.72	19 22 21 18 Ph Ph	131.62 105.99 121.61 108.35 160.88 117.94	p	5.62	23 24 2 1 Ph Ph	105.04 128.61 133.89 124.83 163.09 119.39

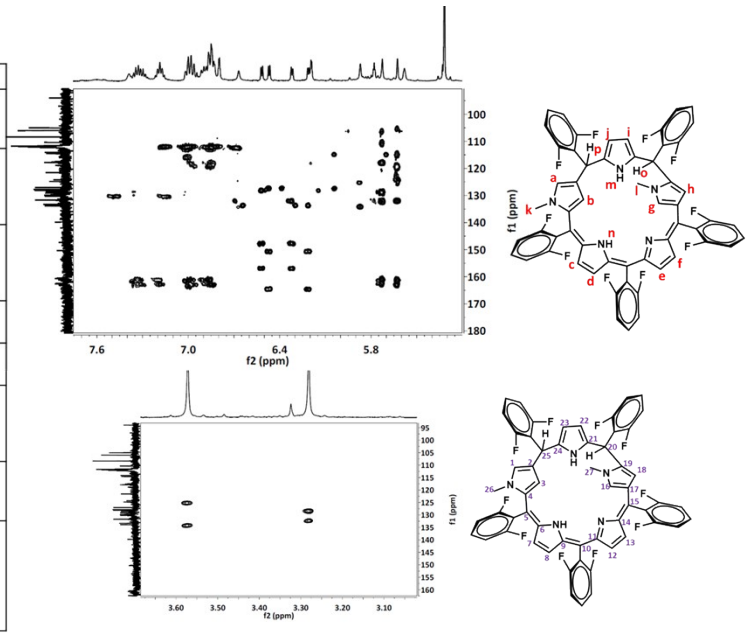

Fig. S41 HMBC NMR spectra of **7** in CD_2Cl_2 at 298 K

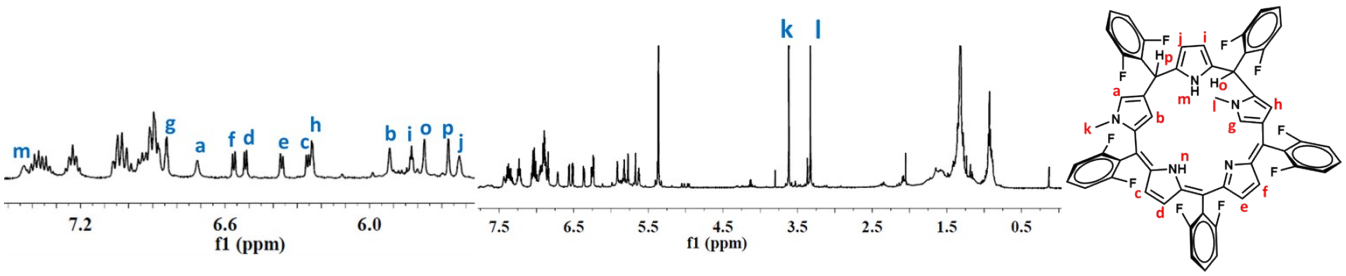

Fig. S42 Complete ^{1}H NMR spectral assignment of **7** in CD_2Cl_2 at 298 K

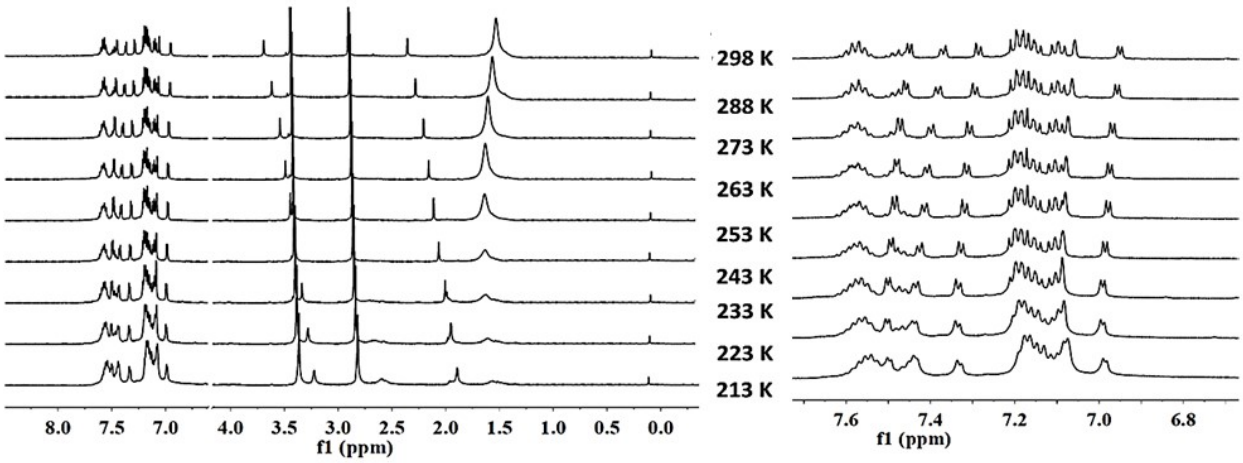

Fig. S43 Low VT ^{1}H NMR spectra of **8** in CD_2Cl_2

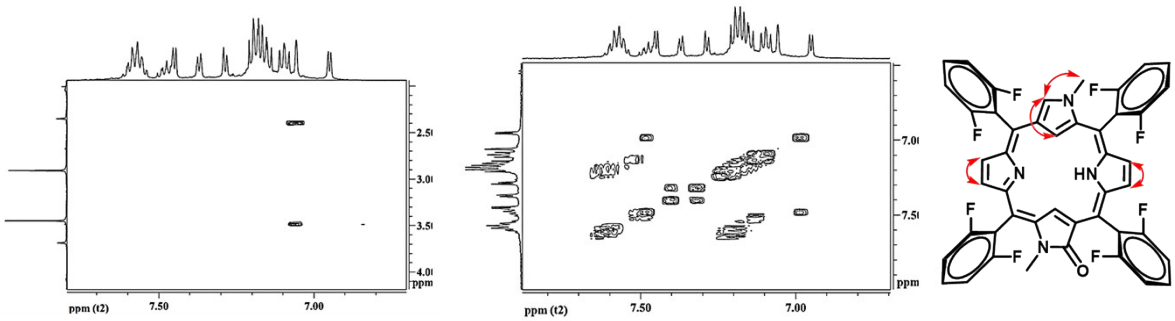

Fig. S44 ^{1}H -^{1}H 2D COSY NMR spectra of **8** in CD_2Cl_2 at 298 K

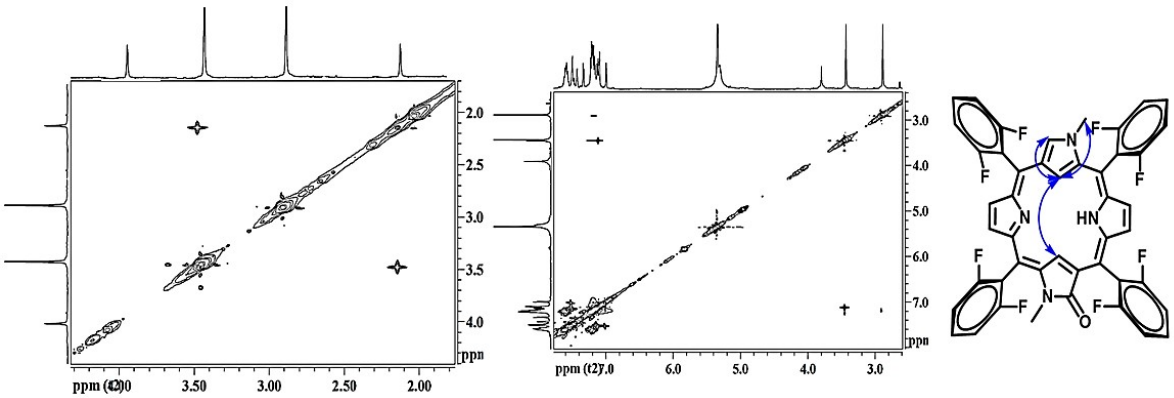

Fig. S45 ^{1}H -^{1}H 2D ROESY NMR spectra of **8** in CD_2Cl_2 at 298 K

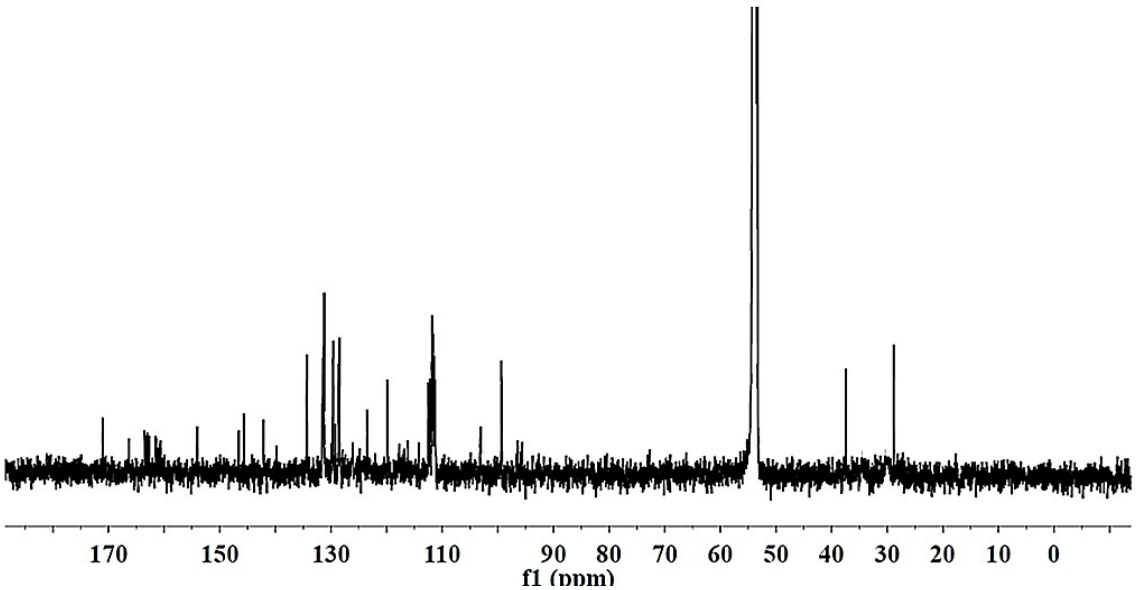

Fig. S46 ^{13}C NMR spectra of **8** in CD_2Cl_2 at 298 K

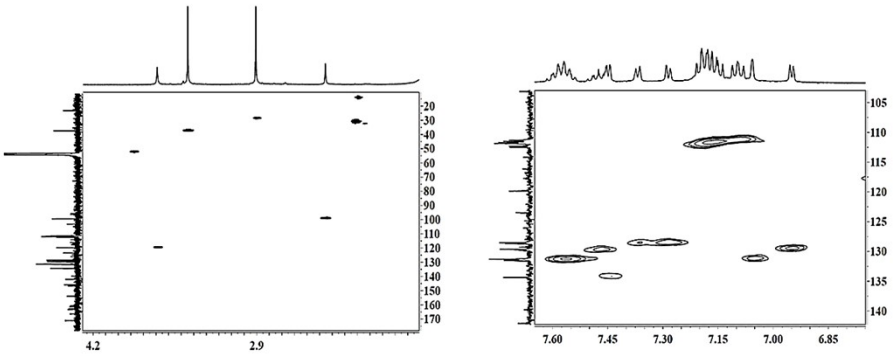

^{1}H	ppm	^{13}C	ppm	^{1}H	ppm	^{13}C	ppm
a	7.05	1	131.28	h	3.45	21	37.40
b	2.36	3	100.14	i	2.91	22	28.77
f	7.37	7	128.54	e	7.45	17	134.23
g	7.28	8	128.36	d	6.95	18	129.51
c	3.70	13	119.59				

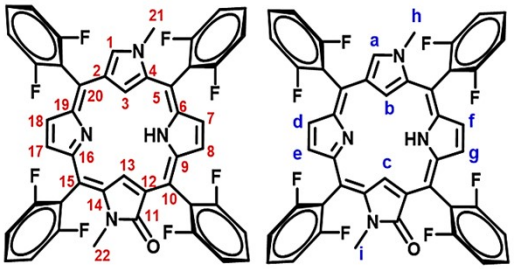

Fig. S47 HSQC NMR spectra of **8** in CD_2Cl_2 at 298 K

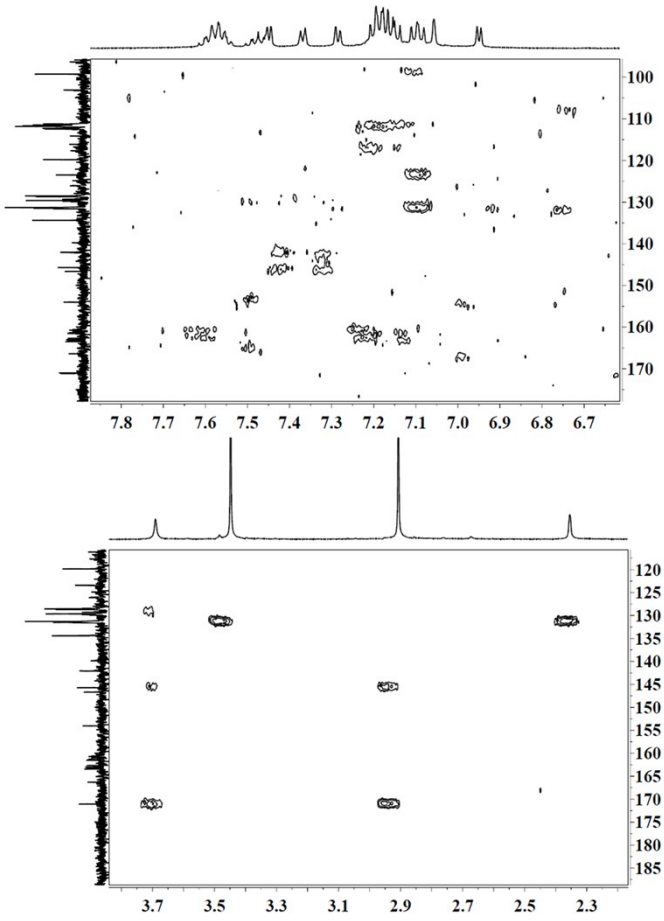

^{1}H	ppm	^{13}C	ppm	^{1}H	ppm	^{13}C	ppm
a	7.05	2 4	123.22 131.40	h	3.45	1	131.28
b	2.36	1	131.28	i	2.91	11 14	170.97 145.47
f	7.37	8 6 9	128.36 153.84 166.09	e	7.45	17 19 16	134.23 147.05 141.31
g	7.28	7 6 9	128.54 153.84 166.09	d	6.95	18 19 16	129.51 147.05 141.31
c	3.70	11 14 12	170.97 145.47 129.16				

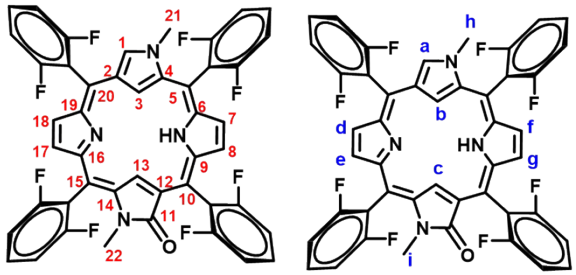

Fig. S48 HMBC NMR spectra of **8** in CD_2Cl_2 at 298 K

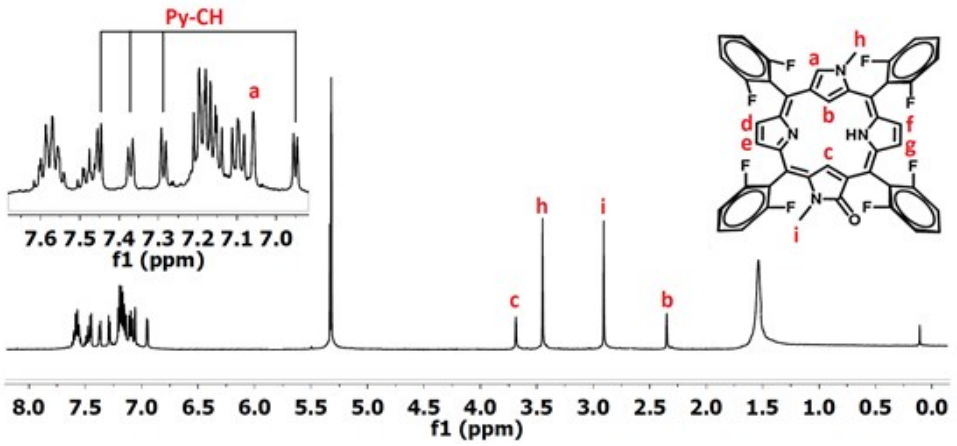

Fig. S49 Complete ^{1}H NMR spectral assignment of **8** in CD_2Cl_2 at 298 K

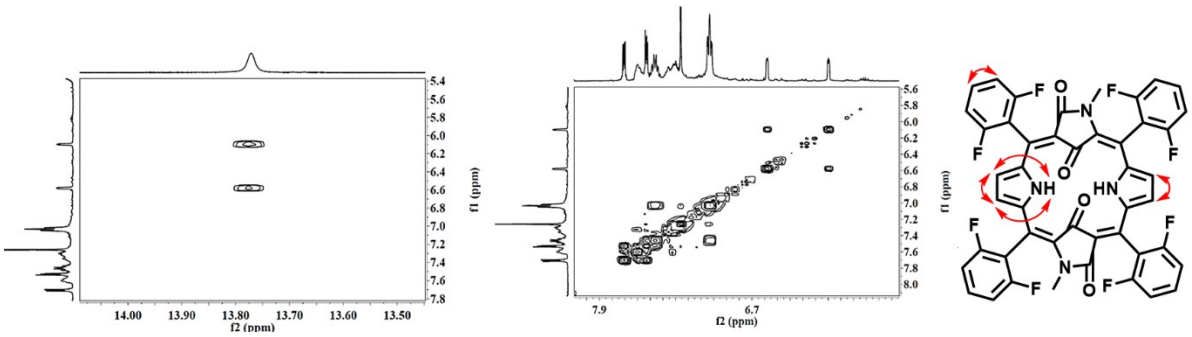

Fig. S50 ^{1}H -^{1}H 2D COSY NMR spectra of **10** in $CDCl_3$ at 298 K

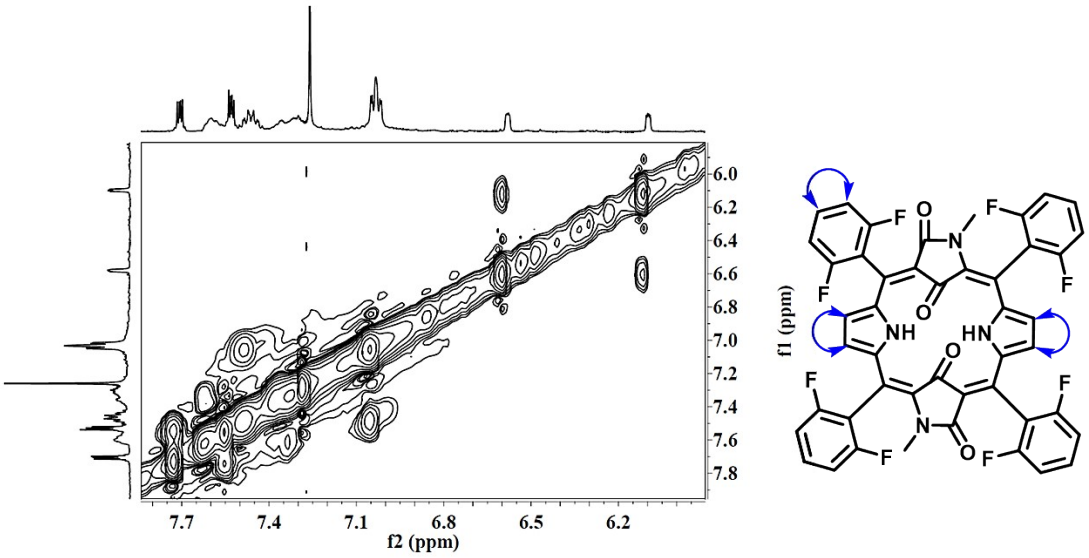

Fig. S51 ^{1}H -^{1}H 2D ROESY NMR spectra of **10** in $CDCl_3$ at 298 K

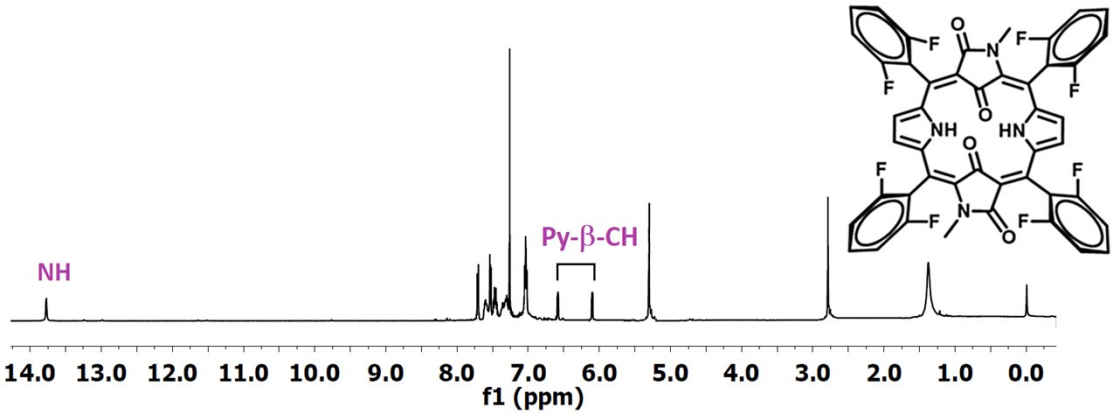

Fig. S52 Complete ^{1}H NMR spectral assignment of **10** in $CDCl_3$ at 298 K

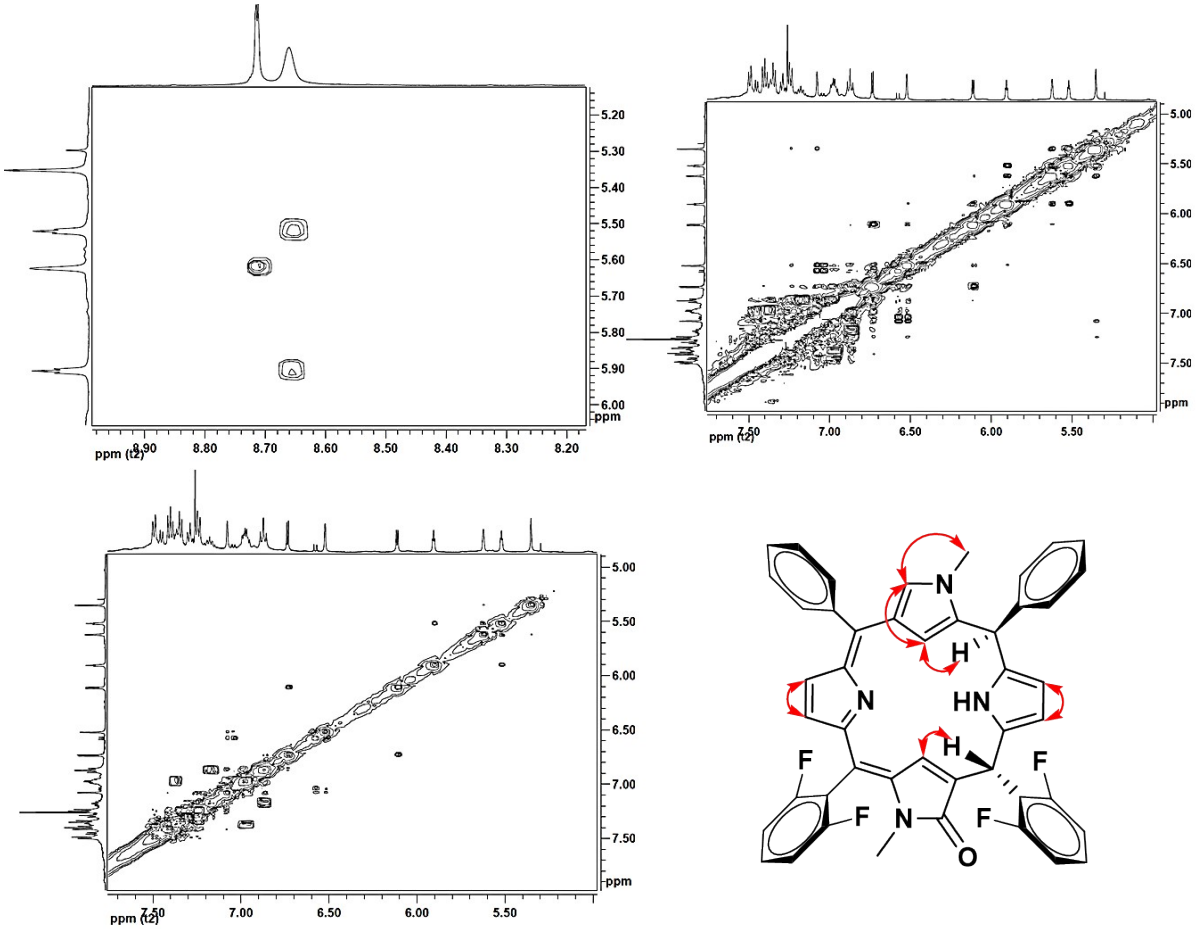

Fig. S53 ^{1}H-^{1}H 2D COSY NMR spectra of **11** in $CDCl_3$ at 298 K

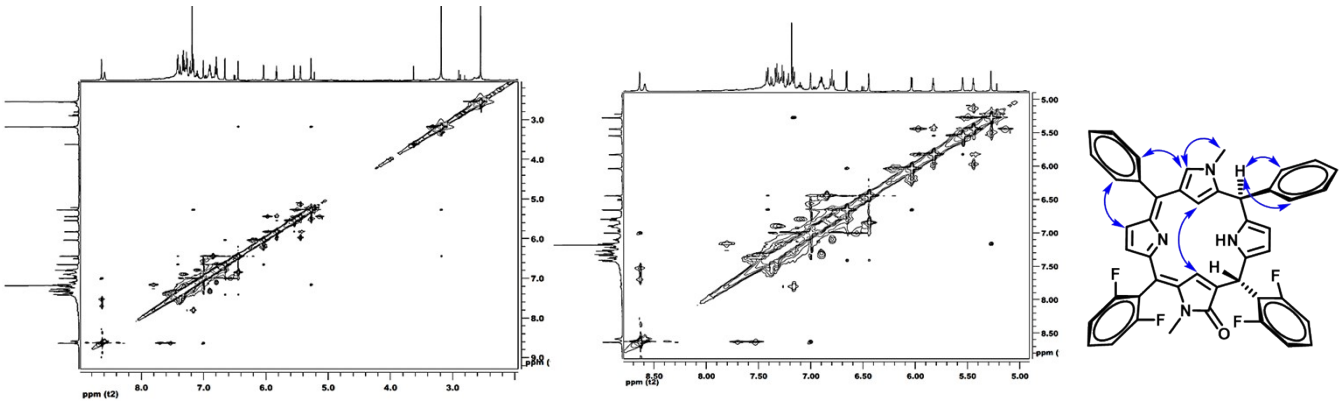

Fig. S54 ^{1}H-^{1}H 2D ROESY NMR spectra of **11** in $CDCl_3$ at 298 K

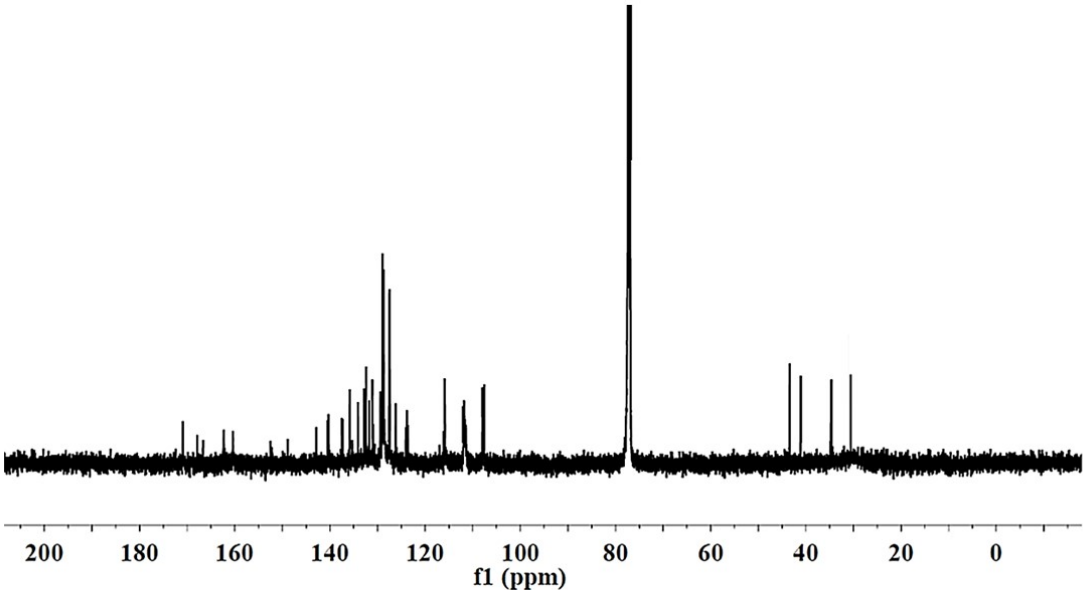

Fig. S55 ^{13}C NMR spectra of **11** in $CDCl_3$ at 298 K

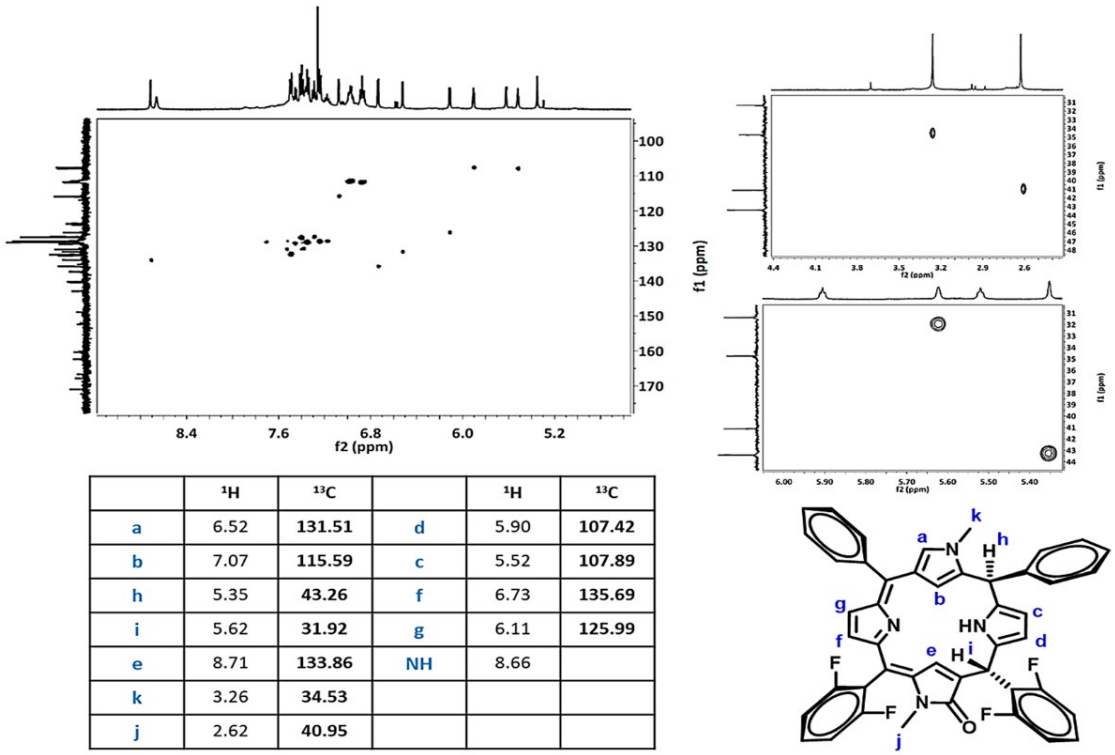

	^{1}H	^{13}C		^{1}H	^{13}C
a	6.52	131.51	d	5.90	107.42
b	7.07	115.59	c	5.52	107.89
h	5.35	43.26	f	6.73	135.69
i	5.62	31.92	g	6.11	125.99
e	8.71	133.86	NH	8.66	
k	3.26	34.53			
j	2.62	40.95			

Fig. S56 HSQC NMR spectra of **11** in $CDCl_3$ at 298 K

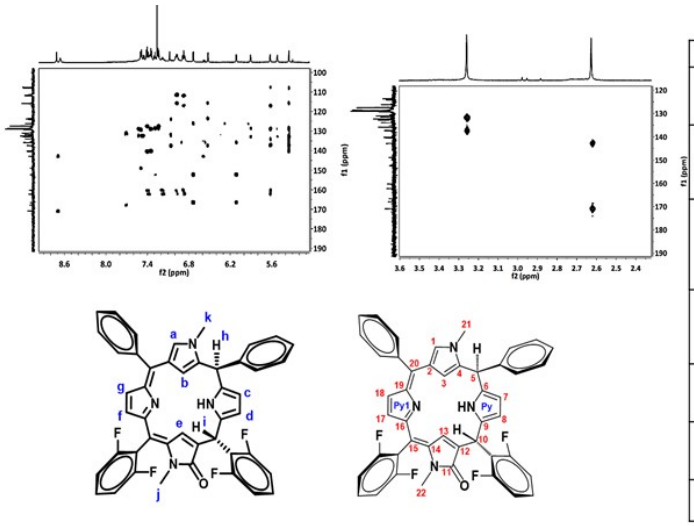

	^{1}H	^{13}C			^{1}H	^{13}C	
a	6.52	115.59 123.52 137.41	3 2 20	d	5.90	128.73 132.69	6 9
b	7.07	137.41 131.51 123.52 132.56	20 1 2 4	c	5.52	128.73 132.69	6 9
h	5.35	115.59 107.89 128.73 132.56 139.91	3 7 6 4 Ph	f	6.73	125.99 152.30 166.47	18 16 15
i	5.62	107.42 132.69 134.16 137.00	8 9 12 Ph	g	6.11	135.69 137.41 152.26 166.47	17 20 19 15
e	8.71	142.80 170.97 134.16	14 11 12				
k	3.26	131.51 137.36 132.56	1 20 4				
j	2.62	142.80 170.97	14 11				

Fig. S57 HMBC NMR spectra of **11** in $CDCl_3$ at 298 K

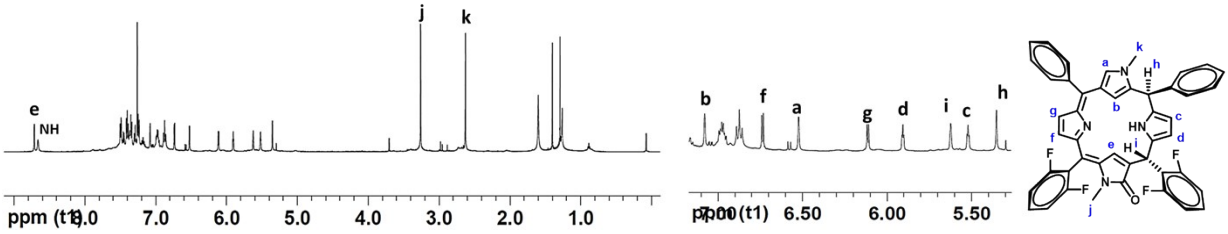

Fig. S58 Complete ^{1}H NMR spectral assignment of **11** in $CDCl_3$ at 298 K

3.0 Electrochemistry:

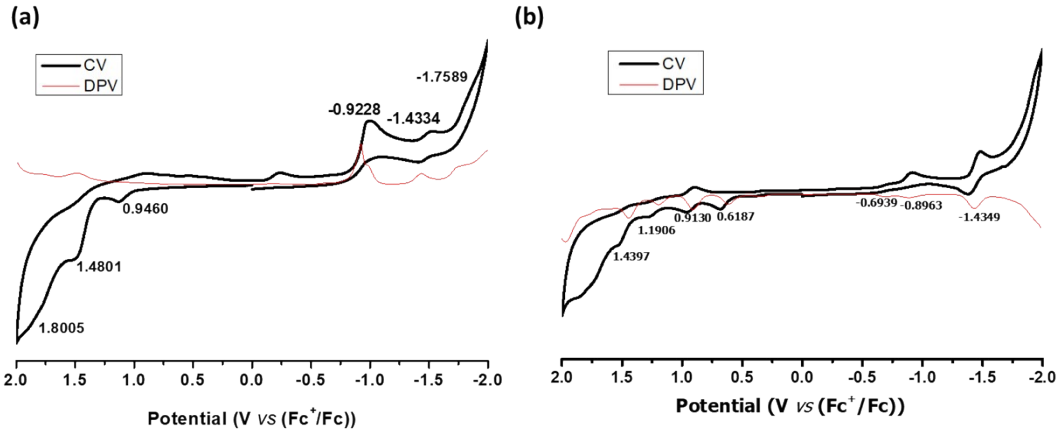

Fig. S59 Cyclic voltammogram of (a) **6** (~10^{-4}M) and (b) **8** (~10^{-4}M) in dichloromethane containing tetrabutylammonium hexafluorophosphate (0.01M) recorded at 100 mVs^{-1}.

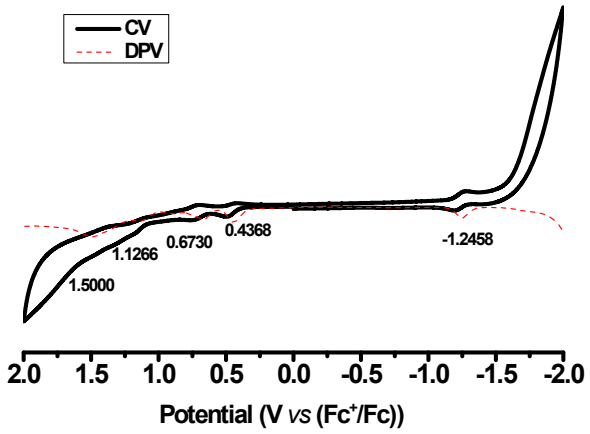

Fig. S60 Cyclic voltammogram of **7** (~10^{-4}M) in dichloromethane containing tetrabutylammonium hexafluorophosphate (0.01M) recorded at 100 mVs^{-1}.

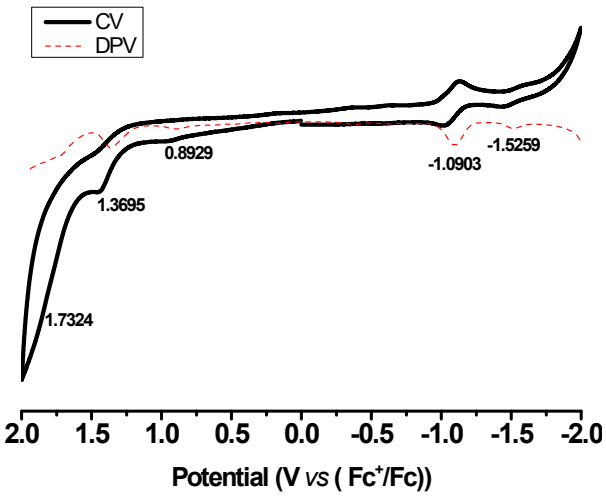

Fig. S61 Cyclic voltammogram of **11** (~10^{-4}M) in dichloromethane containing tetrabutylammonium hexafluorophosphate (0.01M) recorded at 100 mVs^{-1}.

4. 0 Crystallographic Data

Table S1

Parameters	7	8	10
Chemical formula	$C_{57}H_{35}F_{10}N_5$	$C_{46}H_{26}F_8N_4O$	$C_{46}H_{24}F_8N_4O_4$
Formula weight	980.28	802.71	848.69
Temperature	100 K	101 K	110 K
Crystal system	Triclinic	Monoclinic	Triclinic
Space group	P -1	P 2yb	P -1
a (Å); α (°)	11.498(3); 76.103(6)	11.811(4); 90	7.0383(11); 96.192(6)
b (Å); β(°)	12.936(2); 77.831(7)	12.587(4); 106.953(12)	10.8268(16); 98.435(6)
c (Å); γ (°)	20.787(4); 66.872(6)	12.433(4); 90	12.680(2); 103.371(5)
V (Å3); Z	2736.5(10); 2	1768.0(10); 2	919.7(2); 1
ρ (calc.) g m-3	1.498	1.508	1.532
μ(Mo Kα) mm-1	0.394	0.121	0.127
2θmax (°)	50.998	53.000	56.710
R(int)	0.0972	0.0777	0.0636
Completeness to θ	0.991	0.99	0.981
Data / param.	10089/ 733	7260/ 3927	4525 / 3006
GOF	1.050	0.948	1.042
R1 [F>4σ(F)]	0.09715	0.0777	0.063593
wR2 (all data)	0.3067	0.2253	0.1800
max. peak/hole (e.Å-3)	1.431 / -1.225	0.523 / -0.337	0.423 / -0.382
CCDC	2063643	2063644	2063645

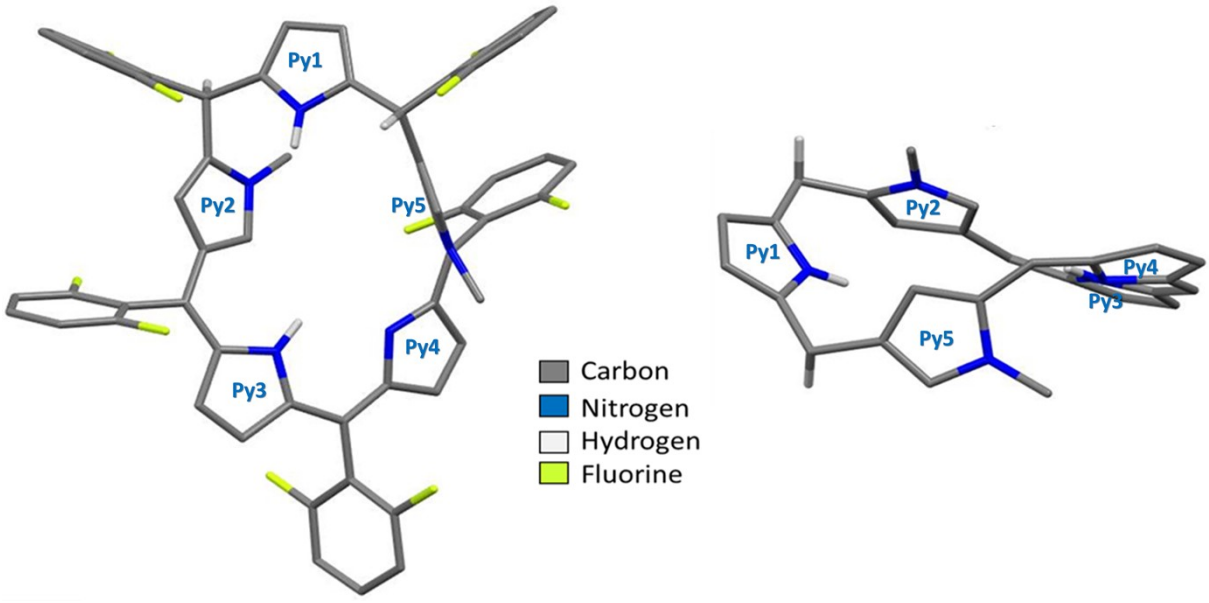

Fig. S62 X-ray crystal structure of **7** (left: Top view, right: side view).

5.0 Theoretical Calculation

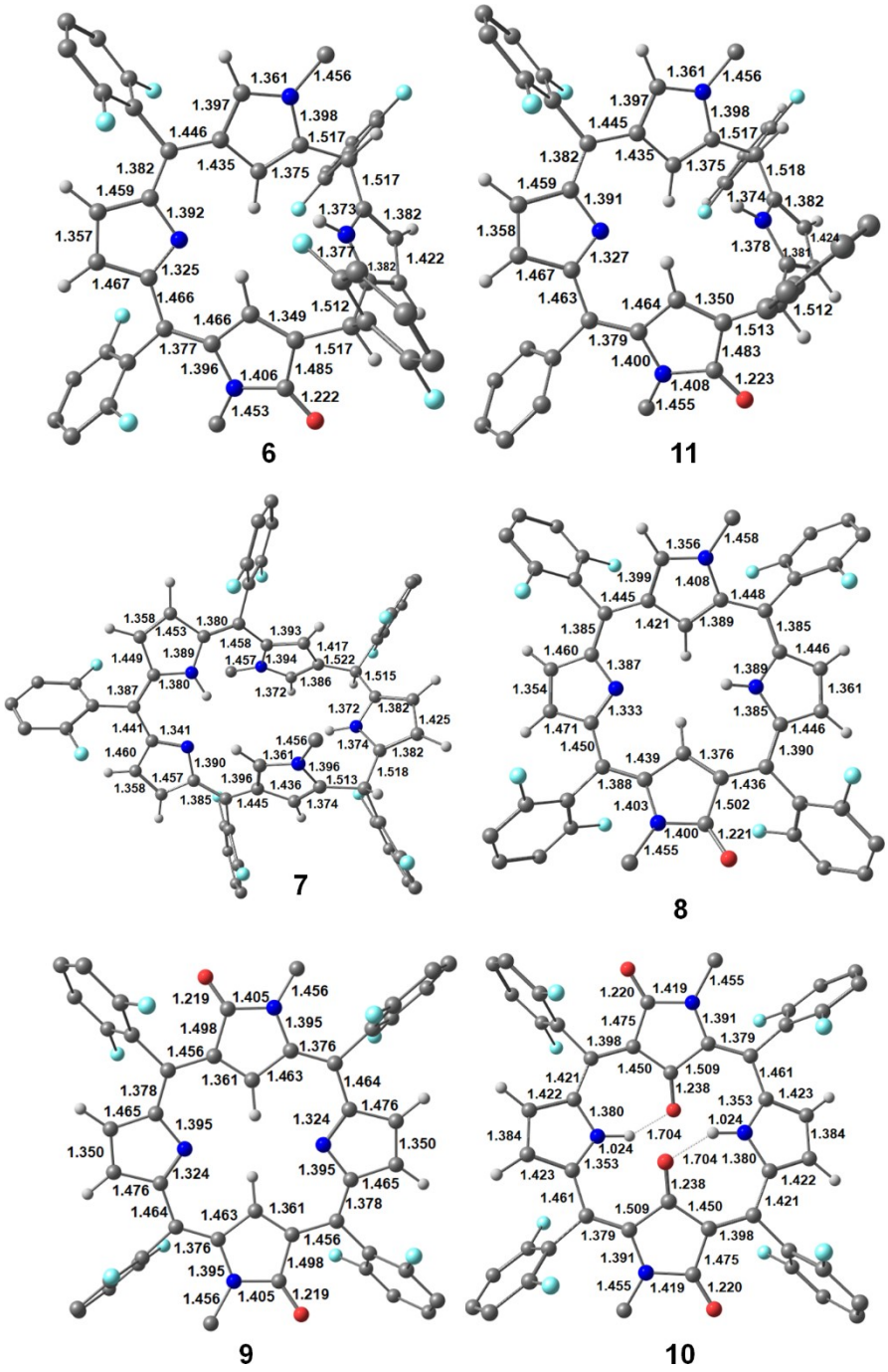

Fig. S63 DFT optimised geometries and key bond length parameters (Å) of **6-11**, at B3LYP/ 6-31+G** level of theory. Note that except for **6** and **11, 8-10** are the optimised geometry of X-ray crystal structures.

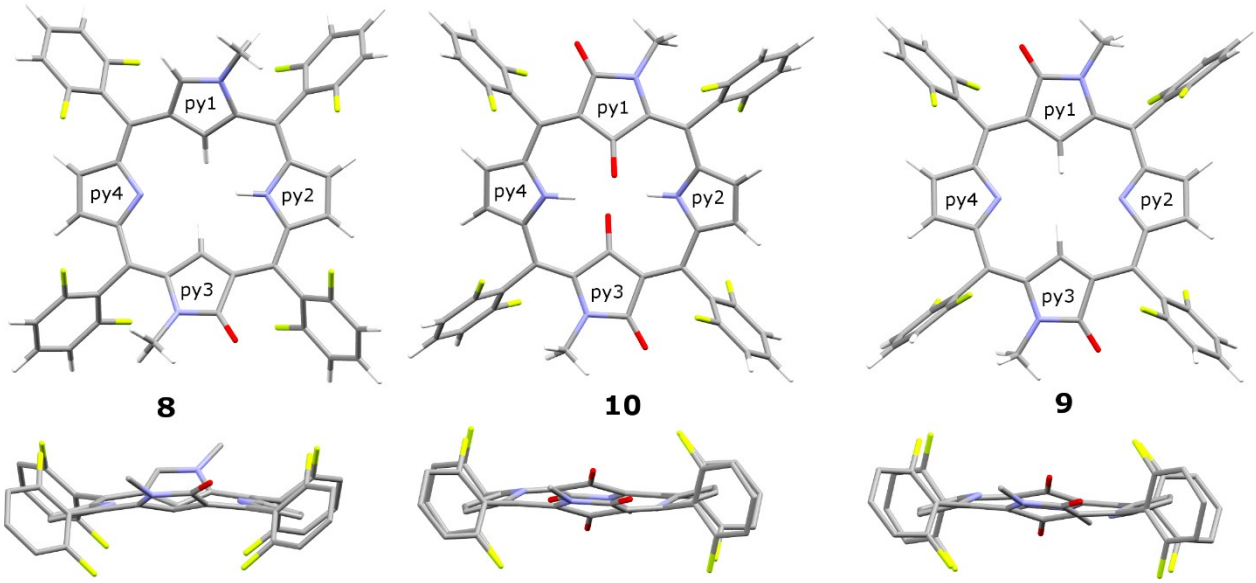

Mean plane of deviation (°)	**8**	**10**	**9**
Py1	30.72	15.97	11.76
Py2	14.45	18.91	2.66
Py3	18.50	15.97	11.76
Py4	12.25	18.91	2.66
Mean plane of deviation (°)	**8a**	**10a**	**9a**
Py1	15.34	14.89	6.03
Py2	5.29	15.86	1.46
Py3	1.55	14.89	6.03
Py4	2.26	15.86	1.46

Fig. S64 Top and side view of DFT optimised geometries of **8-10** and_dihedral angle planes of pyrrole rings with respect to mean plane deviation of meso carbons at B3LYP/6-31+G** level of theory.

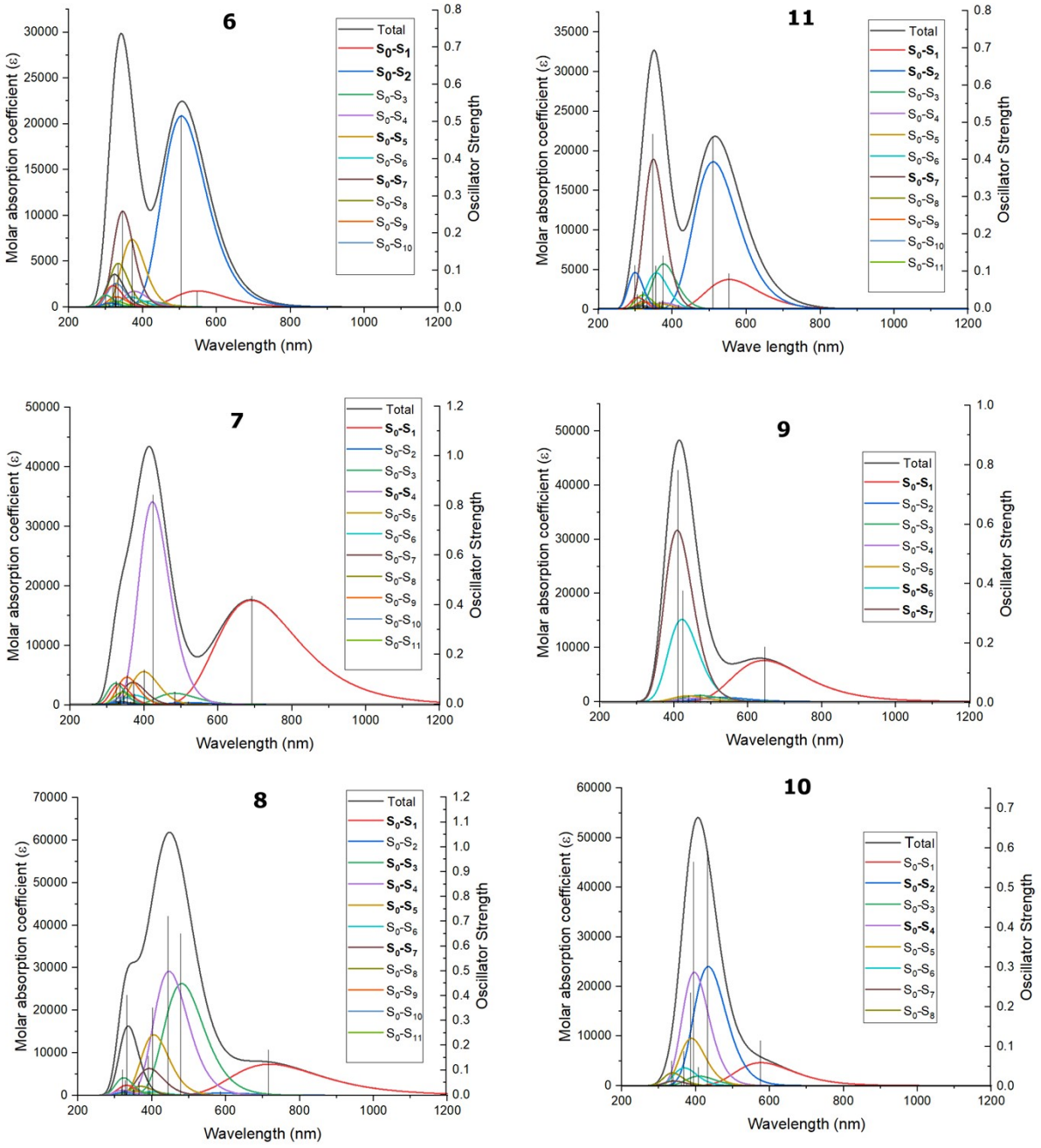

Fig. S65 Steady state absorption spectrum (total) and individual transitions that are predicted from TD-DFT calculation done with solvent (dichloromethane using a polarizable continuum model) and at B3LYP/6-31G** level of theory for **6**, **11**, **7**, **9**, **8** and **10**.

Table S2: Summary of UV-vis spectral data of **6**

No.	Energy (eV)	Wavelength (nm)	Oscillator Strength	Symmetry	Major contributions
1	2.2635	547.75	0.04330	Singlet-A	H-1 -> L 75.9%, H -> L 23.3%
2	**2.4534**	**505.36**	**0.51570**	**Singlet-A**	**H -> L 76.1%, H-1 -> L 23.4%**
3	2.9924	414.33	0.01550	Singlet-A	H-2 -> L 85.9%, H -> L+1 10.1%
4	3.0988	400.10	0.00220	Singlet-A	H-3 -> L 77.7%, H -> L+1 18.0%
5	3.2806	377.93	0.04230	Singlet-A	H-1 -> L+1 86.2%, H -> L+1 7.9%
6	3.3365	371.60	0.18250	Singlet-A	H -> L+1 38.4%, H-5 -> L 22.9%, H-1 -> L+1 10.7%, H-3 -> L 8.5%,
7	3.3707	367.83	0.02670	Singlet-A	H-7 -> L 21.9%, H-4 -> L 19.4%, H-9 -> L 17.1%, H-6 -> L 10.2%,
8	3.4092	363.68	0.00440	Singlet-A	H-4 -> L 70.2%, H-7 -> L 8.7%
9	**3.5826**	**346.07**	**0.25820**	**Singlet-A**	**H-5 -> L 60.1%, H-14 -> L 12.8%, H -> L+1 11.2%**
10	3.6927	335.75	0.00300	Singlet-A	H-10 -> L 90.7%
11	3.7129	333.93	0.11790	Singlet-A	H-9 -> L 54.0%, H-7 -> L 21.8%, H-6 -> L 8.2%, H-10 -> L 6.5%
12	3.7641	329.39	0.02750	Singlet-A	H-8 -> L 77.1%, H-6 -> L 9.1%
13	3.7818	327.84	0.06350	Singlet-A	H-6 -> L 23.6%, H-8 -> L 17.6%, H-11 -> L 12.1%, H-16 -> L 12.1%,
14	3.8016	326.14	0.01550	Singlet-A	H-6 -> L 40.8%, H-7 -> L 32.4%, H-16 -> L 8.6%
15	3.8236	324.26	0.08800	Singlet-A	H-14 -> L 52.4%, H-16 -> L 12.1%, H-11 -> L 7.1%
16	3.8738	320.06	0.05740	Singlet-A	H-13 -> L 54.3%, H-12 -> L 33.3%, H-11 -> L 6.2%
17	3.9699	312.31	0.01040	Singlet-A	H-2 -> L+1 77.6%, H-3 -> L+1 7.8%
18	4.0004	309.93	0.00910	Singlet-A	H-11 -> L 45.8%, H-16 -> L 30.4%, H-12 -> L 6.3%, H-2 -> L+1 5.0%
19	4.0867	303.38	0.00610	Singlet-A	H-12 -> L 48.0%, H-13 -> L 28.1%, H-16 -> L 15.8%
20	4.1305	300.17	0.03200	Singlet-A	H-3 -> L+1 81.0%, H-2 -> L+1 8.6%

Table S3: Summary of UV-vis spectral data of **7**

No.	Energy (eV)	Wavelength (nm)	Oscillator Strength	Symmetry	Major contributions
1	**1.7958**	**690.41**	**0.43470**	**Singlet-A**	**H -> L 100.1%**
2	2.3885	519.09	0.01010	Singlet-A	H-1 -> L 97.2%
3	2.5696	482.50	0.04890	Singlet-A	H -> L+1 53.5%, H-2 -> L 43.1%
4	**2.9336**	**422.63**	**0.84390**	**Singlet-A**	**H-2 -> L 50.8%, H -> L+1 38.8%**
5	3.1053	399.27	0.13890	Singlet-A	H-3 -> L 93.6%
6	3.3174	373.74	0.04080	Singlet-A	H-4 -> L 91.3%
7	3.3504	370.06	0.09460	Singlet-A	H-5 -> L 71.7%, H-6 -> L 15.3%, H-7 -> L 5.3%
8	3.4159	362.96	0.01000	Singlet-A	H-1 -> L+1 95.1%
9	3.5029	353.95	0.11560	Singlet-A	H-7 -> L 50.8%, H-6 -> L 20.5%, H-5 -> L 14.5%, H-2 -> L+1 5.9%
10	3.6052	343.90	0.03230	Singlet-A	H-6 -> L 58.9%, H-7 -> L 26.6%
11	3.6197	342.53	0.05220	Singlet-A	H -> L+3 88.8%
12	3.7009	335.01	0.01430	Singlet-A	H-2 -> L+1 48.1%, H -> L+5 30.3%, H-17 -> L 6.6%
13	3.7164	333.61	0.08790	Singlet-A	H -> L+5 57.7%, H-2 -> L+1 25.4%, H -> L+6 7.8%
14	3.7410	331.42	0.00840	Singlet-A	H -> L+2 81.9%
15	3.7596	329.78	0.00710	Singlet-A	H-8 -> L 69.9%, H -> L+6 13.4%, H -> L+4 8.7%
16	3.7634	329.45	0.00850	Singlet-A	H-8 -> L 28.7%, H -> L+6 27.8%, H -> L+4 20.7%, H-12 -> L 9.1%,
17	3.7720	328.70	0.00500	Singlet-A	H-12 -> L 79.2%, H-10 -> L 5.4%
18	3.7763	328.32	0.00440	Singlet-A	H-10 -> L 72.9%, H -> L+6 7.0%, H-9 -> L 5.8%
19	3.7881	327.30	0.01090	Singlet-A	H -> L+4 54.2%, H -> L+6 21.6%, H -> L+2 10.0%
20	3.8384	323.01	0.09050	Singlet-A	H-17 -> L 37.7%, H-19 -> L 20.6%, H -> L+6 9.7%, H-2 -> L+1 8.1%

Table S4: Summary of UV-vis spectral data of **8**

No.	Energy (eV)	Wavelength (nm)	Oscillator Strength	Symmetry	Major contributions
1	**1.7246**	**718.92**	**0.18090**	**Singlet-A**	**H -> L 94.6%**
2	2.1052	588.94	0.01280	Singlet-A	H-1 -> L 56.8%, H -> L+1 42.1%
3	**2.5772**	**481.08**	**0.65020**	**Singlet-A**	**H -> L+1 40.9%, H-1 -> L 27.6%, H-1 -> L+1 25.5%**
4	**2.7751**	**446.77**	**0.72130**	**Singlet-A**	**H-1 -> L+1 62.8%, H-1 -> L 11.6%, H -> L+1 11.5%, H-2 -> L 7.3%**
5	3.0572	405.55	0.35230	Singlet-A	H-2 -> L 76.1%, H -> L+2 6.8%
6	3.1163	397.86	0.01920	Singlet-A	H -> L+2 63.8%, H-3 -> L 22.9%, H-2 -> L 10.2%
7	3.1544	393.05	0.15600	Singlet-A	H-3 -> L 66.4%, H -> L+2 22.3%
8	3.3601	368.99	0.05280	Singlet-A	H-6 -> L 26.8%, H-4 -> L 22.6%, H-10 -> L 18.6%, H-7 -> L 13.3%, H-5 -> L 5.9%
9	3.4649	357.83	0.00250	Singlet-A	H-4 -> L 54.1%, H-10 -> L 23.2%
10	3.4858	355.68	0.02270	Singlet-A	H-5 -> L 59.3%, H-10 -> L 14.0%, H-7 -> L 8.8%, H-6 -> L 5.7%
11	3.5169	352.54	0.01140	Singlet-A	H-2 -> L+1 33.3%, H-6 -> L 28.5%, H-4 -> L 18.2%, H-10 -> L 8.3%
12	3.5211	352.12	0.02650	Singlet-A	H-1 -> L+2 34.1%, H-2 -> L+1 29.9%, H-6 -> L 15.8%, H-10 -> L 6.7%, H-3 -> L+1 5.7%
13	3.6225	342.26	0.00140	Singlet-A	H-7 -> L 65.0%, H-5 -> L 24.9%, H-10 -> L 5.8%
14	3.6270	341.84	0.00240	Singlet-A	H-8 -> L 94.4%
15	3.6889	336.10	0.40320	Singlet-A	H-1 -> L+2 36.6%, H-2 -> L+1 16.8%, H-6 -> L 15.2%, H-3 -> L+1 7.6%
16	3.7028	334.84	0.00850	Singlet-A	H-9 -> L 93.8%
17	3.7414	331.38	0.05820	Singlet-A	H -> L+3 85.3%, H-11 -> L 9.4%
18	3.7708	328.80	0.01890	Singlet-A	H-3 -> L+1 67.7%, H-1 -> L+2 8.6%, H-11 -> L 5.6%
19	3.8253	324.12	0.10200	Singlet-A	H-12 -> L 77.2%, H-10 -> L 11.0%
20	3.8666	320.65	0.02870	Singlet-A	H-11 -> L 71.9%, H -> L+3 8.5%

Table S5: Summary of UV-vis spectral data of **9**

No.	Energy (eV)	Wavelength (nm)	Oscillator Strength	Symmetry	Major contributions
1	1.1329	1094.40	0.00000	Singlet-A	:H -> L 100.3%
2	**1.9274**	**643.27**	**0.18810**	**Singlet-A**	**:H-1 -> L 92.3%**
3	2.3688	523.41	0.02010	Singlet-A	:H-3 -> L 88.7%
4	2.3716	522.79	0.00000	Singlet-A	:H-2 -> L 87.4%, H-5 -> L 9.2%
5	2.5090	494.16	0.00000	Singlet-A	:H-5 -> L 69.3%, H-8 -> L 18.1%, H-2 -> L 9.8%
6	2.5401	488.11	0.00340	Singlet-A	:H-4 -> L 79.9%, H-9 -> L 6.0%
7	2.5625	483.84	0.00100	Singlet-A	:H-12 -> L 30.7%, H-10 -> L 18.8%, H-6 -> L 17.3%, H-4 -> L 15.5%,
8	2.6086	475.29	0.00000	Singlet-A	:H-8 -> L 72.9%, H-5 -> L 20.3%
9	2.6447	468.80	0.02820	Singlet-A	:H-9 -> L 35.2%, H-6 -> L 21.5%, H-12 -> L 20.4%, H-10 -> L 15.9%
10	2.6979	459.56	0.00000	Singlet-A	:H-7 -> L 95.1%
11	2.7168	456.36	0.01470	Singlet-A	:H-6 -> L 55.3%, H-9 -> L 37.6%
12	2.8041	442.15	0.00000	Singlet-A	:H-11 -> L 63.7%, H-15 -> L 28.4%
13	2.8313	437.91	0.02580	Singlet-A	:H-10 -> L 42.7%, H-12 -> L 19.8%, H -> L+2 17.0%, H -> L+1 10.0%,
14	2.9382	421.97	0.00000	Singlet-A	:H-15 -> L 41.0%, H-11 -> L 26.5%, H-13 -> L 24.9%
15	2.9398	421.74	0.37580	Singlet-A	:H -> L+1 27.3%, H-12 -> L 18.5%, H-14 -> L 16.2%, H-10 -> L 15.7%,
16	3.0147	411.27	0.00000	Singlet-A	:H-13 -> L 71.8%, H-15 -> L 19.1%, H-11 -> L 6.2%
17	**3.0311**	**409.04**	**0.78280**	**Singlet-A**	**:H -> L+1 39.6%, H -> L+2 35.0%, H-14 -> L 12.5%, H-1 -> L 5.4%**
18	3.2598	380.34	0.00000	Singlet-A	:H-1 -> L+1 96.4%
19	3.3123	374.31	0.00000	Singlet-A	:H-16 -> L 82.4%, H-1 -> L+2 6.1%
20	3.3646	368.50	0.00580	Singlet-A	:H-17 -> L 88.9%

Table S6: Summary of UV-vis spectral data of **10**

No.	Energy eV	Wavelength (nm)	Oscillator Strength	Symmetry	Major contributions
1	1.8212	680.78	0.00000	Singlet-A	H-1 -> L 99.1%
2	**2.1486**	**577.05**	**0.11460**	**Singlet-A**	**H -> L 85.2%, H-1 -> L+1 14.7%**
3	2.4622	503.55	0.00000	Singlet-A	H -> L+1 96.2%
4	**2.8566**	**434.03**	**0.59360**	**Singlet-A**	**H-1 -> L+1 55.5%, H-1 -> L+2 29.7%, H -> L 9.1%**
5	2.9137	425.52	0.00000	Singlet-A	H -> L+2 71.9%, H-2 -> L 20.8%
6	3.0135	411.43	0.00000	Singlet-A	H-10 -> L 36.4%, H-3 -> L 34.4%, H-6 -> L 9.0%, H-2 -> L 7.3%
7	3.0299	409.20	0.04750	Singlet-A	H-11 -> L 37.8%, H-5 -> L 21.0%, H-4 -> L 18.1%, H-12 -> L 5.5%
8	**3.1282**	**396.34**	**0.56510**	**Singlet-A**	**H-1 -> L+2 44.9%, H-4 -> L 24.8%, H-1 -> L+1 16.8%**
9	3.1488	393.75	0.00000	Singlet-A	H-2 -> L 57.3%, H-3 -> L 17.6%, H -> L+2 15.2%
10	3.1904	388.62	0.23540	Singlet-A	H-4 -> L 40.4%, H-11 -> L 18.5%, H-1 -> L+2 17.2%, H-1 -> L+1 6.6%
11	3.1990	387.57	0.00000	Singlet-A	H-10 -> L 37.2%, H-3 -> L 29.2%, H-2 -> L 10.3%, H -> L+2 5.7%
12	3.2801	377.99	0.00590	Singlet-A	H-5 -> L 62.1%, H-4 -> L 10.2%, H-9 -> L 8.1%, H-11 -> L 7.4%
13	3.2822	377.75	0.00000	Singlet-A	H-6 -> L 76.7%, H-3 -> L 13.1%
14	3.3551	369.54	0.08810	Singlet-A	H-9 -> L 68.6%, H-7 -> L 10.4%, H-11 -> L 10.0%
15	3.4088	363.72	0.00000	Singlet-A	H-8 -> L 93.0%
16	3.4149	363.07	0.00970	Singlet-A	H-7 -> L 79.7%, H-11 -> L 9.1%
17	3.6288	341.67	0.02350	Singlet-A	H-12 -> L 69.9%, H-11 -> L 9.7%, H-10 -> L+1 7.2%
18	3.6309	341.47	0.00000	Singlet-A	H-13 -> L 52.8%, H-14 -> L 16.3%, H-10 -> L 12.0%, H-11 -> L+1 7.3%
19	3.6765	337.23	0.06350	Singlet-A	H-3 -> L+1 56.2%, H-6 -> L+1 15.1%, H -> L+3 6.7%
20	3.6899	336.01	0.00000	Singlet-A	H-4 -> L+1 57.2%, H-5 -> L+1 20.7%

Table S7: Summary of UV-vis spectral data of **11**

No.	Energy (eV)	Wavelength (nm)	Oscillator Strength	Symmetry	Major contributions
1	2.2434	552.66	0.09360	Singlet-A	H-1 -> L 51.9%, H -> L 47.4%
2	**2.4352**	**509.13**	**0.46040**	**Singlet-A**	**H -> L 52.2%, H-1 -> L 47.5%**
3	2.9774	416.42	0.00910	Singlet-A	H-2 -> L 82.0%, H -> L+1 15.2%
4	3.0972	400.31	0.00600	Singlet-A	H-3 -> L 78.7%, H -> L+1 14.7%
5	3.3054	375.10	0.14230	Singlet-A	H -> L+1 30.0%, H-6 -> L 22.8%, H-1 -> L+1 17.1%, H-5 -> L 13.1%,
6	3.3175	373.73	0.02130	Singlet-A	H-4 -> L 29.3%, H-5 -> L 26.5%, H-10 -> L 17.7%, H-11 -> L 8.0%
7	3.3442	370.74	0.00830	Singlet-A	H-1 -> L+1 71.5%, H-6 -> L 22.0%
8	3.3932	365.39	0.01780	Singlet-A	H-4 -> L 60.4%, H-5 -> L 25.0%
9	3.4926	354.99	0.11450	Singlet-A	H-5 -> L 21.9%, H-10 -> L 15.5%, H-6 -> L 13.5%, H-11 -> L 12.2%,
10	**3.5705**	**347.25**	**0.46850**	**Singlet-A**	**H-6 -> L 32.4%, H -> L+1 20.0%, H-5 -> L 9.8%, H-10 -> L 9.6%,**
11	3.6978	335.29	0.00230	Singlet-A	H-9 -> L 97.7%
12	3.7242	332.91	0.00680	Singlet-A	H-7 -> L 83.2%
13	3.7472	330.87	0.02270	Singlet-A	H-10 -> L 33.0%, H-11 -> L 21.9%, H-14 -> L 16.0%, H-7 -> L 10.8%
14	3.8108	325.35	0.00030	Singlet-A	H-8 -> L 91.7%
15	3.8557	321.56	0.02530	Singlet-A	H-16 -> L 31.9%, H-14 -> L 29.5%, H-11 -> L 17.9%, H-10 -> L 6.4%
16	3.8692	320.44	0.01280	Singlet-A	H-16 -> L 41.4%, H-14 -> L 27.3%, H-11 -> L 15.9%
17	3.8798	319.56	0.04570	Singlet-A	H-13 -> L 65.9%, H-12 -> L 19.1%, H-11 -> L 10.2%
18	4.0202	308.40	0.01140	Singlet-A	H-2 -> L+1 84.7%
19	4.0652	304.99	0.03750	Singlet-A	H-12 -> L 67.3%, H-13 -> L 23.4%
20	4.1619	297.90	0.11560	Singlet-A	H-15 -> L 70.1%, H -> L+3 6.4%, H-12 -> L 5.2%

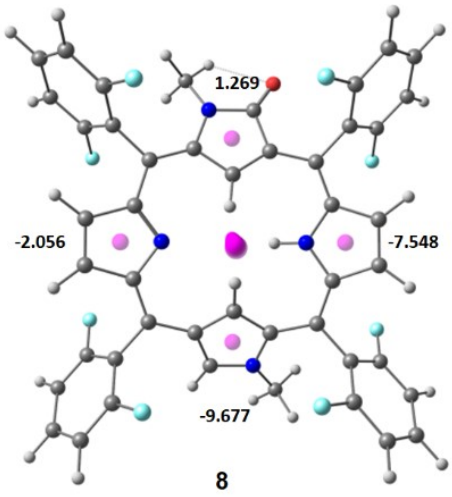

8

8	ppm
NICS(5)	-1.057
NICS(4)	-1.526
NICS(3)	-2.172
NICS(2)	-2.922
NICS(1)	-3.611
NICS(0)	-3.698
NICS(-1)	-4.011
NICS(-2)	-3.340
NICS(-3)	-2.416
NICS(-4)	-1.638
NICS(-5)	-1.109

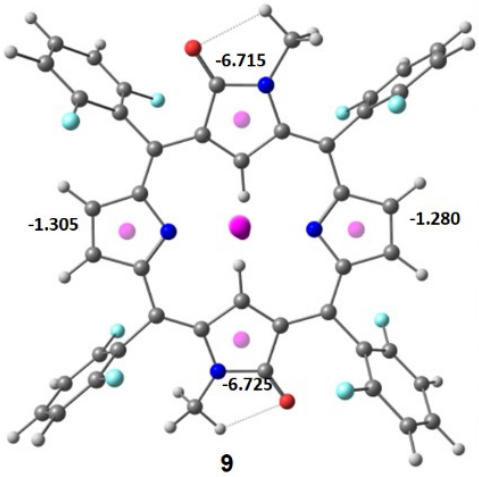

9

9	ppm
NICS(5)	1.295
NICS(4)	2.155
NICS(3)	3.722
NICS(2)	6.413
NICS(1)	9.891
NICS(0)	11.815
NICS(-1)	9.896
NICS(-2)	6.416
NICS(-3)	3.724
NICS(-4)	2.156
NICS(-5)	1.294

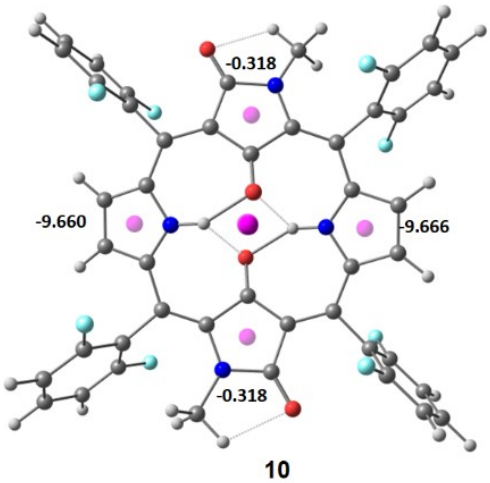

10

10	ppm
NICS(5)	-0.343
NICS(4)	-0.447
NICS(3)	-0.470
NICS(2)	-0.153
NICS(1)	-2.586
NICS(0)	-7.888
NICS(-1)	-2.586
NICS(-2)	-0.153
NICS(-3)	-0.470
NICS(-4)	-0.447
NICS(-5)	-0.344

Fig.S66 NICS values of **8-10** at B3LYP/6-31G** level of theory.

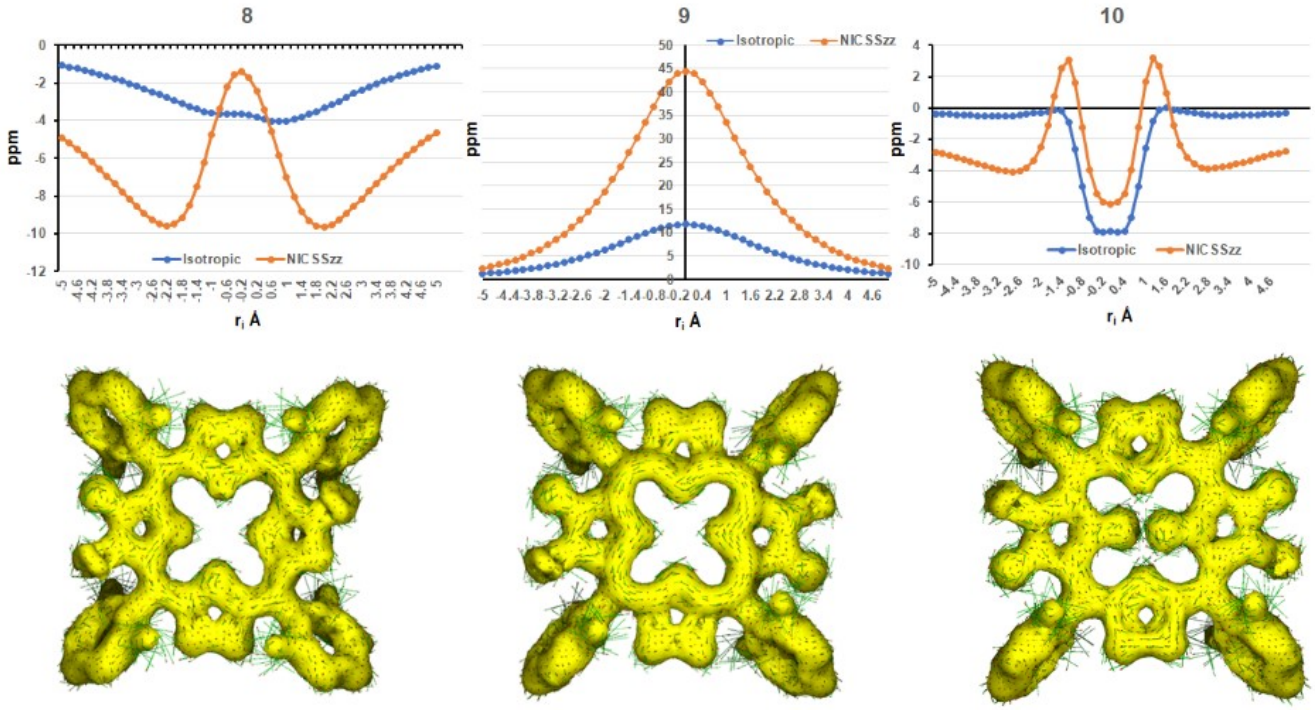

Fig. S67 Isotropic NICS and $NICS_{zz}$ scan values and AICD plot for **8** -**10** at B3LYP/6-31G ** level of theory.

Table S8: Total electronic energy €, zero-point energy (ZPE), free energy (G) XXXartreeree of **6-11** B3LYP/6-31G** level of theory.

Structure	E	E+ZPE	G
6	-2862.68360	-2862.04534	-2862.13043
7	-3465.26919	-3464.48040	-3464.58013
9	-2935.458977	-2934.86524	-2934.95072
8	-2861.46667	-2860.85312	-2860.93782
10	-3085.97500	-3085.37009	-3085.45887
11	-2465.75752	-2465.08693	-2465.16871
8a	-1064.77429	-1064.47406	-1064.51999
9a	-1138.7743936	-1138.49416	-1138.54173
10a	-1289.2923238	-1289.00048	-1289.04788

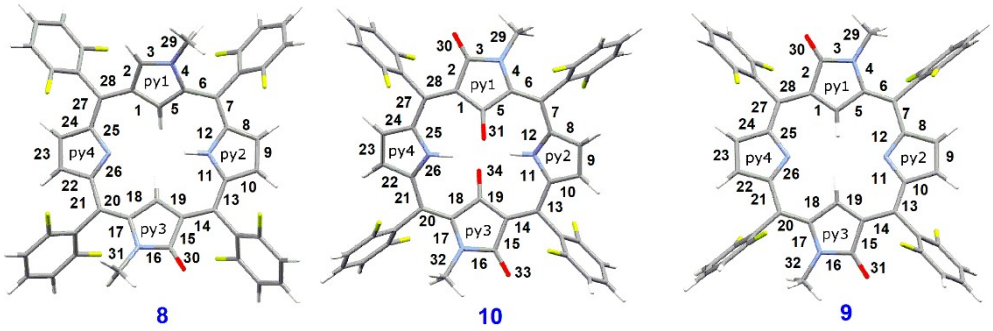

Number of Bond	8		9		10	
	Wieberg Bond Index	π character of the bond	Wieberg Bond Index	π character of the bond	Wieberg Bond Index	π character of the bond
1	1.271	0.384	1.622	0.561	1.145	0.164
2	1.378	0.105	1.009	-	1.052	0.107
3	1.253	0.515	1.051	0.179	1.021	0.164
4	1.083	-	1.095	0.140	1.108	0.150
5	1.466		1.103	0.126	1.006	0.063
6	1.135	0.500	1.523	0.531	1.548	0.547
7	1.446	0.441	1.121	0.169	1.125	0.161
8	1.165	0.467	1.100	0.142	1.297	0.225
9	1.664	0.5911	1.731	0.723	1.518	0.427
10	1.169	0.293	1.100	0.139	1.280	0.202
11	1.133	0.228	1.161	0.191	1.146	0.182
12	1.119	0.156	1.526	0.525	1.263	0.222
13	1.417	0.418	1.512	0.536	1.275	0.291
14	1.193	0.418	1.120	0.156	1.416	0.4255
15	1.033	-	1.009	-	1.052	0.107
16	1.068	0.164	1.051	0.179	1.021	0.165
17	1.072	-	1.095	0.143	1.108	0.150
18	1.184	0.225	1.103	0.126	1.007	0.161
19	1.524	0.658	1.622	0.561	1.145	0.163
20	1.449	0.731	1.523	0.531	1.546	0.547
21	1.165	0.189	1.121	0.169	1.546	0.161
22	1.115	0.454	1.100	0.141	1.125	0.225
23	1.711	0.641	1.731	0.723	1.518	0.427
24	1.117	0.345	1.100	0.139	1.280	0.202
25	1.197	0.202	1.609	0.191	1.146	0.182
26	1.471	0.425	1.523	0.525	1.263	0.222
27	1.458	0.442	1.512	0.536	1.275	0.290
28	1.142	0.144	1.120	0.156	1.416	0.426
29	0.952	-	0.948	-	0.948	-
30	1.678	0.358	1.688	0.483	1.675	0.529
31	0.952	-	1.688	0.483	1.582	0.315
32	-	-	0.948	-	0.948	-
33	-	-	-	-	1.675	0.529
34	-	-	-	-	1.582	0.315

Fig. S68 NBO-Weiberg Bond Index and amount of π character present for each bond of **8** -**10** at B3LYP/6-31G ** level of theory.

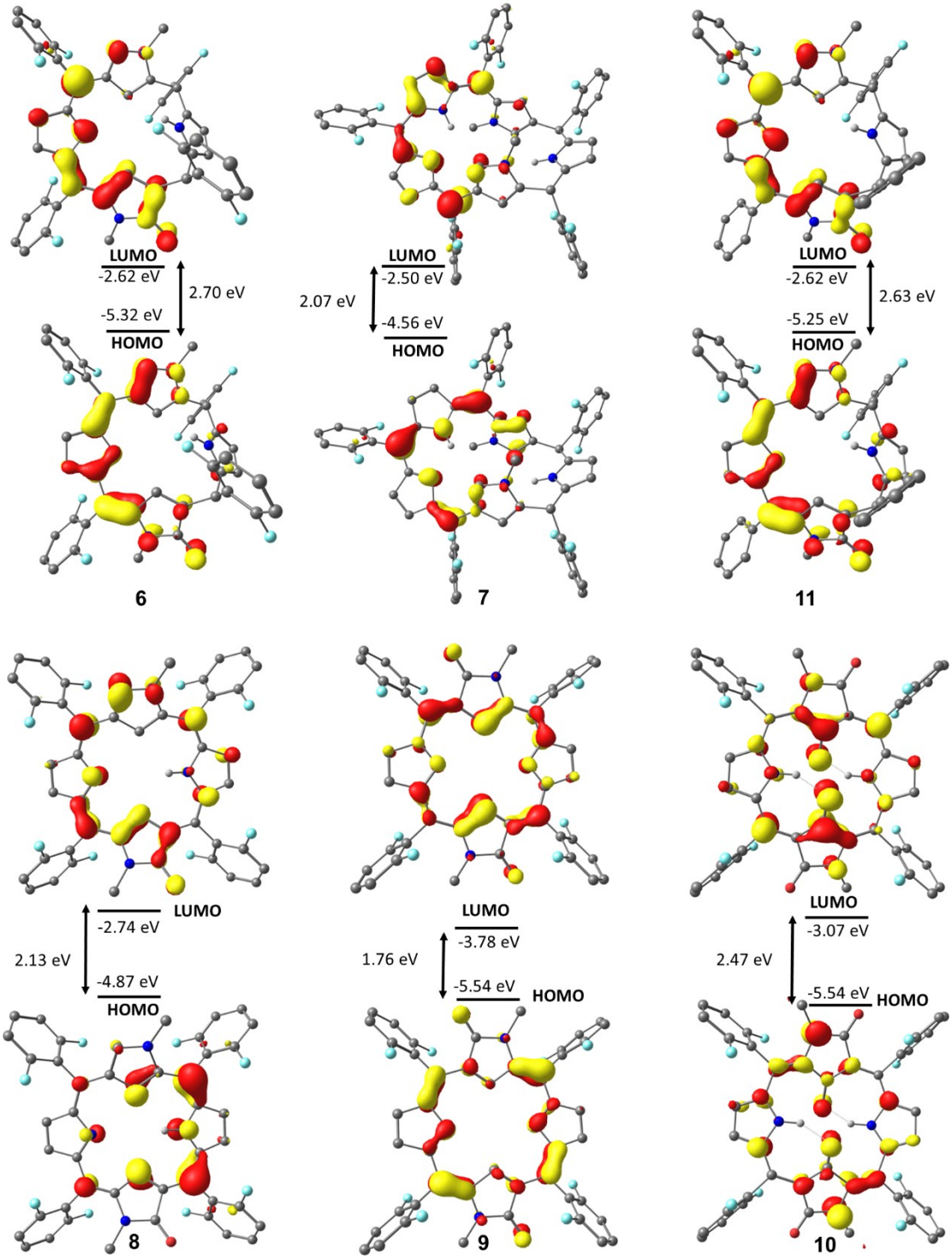

Fig. S69 HOMO-LUMO gap of DFT optimized structures of **6-11** at B3LYP/6-31G** level of theory.

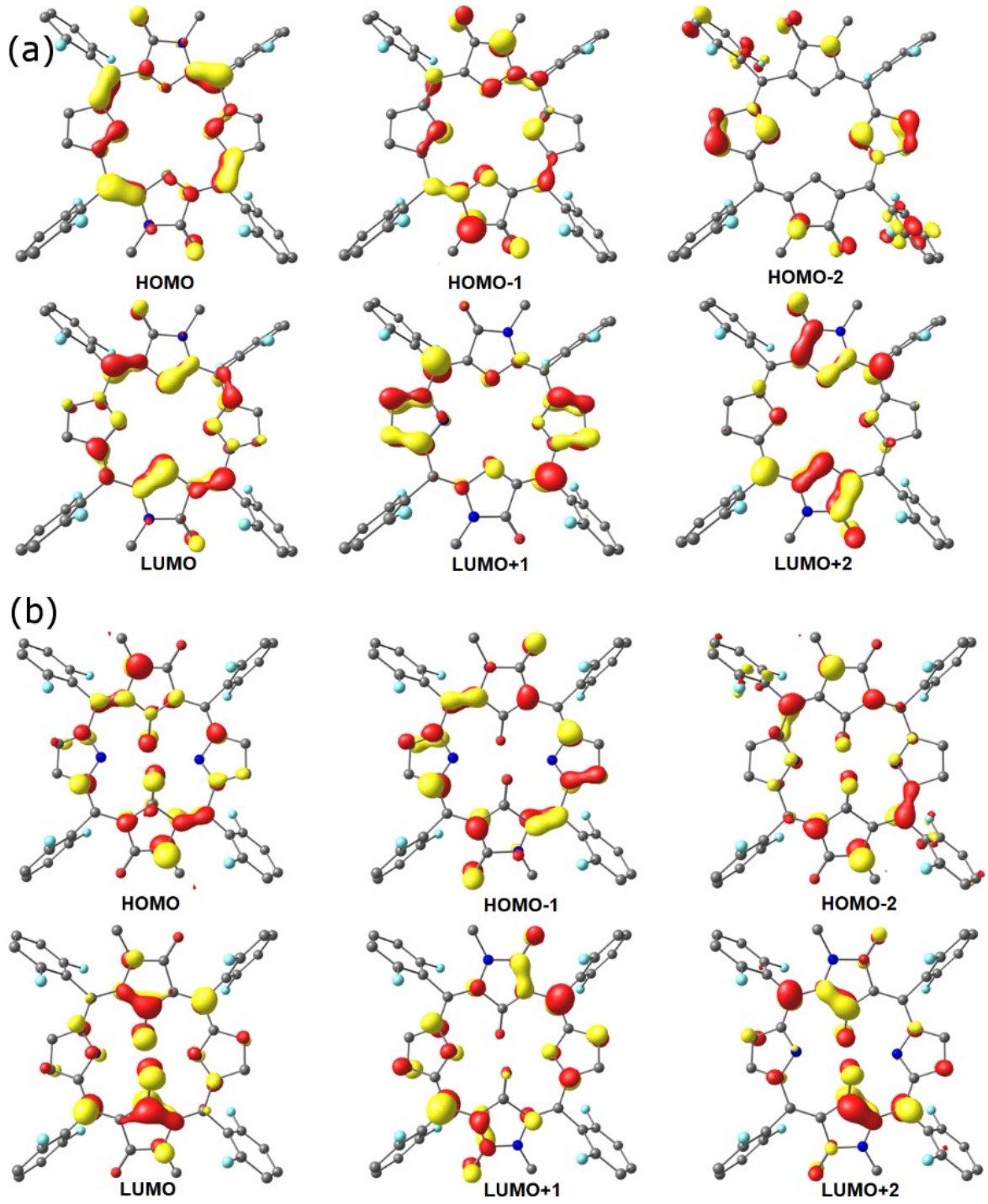

Fig. S70 Frontier kohn sham orbitals of (a) **9** and (b) **10** at B3LYP/6-31G** level of theory. Hydrogen atoms are not shown for the sake of clarity.

6.0 X,Y,Z Coordinates

Cartesian Coordinates

6
Energy = -2862.683596, Nimag=0.0
C, 10.024445, 5.687436, 5.028618
H, 9.126680, 6.286867, 5.005602
C, 10.812486, 5.290770, 6.111427
C, 11.899314, 4.539406, 5.550903
H, 12.678116, 4.060965, 6.119002
C, 11.751103, 4.521850, 4.183922
C, 12.590230, 3.865058, 3.103891
C, 14.078371, 3.908825, 3.395084
C, 15.114259, 3.137432, 2.901939
H, 15.011506, 2.300374, 2.226087
C, 16.323327, 3.641910, 3.455532
H, 17.320130, 3.252221, 3.301622
C, 16.000802, 4.711775, 4.268996
C, 16.888262, 5.507662, 5.199262
C, 17.581577, 4.489728, 7.487916
C, 16.582544, 5.206147, 6.654293
C, 15.485636, 5.394132, 7.416193
H, 14.561011, 5.880457, 7.160994
C, 15.694279, 4.815375, 8.746685
C, 14.760980, 4.787413, 9.758484
C, 13.357057, 5.133745, 9.518831
C, 12.420672, 5.573588, 10.558421
H, 12.645681, 5.695838, 11.608914
C, 11.243208, 5.819583, 9.929532
H, 10.318099, 6.160746, 10.372604
C, 11.463326, 5.519035, 8.518977
C, 10.548771, 5.636413, 7.490001
C, 12.124446, 2.436452, 2.818437
C, 12.260785, 1.394181, 3.743739
C, 11.839239, 0.093708, 3.496249
H, 11.980319, -0.659549, 4.262611
C, 11.248729, -0.200849, 2.267135
H, 10.914348, -1.211562, 2.057501
C, 11.083240, 0.797108, 1.308467
H, 10.628169, 0.603480, 0.344126
C, 11.524520, 2.079913, 1.609907
C, 16.977804, 7.001363, 4.874457
C, 18.179961, 7.557536, 4.420935
C, 18.342068, 8.901842, 4.104541
H, 19.309644, 9.250018, 3.762184
C, 17.251443, 9.757900, 4.239907
H, 17.355524, 10.810861, 3.999865
C, 16.024837, 9.263625, 4.682812
H, 15.153822, 9.897759, 4.800301
C, 15.925208, 7.912306, 4.982651
C, 15.103943, 4.442481, 11.165307
C, 14.462565, 3.404670, 11.858163
C, 14.709095, 3.104929, 13.191960
H, 14.180479, 2.279972, 13.655311
C, 15.636405, 3.877933, 13.891405
H, 15.842909, 3.659780, 14.934106
C, 16.301327, 4.927538, 13.258468
H, 17.023712, 5.547707, 13.776447
C, 16.019680, 5.185405, 11.922201
C, 9.196141, 6.190518, 7.796709
C, 8.997597, 7.512534, 8.215985
C, 7.743072, 8.045966, 8.490565
H, 7.666648, 9.079502, 8.807845
C, 6.621317, 7.231239, 8.343443
H, 5.634644, 7.629384, 8.556813
C, 6.758339, 5.907639, 7.925089
H, 5.905611, 5.248858, 7.808573
C, 8.032538, 5.421160, 7.658944
C, 10.089601, 5.553216, 2.545842
H, 10.097692, 4.673166, 1.901976
H, 9.063374, 5.912678, 2.635403
H, 10.694588, 6.336120, 2.074923
C, 17.670241, 3.501911, 9.752532
H, 18.001861, 4.096100, 10.606946
H, 17.019664, 2.696653, 10.101938
H, 18.546258, 3.076574, 9.260309
N, 10.586741, 5.232269, 3.876357
N, 14.633855, 4.865573, 4.208547
N, 17.000009, 4.320809, 8.756993
N, 12.773547, 5.088832, 8.330270
O, 18.695996, 4.100283, 7.172245
H, 14.105190, 5.557671, 4.716004
H, 12.417334, 4.422461, 2.176190
H, 17.895393, 5.114525, 5.041788
F, 10.071405, 8.313623, 8.348954
F, 8.157613, 4.140681, 7.263658
F, 11.344011, 3.048865, 0.671717
F, 12.826643, 1.663415, 4.933508
F, 16.673762, 6.198197, 11.317447
F, 13.569531, 2.652307, 11.188442
F, 14.711471, 7.459633, 5.407967
F, 19.249080, 6.745680, 4.279956

7
Energy = -3465.269186, NImag=0.0
F, 8.817439, 14.491736, 5.835921
F, 13.439364, 14.441582, 4.861507
F, 14.005463, 4.602561, 4.049654
F, 10.341696, 5.377543, 6.926426
F, 9.320355, 6.343750, 1.222558
F, 13.331672, 6.222443, -1.257334
F, 9.517430, 13.301115, 0.792039
F, 5.420001, 11.242366, 1.938337
F, 16.319135, 9.012198, 8.975629
F, 12.684513, 11.111165, 11.137063
N, 9.492033, 11.035956, 5.467646
N, 12.956013, 8.681693, 2.579184

N, 9.998073, 9.312707, 1.399072
H, 10.090285, 9.011641, 2.358541
N, 12.389059, 11.196759, 7.008127
H, 12.241924, 10.345723, 6.466160
N, 12.960767, 8.518760, 6.877038
C, 16.508912, 9.592772, 11.242264
H, 17.513213, 9.185003, 11.238446
C, 15.945275, 10.164293, 12.382901
H, 16.515594, 10.204491, 13.305215
C, 14.651900, 10.683844, 12.343483
H, 14.182213, 11.126129, 13.214549
C, 13.940452, 10.616403, 11.151306
C, 13.678853, 9.984505, 8.703993
C, 13.199437, 11.150357, 8.124683
C, 12.040952, 12.504003, 6.693568
C, 12.723282, 13.331671, 7.673347
H, 12.639656, 14.407666, 7.716800
C, 13.394762, 12.526302, 8.536034
H, 13.979335, 12.830493, 9.391276
C, 13.427608, 8.690467, 8.122265
C, 12.815647, 7.147530, 6.702470
C, 13.173593, 6.456832, 7.934701
H, 13.164776, 5.386051, 8.083387
C, 13.591476, 7.410649, 8.805871
H, 13.948769, 7.273269, 9.817051
C, 11.166834, 12.924528, 5.712645
C, 10.262482, 12.074578, 4.947684
C, 8.689281, 10.545339, 4.469307
H, 7.981642, 9.753859, 4.674100
C, 8.925394, 11.245557, 3.296852
C, 9.919126, 12.207548, 3.604105
H, 10.353840, 12.923311, 2.924475
C, 12.510030, 6.540565, 5.495888
C, 12.507164, 7.219972, 4.220466
C, 13.137631, 8.424770, 3.903307
H, 13.715068, 9.078883, 4.536068
C, 12.205615, 7.654822, 2.003992
C, 11.922814, 6.748103, 2.996443
H, 11.340664, 5.847579, 2.877957
C, 11.128964, 14.369569, 5.370853
C, 9.936478, 15.111502, 5.414266
C, 9.852681, 16.453516, 5.070395
H, 8.895889, 16.958071, 5.139284
C, 11.011049, 17.113355, 4.657373
H, 10.966476, 18.163019, 4.385856
C, 12.225487, 16.431894, 4.593878
H, 13.140233, 16.914458, 4.269447
C, 12.258228, 15.087567, 4.946599
C, 9.359478, 10.644369, 6.865224
H, 8.342176, 10.285012, 7.032512
H, 9.533468, 11.510122, 7.505554
H, 10.066595, 9.855891, 7.137322
C, 8.227755, 10.967762, 1.973184
H, 7.427419, 10.255367, 2.204989
C, 9.146176, 10.299654, 0.970289
C, 10.720028, 8.801924, 0.347445
C, 10.314213, 9.477955, -0.787806
H, 10.695154, 9.318691, -1.787590
C, 9.316006, 10.415906, -0.396233
H, 8.790209, 11.104289, -1.041828
C, 12.197495, 5.084506, 5.489800
C, 12.945193, 4.156932, 4.748211
C, 12.662852, 2.797183, 4.714141
H, 13.294677, 2.141518, 4.126265
C, 11.577655, 2.319118, 5.448532
H, 11.341693, 1.259986, 5.434617
C, 10.795276, 3.193343, 6.201499
H, 9.941887, 2.852970, 6.776484
C, 11.118982, 4.545345, 6.206727
C, 13.517499, 9.825028, 1.873185
H, 12.743167, 10.334649, 1.295446
H, 14.320423, 9.511547, 1.197578
H, 13.926941, 10.520378, 2.606513
C, 11.769711, 7.725566, 0.556752
H, 12.640670, 8.013429, -0.041853
C, 11.345806, 6.365185, 0.011148
C, 10.139239, 5.738295, 0.335200
C, 9.740449, 4.517877, -0.195288
H, 8.788662, 4.096492, 0.106813
C, 10.582613, 3.874141, -1.102041
H, 10.288809, 2.920575, -1.528395
C, 11.800149, 4.449315, -1.461660
H, 12.477740, 3.976058, -2.162712
C, 12.148544, 5.671106, -0.898001
C, 7.517607, 12.189687, 1.402329
C, 8.166077, 13.297403, 0.846568
C, 7.500755, 14.408193, 0.341510
H, 8.080353, 15.224704, -0.073456
C, 6.107496, 14.434686, 0.385878
H, 5.570026, 15.293524, -0.002703
C, 5.403949, 13.361480, 0.928707
H, 4.321451, 13.346449, 0.979202
C, 6.121580, 12.276200, 1.417725
C, 14.453472, 10.062626, 9.968744
C, 15.759045, 9.557567, 10.073158

8

Energy = -2861.466670, Nimag =0.0
F, -3.243248, -0.880734, -1.668464
F, -5.936454, -4.154315, 0.386239
F, -2.464159, -2.106520, -6.800095
F, -4.183017, -6.304320, -8.113554
F, -1.960172, -10.312086, -6.554670
F, 2.222757, -10.009163, -4.393694
F, -3.153823, -8.194624, 2.014945
F, 1.431535, -8.472306, 0.943652
O, -1.299085, -5.556998, 2.227711
N, -0.893052, -8.046081, -2.379974
H, -1.017698, -7.084988, -2.662625
N, -3.214603, -4.549275, -3.597716
N, -2.609163, -4.377672, 0.723132

N, -0.412275, -7.295798, -6.543277
C, -1.662099, -9.103636, 3.585224
H, -2.496228, -9.249943, 4.261531
C, -1.844324, -5.474625, 1.138349
C, -1.805285, -6.429908, -0.019809
C, -2.472942, -5.808602, -1.050548
H, -2.708369, -6.182734, -2.030731
C, -2.992767, -4.538944, -0.617218
C, -3.772611, -3.662763, -1.359474
C, -3.919396, -3.746838, -2.799883
C, -4.828166, -2.891120, -3.577499
H, -5.529591, -2.173398, -3.176739
C, -4.611781, -3.190186, -4.880394
H, -5.104591, -2.769646, -5.745742
C, -3.588174, -4.231847, -4.894867
C, -3.013418, -4.800872, -6.019237
C, -2.095284, -5.914855, -5.962525
C, -1.957146, -6.914366, -4.962344
H, -2.620178, -7.038072, -4.123957
C, -0.924708, -7.771531, -5.320921
C, -1.117940, -6.201864, -6.922102
H, -0.855310, -5.658679, -7.818176
C, -0.416912, -8.939455, -4.631708
C, -0.481396, -9.044823, -3.252541
C, -0.175801, -10.184099, -2.416679
H, 0.132404, -11.148560, -2.791587
C, -0.375952, -9.837767, -1.116157
H, -0.258012, -10.469768, -0.249045
C, -0.833842, -8.467306, -1.062436
C, -1.175327, -7.718021, 0.057346
C, -2.612372, -3.168237, 1.531686
H, -2.254728, -2.313492, 0.951763
H, -1.933123, -3.355644, 2.364725
H, -3.603647, -2.940994, 1.930058
C, 0.787663, -7.751629, -7.235545
H, 0.607482, -8.674889, -7.791508
H, 1.593061, -7.921410, -6.518412
H, 1.099559, -6.972919, -7.933314
C, -4.548028, -2.578606, -0.686986
C, -5.634389, -2.863614, 0.150266
C, -6.413109, -1.883216, 0.755513
H, -7.239778, -2.180632, 1.390280
C, -6.104681, -0.543865, 0.519542
H, -6.700350, 0.235840, 0.983035
C, -5.034111, -0.199116, -0.306198
H, -4.766291, 0.832802, -0.501608
C, -4.287609, -1.217324, -0.886454
C, -3.315717, -4.239566, -7.364359
C, -3.877794, -5.021901, -8.385817
C, -4.157251, -4.537593, -9.657556
H, -4.605956, -5.200167, -10.388569
C, -3.859076, -3.206191, -9.947514
H, -4.070603, -2.809040, -10.934988
C, -3.291372, -2.382273, -8.976674
H, -3.039879, -1.346905, -9.175390
C, -3.033245, -2.910603, -7.716694
C, 0.091282, -10.101186, -5.406635
C, 1.385785, -10.620793, -5.256952
C, 1.865036, -11.711795, -5.971836
H, 2.880131, -12.051324, -5.801151
C, 1.023852, -12.326666, -6.899032
H, 1.379253, -13.179947, -7.467264
C, -0.271765, -11.849692, -7.101023
H, -0.950868, -12.310277, -7.809234
C, -0.706432, -10.759890, -6.356662
C, -0.884345, -8.313552, 1.391092
C, 0.404898, -8.680224, 1.795798
C, 0.688884, -9.249352, 3.031823
H, 1.714584, -9.503500, 3.272950
C, -0.357256, -9.459353, 3.928318
H, -0.155634, -9.899658, 4.899469
C, -1.891385, -8.540284, 2.338792

8a

Energy = -1064.77429, Nimag =0.0

8	-2.056219	-6.022420	2.390094
7	-0.872691	-8.052385	-2.361856
1	-1.065268	-7.110385	-2.659270
7	-3.303384	-4.577886	-3.596390
7	-3.035089	-4.652302	0.780570
7	-0.825627	-7.603113	-6.668513
6	-2.289827	-5.742748	1.226278
6	-1.859050	-6.465240	-0.024756
6	-2.376465	-5.753675	-1.088625
1	-2.321771	-5.914763	-2.148576
6	-3.117212	-4.625615	-0.615916
6	-3.788555	-3.683692	-1.364862
6	-3.852340	-3.660730	-2.797664
6	-4.498624	-2.599295	-3.581600
1	-5.016406	-1.739294	-3.175038
6	-4.294130	-2.910537	-4.887275
1	-4.614775	-2.359900	-5.762730
6	-3.529953	-4.158623	-4.895108
6	-3.037474	-4.808172	-6.006336
6	-2.240103	-6.000796	-5.992468
6	-1.956853	-6.865692	-4.896361
1	-2.457385	-6.794670	-3.949706
6	-1.059031	-7.846310	-5.308102
6	-1.516609	-6.511809	-7.081660
1	-1.439057	-6.147704	-8.096343
6	-0.405738	-8.905034	-4.603864
6	-0.355660	-9.001830	-3.230444
6	0.187436	-10.040773	-2.384447
1	0.637221	-10.952501	-2.753779
6	-0.000059	-9.682628	-1.078873
1	0.274336	-10.249183	-0.199492
6	-0.672321	-8.403121	-1.038771
6	-1.099242	-7.659368	0.045837
1	-0.173659	-8.121219	-7.237224
1	0.097218	-9.678042	-5.177312

1	-0.859574	-8.023512	1.039707
1	-3.462472	-3.994569	1.413258
1	-3.232605	-4.354875	-6.975678
1	-4.298932	-2.877931	-0.843142

9

Energy = -2935.458977, Nimag=0.0
F, 2.788530, 1.510875, 1.461553
F, -1.382230, 3.699223, 1.538910
F, 4.018656, 8.616690, 3.611559
F, 6.764749, 5.298432, 5.506985
O, 3.661222, 7.898222, 9.508558
N, 2.400260, 4.569704, 4.370718
N, 4.205589, 7.272934, 7.346149
C, 0.726200, 2.657666, 1.563157
C, 1.633384, 1.858874, 0.859490
C, 1.399769, 1.398949, -0.431137
H, 2.146636, 0.779593, -0.913995
C, 0.202809, 1.740856, -1.058163
H, 0.004155, 1.391342, -2.066072
C, -0.743760, 2.525423, -0.398276
H, -1.685608, 2.801693, -0.857527
C, -0.465220, 2.952648, 0.890849
C, 0.981147, 3.157926, 2.945707
C, 0.094916, 2.702054, 4.007601
C, -0.060136, 3.153127, 5.281800
C, 3.734694, 6.338413, 6.422997
C, 4.128642, 6.197293, 5.111654
C, 3.444356, 5.349106, 4.134443
C, 2.042040, 4.016037, 3.141540
C, 2.945471, 4.504216, 2.096470
H, 2.893925, 4.258643, 1.046424
C, 3.826255, 5.323393, 2.709356
H, 4.645951, 5.861610, 2.257091
C, 3.510248, 7.146620, 8.560489
C, 5.030756, 8.452317, 7.126864
H, 5.010843, 9.012497, 8.062360
H, 4.620557, 9.071348, 6.324898
H, 6.062320, 8.187194, 6.889810
C, 5.327952, 6.921676, 4.583466
C, 5.241391, 8.085603, 3.813951
C, 6.346319, 8.732400, 3.275030
H, 6.203557, 9.636987, 2.695383
C, 7.611827, 8.191246, 3.506120
H, 8.488867, 8.680171, 3.094799
C, 7.759468, 7.029388, 4.262977
H, 8.730127, 6.587582, 4.456005
C, 6.620003, 6.420874, 4.778861
F, -0.113786, 7.174631, 10.944447
F, 4.056968, 4.986269, 10.867046
F, -1.343930, 0.068799, 8.794379
F, -4.090022, 3.387103, 6.899033
O, -0.986524, 0.787312, 2.897405
N, 0.274464, 4.115810, 8.035256
N, -1.530882, 1.412593, 5.059817
C, 1.948540, 6.027832, 10.842820
C, 1.041364, 6.826622, 11.546500
C, 1.274991, 7.286539, 12.837127
H, 0.528129, 7.905895, 13.319994
C, 2.471954, 6.944626, 13.464141
H, 2.670617, 7.294133, 14.472051
C, 3.418516, 6.160061, 12.804243
H, 4.360367, 5.883785, 13.263484
C, 3.139965, 5.732843, 11.515117
C, 1.693582, 5.527580, 9.460269
C, 2.579801, 5.983463, 8.398370
C, 2.734851, 5.532392, 7.124170
C, -1.059978, 2.347106, 5.982974
C, -1.453918, 2.488218, 7.294320
C, -0.769625, 3.336397, 8.271532
C, 0.632692, 4.669465, 9.264438
C, -0.270723, 4.181264, 10.309512
H, -0.219166, 4.426822, 11.359561
C, -1.151508, 3.362089, 9.696625
H, -1.971195, 2.823859, 10.148892
C, -0.835549, 1.538914, 3.845474
C, -2.356056, 0.233214, 5.279097
H, -2.336155, -0.326956, 4.343594
H, -1.945854, -0.385829, 6.081052
H, -3.387616, 0.498342, 5.516162
C, -2.653226, 1.763836, 7.822512
C, -2.566664, 0.599897, 8.592009
C, -3.671590, -0.046899, 9.130935
H, -3.528827, -0.951495, 9.710568
C, -4.937097, 0.494266, 8.899868
H, -5.814135, 0.005342, 9.311192
C, -5.084739, 1.656136, 8.143028
H, -6.055397, 2.097952, 7.950018
C, -3.945276, 2.264649, 7.627140
H, 0.431250, 3.989363, 5.744894
H, 2.243473, 4.696149, 6.661080

9a

Energy =-1138.7743936, Nimag=0.0

8	3.809649	7.707297	9.593466
7	2.355244	4.647397	4.325476
7	4.221030	7.186923	7.358403
6	1.016805	3.133066	2.975096
6	0.117008	2.715033	4.019984
6	-0.004534	3.149051	5.304470
6	3.689919	6.322103	6.406187
6	4.037140	6.261126	5.086820
6	3.403880	5.416871	4.092198
6	2.051320	4.017905	3.120470
6	2.995378	4.450069	2.085357
1	2.994173	4.120846	1.054422
6	3.838705	5.324940	2.685405
1	4.674098	5.855166	2.245744
6	3.570677	7.058195	8.591573
8	-1.134926	0.978218	2.812505
7	0.319481	4.038113	8.080499
7	-1.546305	1.498585	5.047570

6	1.657911	5.552453	9.430875
6	2.557693	5.970501	8.385982
6	2.679228	5.536488	7.101493
6	-1.015203	2.363414	5.999784
6	-1.362402	2.424369	7.319157
6	-0.729143	3.268625	8.313780
6	0.623407	4.667601	9.285505
6	-0.320639	4.235421	10.320623
1	-0.319431	4.564639	11.351559
6	-1.163955	3.360537	9.720578
1	-1.999336	2.830297	10.160243
6	-0.896009	1.627374	3.814376
1	0.537621	3.943627	5.779148
1	2.137078	4.741907	6.626818
1	-2.156009	1.772534	7.675847
1	-2.240898	0.787205	5.216702
1	0.857931	2.670954	2.003989
1	4.830763	6.912943	4.730135
1	4.915659	7.898270	7.189281
1	1.816784	6.014569	10.401982

10

Energy = -3085.975001, Nimag=0.0

F, 2.718781, 0.780861, 1.827410
F, -0.821519, 3.832122, 1.309521
F, 4.111025, 9.150332, 4.757792
F, 6.443240, 5.099605, 4.170919
O, 1.331177, 3.003763, 6.155796
O, 3.996541, 7.613146, 9.629678
N, 2.643883, 4.371635, 4.311504
H, 2.325753, 4.022525, 5.219859
N, 4.277445, 7.175760, 7.376736
C, 0.957415, 2.328709, 1.626924
C, 1.754278, 1.332199, 1.063413
C, 1.598655, 0.886851, -0.244248
H, 2.250506, 0.106847, -0.619978
C, 0.601330, 1.463028, -1.029384
H, 0.463183, 1.129579, -2.052763
C, -0.221745, 2.464294, -0.512046
H, -1.007207, 2.925041, -1.099531
C, -0.028751, 2.870179, 0.800770
C, 1.186900, 2.804972, 3.032358
C, 0.341879, 2.343608, 4.045769
C, 0.382583, 2.596007, 5.472847
C, 3.613298, 6.520398, 6.344495
C, 4.042904, 6.331491, 5.047922
C, 3.424915, 5.447615, 4.061686
C, 2.214949, 3.780517, 3.140931
C, 2.831394, 4.503231, 2.083381
H, 2.691812, 4.306032, 1.031476
C, 3.567757, 5.529843, 2.647931
H, 4.136038, 6.282699, 2.123484
C, 3.566275, 7.114384, 8.602820
C, 5.637253, 7.693531, 7.397480
H, 5.878372, 7.879600, 8.443888
H, 5.719272, 8.631688, 6.844615
H, 6.334149, 6.964366, 6.978872
C, 5.211201, 7.081540, 4.493768
C, 5.188052, 8.470366, 4.317784
C, 6.225351, 9.184944, 3.729105
H, 6.136641, 10.260263, 3.626919
C, 7.349043, 8.488412, 3.286213
H, 8.169975, 9.028267, 2.825805
C, 7.427845, 7.102675, 3.433109
H, 8.291271, 6.536685, 3.103388
C, 6.363132, 6.435248, 4.024277
F, -0.044010, 7.904628, 10.578528
F, 3.496251, 4.853336, 11.096519
F, -1.436333, -0.464838, 7.648261
F, -3.768489, 3.585946, 8.234982
O, 1.343609, 5.681590, 6.250219
O, -1.321800, 1.072380, 2.776278
N, 0.030888, 4.313833, 8.094476
H, 0.349022, 4.662945, 7.186123
N, -1.602707, 1.509736, 5.029225
C, 1.717339, 6.356766, 10.779064
C, 0.920475, 7.353290, 11.342550
C, 1.076079, 7.798652, 12.650208
H, 0.424229, 8.578667, 13.025916
C, 2.073385, 7.222475, 13.435368
H, 2.211517, 7.555935, 14.458746
C, 2.896459, 6.221194, 12.918058
H, 3.681905, 5.760447, 13.505562
C, 2.703484, 5.815295, 11.605243
C, 1.487872, 5.880486, 9.373633
C, 2.332894, 6.341840, 8.360220
C, 2.292193, 6.089405, 6.933148
C, -0.938547, 2.165067, 6.061481
C, -1.368161, 2.353994, 7.358050
C, -0.750158, 3.237861, 8.344287
C, 0.459819, 4.904946, 9.265054
C, -0.156639, 4.182236, 10.322598
H, -0.017063, 4.379432, 11.374504
C, -0.893011, 3.155634, 9.758041
H, -1.461307, 2.402785, 10.282483
C, -0.891513, 1.571087, 3.803153
C, -2.962538, 0.992030, 5.008449
H, -3.203643, 0.805980, 3.962035
H, -3.044613, 0.053872, 5.561304
H, -3.659410, 1.721224, 5.427046
C, -2.536479, 1.603980, 7.912204
C, -2.513355, 0.215159, 8.088232
C, -3.550675, -0.499384, 8.676916
H, -3.461984, -1.574702, 8.779136
C, -4.674362, 0.197179, 9.119771
H, -5.495309, -0.342649, 9.580184
C, -4.753139, 1.582913, 8.972835
H, -5.616559, 2.148927, 9.302527
C, -3.688406, 2.250306, 8.381663

10a

Energy= -1289.2923238, Nimag =0.0

8	1.408715	3.030606	6.172452
8	3.967167	7.554287	9.611300
7	2.634134	4.407792	4.262122
1	2.315318	4.068826	5.175052
7	4.164929	7.219300	7.320659
6	1.172726	2.853119	3.046481
6	0.377535	2.374622	4.077516
6	0.455452	2.606193	5.504868
6	3.523043	6.525706	6.299605
6	4.001671	6.318257	5.038676
6	3.450557	5.454255	4.015622
6	2.209418	3.809540	3.096363
6	2.868029	4.494906	2.039183
1	2.743718	4.281306	0.986539
6	3.638616	5.503695	2.605150
1	4.249803	6.227829	2.084945
6	3.526503	7.098387	8.571116
8	1.266035	5.654963	6.233482
8	-1.292394	1.131130	2.794695
7	0.040600	4.277686	8.143852
1	0.359421	4.616646	7.230920
7	-1.490136	1.466123	5.085337
6	1.502003	5.832373	9.359482
6	2.297218	6.310848	8.328453
6	2.219317	6.079280	6.901098
6	-0.848259	2.159741	6.106380
6	-1.326890	2.367187	7.367310
6	-0.775803	3.231212	8.390359
6	0.465309	4.875954	9.309606
6	-0.193309	4.190599	10.366790
1	-0.069008	4.404214	11.419432
6	-0.963875	3.181789	9.800830
1	-1.575054	2.457653	10.321041
6	-0.851726	1.587042	3.834873
1	-2.244750	1.853581	7.646268
1	-2.421289	1.079148	5.147035
1	5.096091	7.606253	7.258972
1	1.783626	6.174347	10.354024
1	4.919543	6.831845	4.759720
1	0.891104	2.511143	2.051940

11

Energy = -2465.757521, Nimag=0.0
C, 10.125558, 5.655425, 4.911434
H, 9.231071, 6.255614, 4.837355
C, 10.873415, 5.291779, 6.033679
C, 11.975888, 4.519125, 5.535827
H, 12.731822, 4.057157, 6.146668
C, 11.876703, 4.459279, 4.165696
C, 12.759664, 3.774168, 3.140267
C, 14.239744, 3.877955, 3.460265
C, 15.314622, 3.153055, 2.981002
H, 15.256996, 2.315143, 2.300675
C, 16.495111, 3.708891, 3.550899
H, 17.509891, 3.364530, 3.407057
C, 16.117423, 4.762793, 4.360193
C, 16.923014, 5.639668, 5.291205
C, 17.533762, 4.444126, 7.529513
C, 16.601328, 5.267706, 6.721737
C, 15.499946, 5.483096, 7.472795
H, 14.618798, 6.052622, 7.224923
C, 15.644624, 4.830486, 8.775221
C, 14.702507, 4.817319, 9.782436
C, 13.313887, 5.189720, 9.509395
C, 12.358950, 5.673679, 10.512589
H, 12.561516, 5.816756, 11.564684
C, 11.203151, 5.926356, 9.845583
H, 10.274252, 6.298743, 10.254525
C, 11.453871, 5.585069, 8.449253
C, 10.569443, 5.683753, 7.391338
C, 12.340897, 2.320539, 2.914604
C, 12.503127, 1.323544, 3.884230
C, 12.124652, 0.001098, 3.690140
H, 12.284115, -0.714366, 4.488444
C, 11.551813, -0.363724, 2.471470
H, 11.250778, -1.392476, 2.303233
C, 11.361233, 0.587004, 1.470391
H, 10.918712, 0.338309, 0.512873
C, 11.759905, 1.894729, 1.719334
C, 16.811987, 7.140359, 4.973408
C, 16.625775, 7.563771, 3.649728
H, 16.511521, 6.820078, 2.866984
C, 16.589530, 8.920663, 3.329319
H, 16.443341, 9.224461, 2.296343
C, 16.739170, 9.884078, 4.327890
H, 16.707303, 10.941165, 4.080141
C, 16.930892, 9.475048, 5.647292
H, 17.051540, 10.213463, 6.435080
C, 16.967660, 8.116448, 5.965881
H, 17.117086, 7.813929, 6.996929
C, 15.026866, 4.458454, 11.191770
C, 14.294817, 3.471515, 11.874725
H, 13.509324, 2.936556, 11.349569
C, 14.575458, 3.167279, 13.205862
H, 14.005957, 2.393368, 13.712428
C, 15.584171, 3.852821, 13.886355
H, 15.799846, 3.617998, 14.924509
C, 16.308927, 4.846224, 13.225995
H, 17.086899, 5.393381, 13.750677
C, 16.032029, 5.146749, 11.892343
H, 16.586890, 5.930627, 11.385260
C, 9.216698, 6.264654, 7.639625
C, 9.025614, 7.599601, 8.020190
C, 7.771445, 8.158390, 8.240122
H, 7.701101, 9.200577, 8.529208
C, 6.642308, 7.357267, 8.075793
H, 5.655658, 7.775480, 8.246541
C, 6.771803, 6.021717, 7.694575
H, 5.912929, 5.373226, 7.566106
C, 8.046075, 5.509705, 7.482632
C, 10.273871, 5.434191, 2.437479
H, 10.293403, 4.528375, 1.830375

H, 9.248986, 5.805618, 2.480857
H, 10.900640, 6.192756, 1.955639
C, 17.466946, 3.272195, 9.707272
H, 17.828186, 3.734309, 10.628521
H, 16.715437, 2.521891, 9.965318
H, 18.304091, 2.797097, 9.193549
N, 10.726535, 5.161881, 3.794747
N, 14.745377, 4.858059, 4.280081
N, 16.920078, 4.253261, 8.782113
N, 12.759561, 5.126872, 8.305651
O, 18.626358, 3.997594, 7.210511
H, 14.170385, 5.498972, 4.805111
H, 12.594159, 4.279993, 2.182573
H, 17.970496, 5.346062, 5.142409
F, 10.107101, 8.387142, 8.169052
F, 8.163802, 4.217588, 7.123489
F, 11.556460, 2.817064, 0.739679
F, 13.051215, 1.661607, 5.065394